

SRG/ART-XC all-sky X-ray survey: Catalog of sources detected during the first five surveys^{*}

S. Sazonov^{1**}, R. Burenin¹, E. Filippova¹, R. Krivonos¹, V. Arefiev¹, K. Borisov², M. Buntov¹, C.-T. Chen³, S. Ehlert⁵, S. Gararin⁴, M. Garin⁴, S. Grigorovich⁴, I. Lapshov¹, V. Levin¹, A. Lutovinov¹, I. Mereminskiy¹, S. Molkov¹, M. Pavlinsky¹, B. D. Ramsey⁵, A. Semena¹, N. Semena¹, A. Shtykovsky¹, R. Sunyaev¹, A. Tkachenko¹, D. A. Swartz³, G. Uskov¹, A. Vikhlinin^{1,6}, V. Voron², E. Zakharov¹, and I. Zaznabin¹

¹ Space Research Institute, 84/32 Profsovnaya str., Moscow 117997, Russian Federation

² State Space Corporation Roscosmos, 42 Schepkina str., Moscow 107996, Russia

³ Universities Space Research Association, Huntsville, AL 35805, USA

⁴ VNIIEF, Nizhny Novgorod region 607188, Russia

⁵ NASA/Marshall Space Flight Center, Huntsville, AL 35812 USA

⁶ Harvard-Smithsonian Center for Astrophysics, 60 Garden Street, Cambridge, MA 02138, USA

May 16, 2024

ABSTRACT

We present an updated catalog of sources detected by the *Mikhail Pavlinsky* ART-XC telescope aboard the Spektrum-Roentgen-Gamma (SRG) observatory during its all-sky survey. It is based on the data of the first four and the partially completed fifth scans of the sky (ARTSS1-5). The catalog comprises 1545 sources detected in the 4–12 keV energy band. The achieved sensitivity ranges between $\sim 4 \times 10^{-12}$ ergs⁻¹ cm⁻² near the ecliptic plane and $\sim 7 \times 10^{-13}$ ergs⁻¹ cm⁻² near the ecliptic poles, which is a ~ 30 –50% improvement over the previous version of the catalog based on the first two all-sky scans (ARTSS12). There are ~ 130 objects, excluding the expected contribution of spurious detections, that were not known as X-ray sources before the SRG/ART-XC all-sky survey. We provide information, partly based on our ongoing follow-up optical spectroscopy program, on the identification and classification of the majority of the ARTSS1-5 sources (1463), of which 173 are tentative at the moment. The majority of the classified objects (964) are extragalactic, a small fraction (30) are located in the Local Group of galaxies, and 469 are Galactic. The dominant classes of objects in the catalog are active galactic nuclei (911) and cataclysmic variables (192).

Key words. Surveys – Catalogs – X-rays: general

1. Introduction

The Spektrum-Roentgen-Gamma (SRG) orbital observatory¹ (Sunyaev et al. 2021) was designed to survey the entire sky in X-rays with better sensitivity, angular resolution, and energy coverage compared to its predecessors, such as *Uhuru* (1970–1973), High Energy Astronomy Observatory 1 (HEAO-1; 1977–1979), and Röntgensatellit (ROSAT; 1990–1991). The spacecraft was launched on July 13, 2019, from the Baikonur Cosmodrome to a halo orbit near the L2 point of the Sun–Earth system, from where it started scanning the sky on December 12, 2019. The observatory is equipped with two grazing incidence telescopes: the extended ROentgen Survey with an Imaging Telescope Array (eROSITA; Predehl et al. 2021) and the *Mikhail Pavlinsky* Astronomical Roentgen Telescope–X-ray Concentrator (ART-XC; Pavlinsky et al. 2021), which operate in overlapping energy bands of 0.2–8 keV and 4–30 keV, respectively. ART-XC is a key component of the SRG mission because it provides a better

sensitivity than eROSITA at energies higher than 6 keV, which is particularly important for the systematic search for and exploration of absorbed X-ray sources. Together, the eROSITA and ART-XC all-sky surveys occupy a unique position in the parameter space of X-ray surveys performed thus far (see a recent review by Brandt & Yang 2022 and in particular Fig. 2 in that paper).

The SRG all-sky survey consists of repeat full scans of the sky, each lasting six months. The original plan was to conduct eight such scans. However, on February 26, 2022, the eROSITA telescope was switched to sleeping mode, and on March 7, 2022, the all-sky survey was interrupted in favor of a deep survey of the Galactic plane region with the ART-XC telescope (the Galactic plane and Galactic center regions had also been observed by SRG during the Calibration and Performance Verification phase in 2019, and the resulting catalogs of sources detected by ART-XC are presented by Karasev et al. 2023 and Semena et al. 2024a). This complementary survey was completed in October 2023, after which ART-XC resumed the all-sky survey. Hence, by early March 2022, the entire sky had been scanned by SRG four times, and about 40% of the sky had also been covered for a fifth time.

^{*} The catalog is only available in electronic form at the CDS via anonymous ftp to cdsarc.u-strasbg.fr (130.79.128.5) or via <http://cdsweb.u-strasbg.fr/cgi-bin/qcat?J/A+A/> and at <http://srg.cosmos.ru>.

^{**} E-mail: sazonov@cosmos.ru

¹ <http://srg.cosmos.ru>

After completion of the first two all-sky scans (December 2019–December 2020), we compiled a catalog of sources detected by ART-XC in the 4–12 keV energy band (ARTSS12; Pavlinsky et al. 2022)². It comprised 867 X-ray sources, of which nearly 10% are expected to be spurious due to the design of the catalog.

Here we present an updated version of this catalog, which is based on the entire dataset accumulated by SRG/ART-XC during the first ~ 4.4 all-sky surveys. The ART-XC survey significantly exceeds previous all-sky X-ray surveys carried out in similar energy bands in terms of the combination of angular resolution, sensitivity, and uniformity. Therefore, the presented catalog can be a valuable new source of information for studies of Galactic and extragalactic X-ray source populations.

2. Data analysis

During the all-sky survey, the optical axes of the ART-XC and eROSITA telescopes are rotating with a period of 4 hours around the spacecraft Z -axis, which is always pointed toward the Sun (this regime of observations is called “survey mode”). This provides full sky coverage every 6 months (see Sunyaev et al. 2021 for further details). The catalog of sources presented in this paper is based on the ART-XC data accumulated between December 12, 2019, and March 7, 2022, during the first four and the incomplete fifth all-sky surveys, hereafter referred to as ART-XC sky surveys 1–5, or ARTSS1-5 for short.

We only used ART-XC data that were obtained in survey mode and disregarded data acquired in other (scanning or pointing) observational regimes. We also excised those time intervals when the calibration sources were inserted into the collimators or when high voltage was switched off on the detectors for depolarization (Pavlinsky et al. 2021). As the background of the ART-XC detector has proved to be exceptionally stable (Pavlinsky et al. 2021), virtually no cleaning of the ART-XC X-ray data was necessary for periods of high background. Only events detected in one or two upper detector strips and in one or two lower strips³ were selected. Events detected in a larger number of strips were not used in the analysis because such events are much more likely to be charged particles than photons.

In constructing the ARTSS1-5 X-ray map and catalog of sources, we adopted largely the same approach as previously for ARTSS12. Therefore, we refer the reader to Pavlinsky et al. (2022) for a detailed description of the different stages of the data analysis. However, we introduced several novel aspects and modifications. In the following subsections, we describe these improvements and briefly outline the components of the analysis that have remained unchanged with respect to the previous version.

² Note that due to software issues all ARTSS12 source fluxes and survey flux limits reported in Pavlinsky et al. (2022) were underestimated by $\sim 30\%$.

³ The coordinate resolution of each ART-XC telescope module is provided by two mutually perpendicular sets of 48 strips on the two sides of a CdTe crystal. The strip width corresponds to an angular resolution of $45''$ (Pavlinsky et al. 2021).

2.1. Construction of maps

As in Pavlinsky et al. (2022), to construct all-sky maps, the ART-XC survey data were split into 4,700 overlapping 3.6×3.6 deg sky tiles in equatorial coordinates. For each tile, a set of standard maps were prepared, including an exposure map, particle and photon background maps, and sky images. All maps consist of 1024×1024 pixels of $12.66''$. The maps were prepared separately for each of the ART-XC surveys (1–5) and then combined. Exposure maps were corrected for vignetting.

Figure 1 shows the all-sky vignetting-corrected ARTSS1-5 exposure map in the 4–12 keV band. Due to the strategy of the SRG all-sky survey (Sunyaev et al. 2021), the accumulated exposure time is lowest near the ecliptic plane, where it varies between ~ 100 and ~ 300 s, and highest near the ecliptic poles, where it reaches ~ 38 ks.

2.2. Background estimation

The SRG/ART-XC data are essentially particle background-limited for sources near the detection threshold. As in Pavlinsky et al. (2022), the particle background was estimated using the data in a hard (30–70 keV) energy band, where the efficiency of the ART-XC X-ray optics vanishes. Because the particle background measured in the SRG orbit is extremely stable, apart from the gradual multiyear trend associated with the solar cycle activity and rare intense solar flares (see Fig. 2, based on data from the SRG Space Weather Monitor⁴), this method of background estimation is highly robust.

The cosmic X-ray background provides a negligible contribution ($\sim 3.4\%$ in the extragalactic sky) to the total background in the 4–12 keV energy band and, moreover, the cosmic X-ray background is highly uniform over the sky, except near the Galactic plane and within a few degrees of the Galactic center, where there is strong Galactic ridge X-ray emission (Revnivtsev et al. 2006). However, even in the innermost region of the Galaxy, the contribution of diffuse X-ray emission does not exceed 30% of the total background and thus has a small effect on the sensitivity to detection of point sources.

The residual background, associated with the uncertainty in particle background estimation and with large-scale X-ray structures in the sky (in particular, Galactic ridge X-ray emission), was assessed from the X-ray images themselves. To this end, the estimated particle background and the point spread function (PSF) models of all bright sources (with X-ray fluxes higher than $\sim 10^{-10}$ erg s⁻¹ cm⁻²) are subtracted from a given X-ray image, and then all significant details at angular scales smaller than $10'$ are eliminated from the X-ray image by wavelet decomposition (wvdecomp; Vikhlinin et al. 1998).

2.3. Detection of sources

We have introduced significant modifications to the source detection procedures compared to the ARTSS12 catalog (Pavlinsky et al. 2022). They are explained below. In constructing the ARTSS1-5 source catalog, we have focused on the detection of point sources, which constitute the vast majority of sources detected by ART-XC during the all-sky

⁴ <https://monitor.srg.cosmos.ru/>

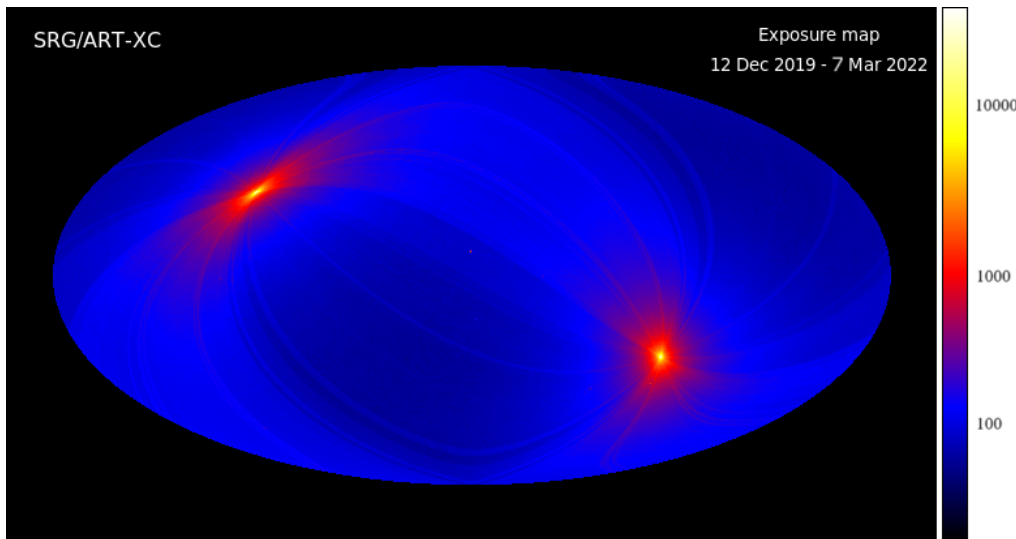


Fig. 1. ARTSS1-5 exposure map in Galactic coordinates in the 4–12 keV energy band, with vignetting corrected. The exposure time is given in seconds (see the color scale on the right-hand side).

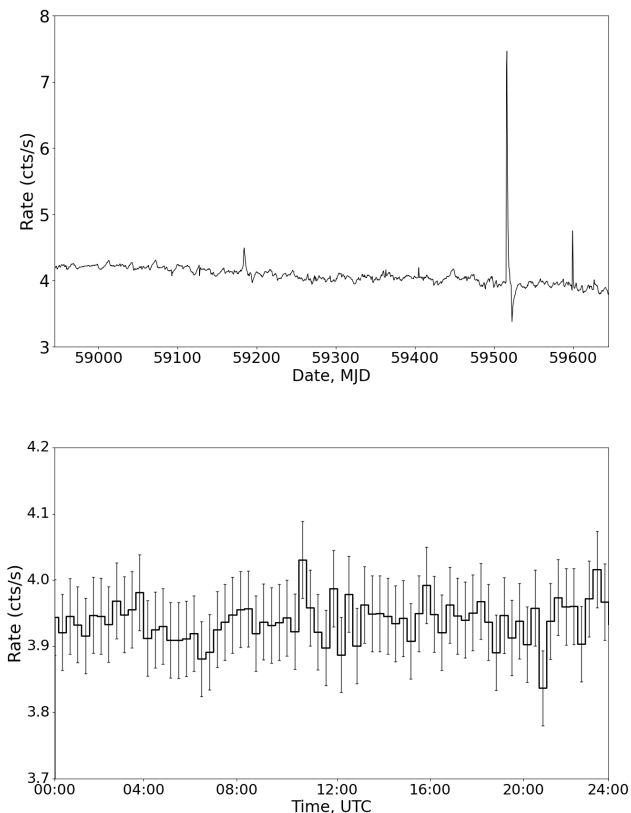


Fig. 2. Particle background measured by one of the ART-XC detectors in the 60–120 keV energy band over the course of the SRG all-sky survey (top panel) and on an arbitrary day of the survey (bottom panel, with the error bars showing the corresponding Poisson uncertainties). The few sharp variations visible in the long-term light curve are due to solar flares, and such short periods are excised from the data analysis.

survey. We made no attempt to consistently detect extended sources, such as clusters of galaxies or supernova remnants. Nevertheless, many extended sources are still detected with

our algorithms designed for the detection of point sources and are thus included in the resulting catalog. However, their estimated X-ray fluxes should be taken with caution.

2.3.1. Optimal matched filtering

In ART-XC X-ray images, the noise statistics is close to the Poisson distribution in most cases, and the PSF and vignetting strongly vary across the field of view. We thus adopted the following optimal matched filter, which maximizes the probability of detecting real sources and minimizes the probability of spurious detections of statistical fluctuations:

$$\Phi(x) = \ln \left[\frac{f(e)v(x,e)p_s(g)}{b(x,e)p_b(g)} P(x_0|x) + 1 \right]. \quad (1)$$

Here, x_0 are the photon coordinates, e is the photon energy, $f(e)$ is the expected spectral energy distribution of X-ray sources, $v(x,e)$ is the vignetting function, $b(x,e)$ is the spectral brightness of the background as a function of coordinates and energy, $p_s(g)$ and $p_b(g)$ are the probability distributions of observed event grades (see below) for source photons and background events, respectively, and $P(x_0|x)$ is the PSF value at x_0 under the assumption that the source is located at x .

The optimal matched filter given by Eq. (1) thus depends on the energy of every photon, expected source flux, and estimated background at every position in the image. It is applied to ART-XC data on an event-by-event basis. We derived this filter as a further development of the Poisson optimal matched filter described in previous works (Lynx X-ray Observatory Concept Study Report 2019; Ofek & Zackay 2018; Pavlinsky et al. 2022; Semena et al. 2024b).

The effective energy band of ART-XC in survey observational regime is 4–12 keV, with sensitivity dropping dramatically below 4 keV and above 12 keV. However, because of the finite spectral resolution (FWHM \sim 1.3 keV), a significant fraction of photons with intrinsic energies \sim 4 keV are registered as events with energies between 3 and 4 keV. For this reason, we used the energy range 3 to 12 keV for the detection of sources.

We adopted the same ART-XC vignetting function, PSF model, and source spectral shape (namely, a power law with photon index $\Gamma = 1.4$) as in our previous work (Pavlinisky et al. 2022). In particular, we refer the reader to Sect. 2.3 of Pavlinisky et al. (2022) as well as to Krivonos et al. (2017) and Pavlinisky et al. (2021) for further details on ART-XC PSF calibration and modeling. In particular, Figs. 12-14 in Pavlinisky et al. (2021) illustrate the behavior of the PSF at different offset angles and energies. We note that the current PSF model does not take into account the dependence on photon energy. This dependence is only significant in the distant wings of the PSF and is thus more important for offset pointing observations than for the all-sky survey. As regards the background spectrum, we adopted an actually measured spectrum, which was obtained by averaging over the whole set of all-sky survey data.

Each event registered by the ART-XC detectors is characterized by a “grade” of 0, 1, 2, 3, and so on, which refers to a particular detection pattern in the 3×3 pixel area where the event has been registered. The probability of being detected with a given grade is different for photons and charged particles. For example, an event detected in three pixels is most probably a charged particle. We determined the probability distributions $p_s(g)$ and $p_b(g)$ for X-ray sources and background events based on real data of the ART-XC all-sky survey.

To determine the flux-to-background ratio involved in the calculation of the optimal matched filter (Eq. 1), we assumed that point sources have a diameter of $90''$. This region contains approximately 95% of the photons from a source observed at an offset of less than $10'$, whereas source photons detected from larger offsets are included in the background. The PSF large-angular-scale wings of very bright X-ray sources are also added to the background at this stage. We then adopted the source flux within the $90''$ diameter aperture that corresponds to a Poisson detection significance of 4.5 for a given background level and substitute this flux for $f(e)$ in Eq. (1). The filter thus defined is close to optimal for detecting faint sources (with Poisson detection significance $\gtrsim 4.5$). For brighter sources, this filter is not optimal but such sources will also be detected with confidence with this filter (see section A.3.2 in [Lynx X-ray Observatory Concept Study Report 2019](#)). The filter is only weakly sensitive to the choice of a fiducial source flux.

Sources are detected in images that are obtained by convolution of raw photon images with the optimal filter given by Eq. (1) as peaks above some low threshold. Figure 3 shows an example of a raw image and the resulting “convolution image”; the latter clearly reveals the presence of an X-ray source. Specifically, we adopted a threshold that yielded a raw catalog of nearly 7000 sources, most of them presumably being spurious detections. At a later stage of the analysis (see below), we adopted a significantly higher threshold, specified in terms of maximum likelihood detection significance and determined by the desired (low) fraction of spurious detections, to construct the final catalog of sources.

In the case of multiple detections within $52''$ of each other, that is, within a distance smaller than the ART-XC PSF full width at half maximum (FWHM; Pavlinisky et al. 2021), only the highest peak in the convolution image is taken into account (with the corresponding coordinates and amplitude).

2.3.2. Maximum likelihood fitting

For all the sources detected with optimal matched filtering technique, we performed a maximum likelihood (ML) fit using the following logarithmic likelihood function (Cash 1979):

$$-2 \ln L = 2 \left(\sum_i \ln m_i - \int m \right), \quad (2)$$

where the sum is taken over all the detected events, and the source plus background model is taken as follows:

$$m(x, e, g) = \sum_j [f(e)v(x, e)p_s(g)P(x_0|x) + b(x, e)p_b(g)]_j. \quad (3)$$

Here, the sum is taken over closely located sources, namely within $5.2'$ of each other. To fit the model, we used the data within $2.6'$ of each source; for closely located sources, these data regions were merged. We simultaneously fit the fluxes and coordinates of all sources in the given data region. With this likelihood function, the ART-XC PSF and vignetting models as well as information on the event grades are self-consistently taken into account. In reality, the vast majority of sources in the ARTSS1-5 catalog were fitted separately. The data regions of two or more sources were merged only in a very small number of cases, because the typical flux threshold for the catalog is much higher than the effective confusion limit.

Sources were sorted by their X-ray fluxes. The brighter ones were fitted first, and their PSF model was then added to the background, including the PSF wings at large angular scales, up to $\approx 50'$. The significance of source detection, that S/N, is calculated from the difference of the logarithmic likelihood function between the best-fit and zero fluxes. The flux and position errors are calculated from the appropriate variation in $-2 \ln L$, by varying the parameter of interest with all other parameters frozen at their best fit values.

2.3.3. Monte Carlo simulations

To specify thresholds for source detection in convolution images and validate the detection significance obtained by ML fitting, we carried out Monte Carlo simulations of empty fields. Only the particle background was simulated, because it strongly dominates the ART-XC background. Specifically, we computed the expected number of peaks of a given amplitude per square degree in the convolution image of an empty field for different background levels and obtained ML fits for all detected peaks.

Figure 4 shows the expected number of spurious sources per square degree, f_{sp} , as a function of ML detection significance. There is only a weak dependence on the background.

2.4. Merging sky tiles and calibration of source fluxes

Using the procedures described above, we obtained catalogs of sources detected in each sky tile. We then merged these individual catalogs into a composite all-sky catalog, taking the overlap of tiles into account. Specifically, sources that are located closer than $3'$ to the tile edge were rejected and if a source was detected in two or more tiles, the detection at the larger distance from the tile edge was selected. Figure 5

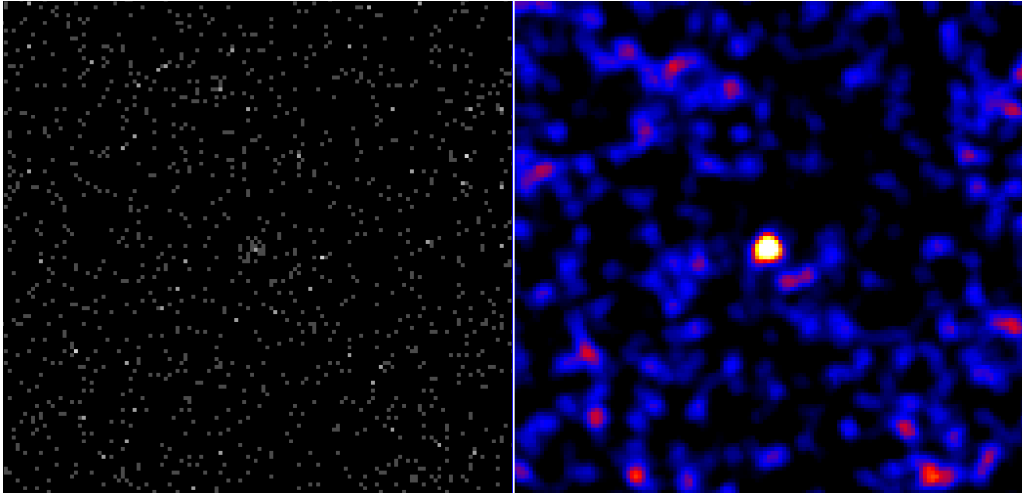


Fig. 3. Example of a detection of a faint source using the optimal matched filter given by Eq. (1). *Left:* Raw photon image in the 4–12 keV energy band. *Right:* Convolution with the filter. The size of the images is approximately $25' \times 25'$.

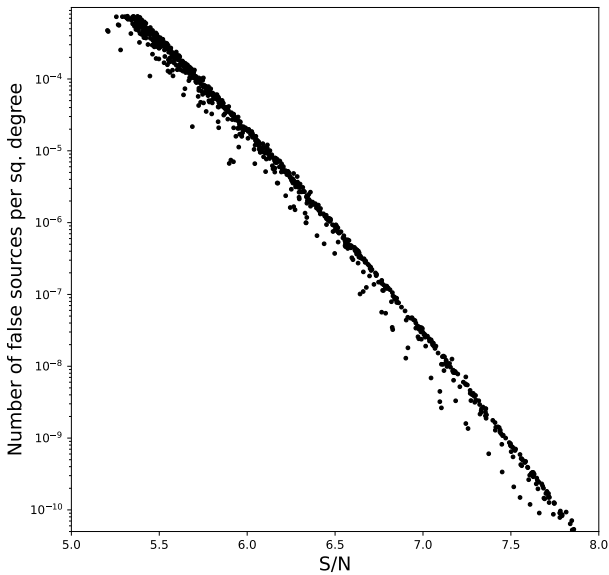


Fig. 4. Correlation between the S/N and the expected number of spurious source detections per square degree obtained via simulations of empty fields. The observed scatter reflects a weak dependence on the background.

shows an example of a merged convolution image of a large, crowded region of the sky near the Galactic center.

As was described above, the ML fitting procedure provides the fluxes of detected sources and the corresponding errors. We calibrated the energy flux to count rate conversion factor for the 4–12 keV energy band using the available ART-XC observations of the Crab nebula (see Pavlinsky et al. 2022 for details). This coefficient in general depends on the adopted procedure of selecting various types of ART-XC detector events. For the criteria adopted in this work, a count rate of 1 cnt s^{-1} corresponds to a flux of $4.0 \times 10^{-11} \text{ erg cm}^{-2} \text{ s}^{-1}$ in the 4–12 keV energy band. This takes into account the difference between the slopes of the fiducial source spectrum adopted in this work

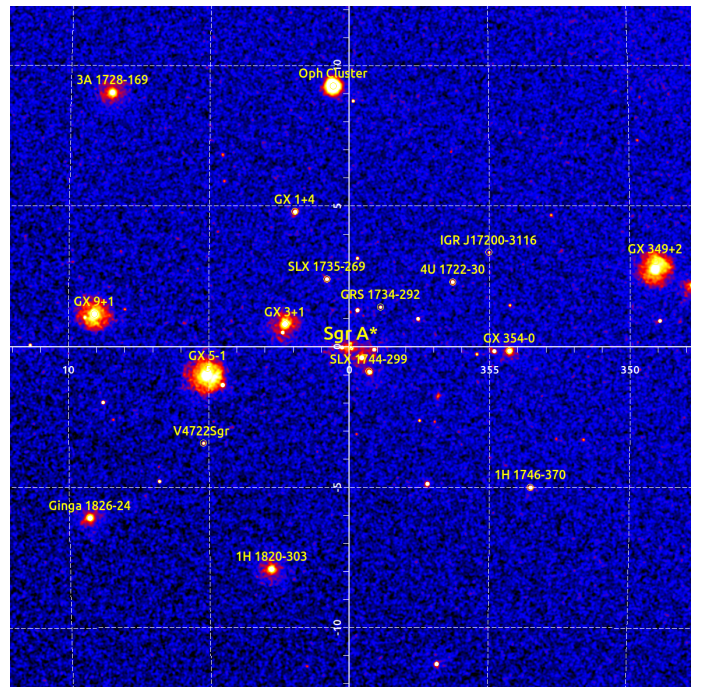


Fig. 5. Image of a $25^\circ \times 25^\circ$ region of the sky near the Galactic center in the 4–12 keV energy band, obtained by convolving the raw photon images with the optimal matched filter, in Galactic coordinates. Some bright sources are labeled. The faintest sources in this region that have been included in the ARTSS1-5 catalog have fluxes $\sim 3 \times 10^{-12} \text{ erg s}^{-1} \text{ cm}^{-2}$.

($\Gamma = 1.4$) and the Crab spectrum ($\Gamma = 2.1$). The energy flux to count rate conversion factor only weakly depends on the spectral shape, namely it varies by less than 4% for Γ between 1.4 and 2.1 and for line-of-sight absorption column densities up to $N_{\text{H}} = 10^{23} \text{ cm}^{-2}$. This is comparable to current uncertainties in the instrument’s calibration.

3. Construction of the final catalog

To construct the final source catalog, we adopted a threshold of $f_{\text{sp}} = 7.475 \times 10^{-4}$ spurious sources per square degree, which typically corresponds to an ML detection significance

limit of $S/N \approx 5.3$ (see Fig. 4). At this f_{sp} threshold, the total number of detected sources is 1545, with 2% of them expected to be spurious.

3.1. Identification and classification of ART-XC sources

For identification of ARTSS1-5 sources, we carried out the same kind of analysis as previously for the ARTSS12 catalog (Pavlinisky et al. 2022). Namely, we cross-correlated the ARTSS1-5 catalog with the SIMBAD Astronomical Database (Wenger et al. 2000), the NASA/IPAC Extragalactic Database⁵ (NED), and the X-ray astronomy database provided by the High Energy Astrophysics Science Archive Research Center (HEASARC). We further searched for possible counterparts in catalogs of optical, infrared (IR), and radio all-sky surveys, in particular *Gaia* Data Release 3 (*Gaia* DR3, *Gaia* Collaboration et al. 2023), the Sloan Digital Sky Survey (SDSS; Ahumada et al. 2020), the 6dF Galaxy Survey (Jones et al. 2009), the DECam Plane Survey (DECaPS; Schlafly et al. 2018), the Wide-field Infrared Survey Explorer (WISE) observatory’s AllWISE (Cutri et al. 2021) and CatWISE2020 (Marocco et al. 2021) catalogs, the Very Large Array (VLA) Faint Images of the Radio Sky at Twenty-Centimeters Survey (FIRST; Helfand et al. 2015), the National Radio Astronomy Observatory (NRAO) VLA Sky Survey (NVSS; Condon et al. 1998), the Sydney University Molonglo Sky Survey (SUMSS; Mauch et al. 2003), and the Very Large Array Sky Survey (VLASS; Gordon et al. 2021).

The search for counterparts was conducted within the 98%-confidence error radii (R_{98}) of ARTSS1-5 sources, which does not exceed 30" even for the lowest S/N detections, and within some margin outside these regions. In most cases, the positional precision provided by ART-XC enables a straightforward selection of a likely counterpart. Often, previous detections in soft X-rays provide a significantly better localization, which further facilitated this selection. The resulting identifications and classifications as well as redshifts for extragalactic sources were adopted from SIMBAD and/or NED in most cases.

In cases of dubious identification or classification and for recently or newly discovered X-ray sources, we used additional information from the literature, from our multiwavelength cross-correlation analysis and our optical follow-up campaign (see below). Various photometric (and spectroscopic if available) signatures were taken into account. In particular, the presence of an extended optical object, an IR source with $W1 - W2 \gtrsim 0.5$ (the color provided by WISE, Assef et al. 2013), or a radio source usually indicate an active galactic nucleus (AGN) origin, whereas the presence of a bright star suggests a Galactic nature. All nontrivial cases are discussed on a source by source basis in Appendix A. If the identification and/or classification of a given ARTSS1-5 source is not robust, we denote such information as tentative in the catalog.

3.2. Follow-up optical program

Since the beginning of the SRG all-sky survey in December 2019, we have been conducting an extensive program of

⁵ The NASA/IPAC Extragalactic Database is funded by the National Aeronautics and Space Administration and operated by the California Institute of Technology.

optical spectroscopy of X-ray sources that have either been discovered by ART-XC or were known as X-ray sources from previous missions but have remained unidentified so far. This follow-up campaign is focused on the northern sky ($\text{Dec} > -25^\circ$) and is mostly implemented using two telescopes: the Sayan observatory’s 1.6 m telescope (AZT-33IK; Burenin et al. 2016), operated by the Institute of Solar-Terrestrial Physics of the Siberian branch of the Russian Academy of Sciences, and the Russian-Turkish 1.5 m telescope (RTT-150), operated jointly by the Kazan Federal University, the Space Research Institute (IKI, Moscow), and the TÜBİTAK National Observatory (TUG, Turkey).

This program has already allowed us to identify and classify ~ 60 AGN and several cataclysmic variables (Zaznobin et al. 2021, 2022a; Uskov et al. 2022, 2023, 2024). In addition, the ARTSS1-5 catalog includes a number of Galactic X-ray transients that were discovered during the SRG all-sky survey by eROSITA and/or ART-XC and later followed up in the optical (e.g., Mereminskiy et al. 2022; Schwöpe et al. 2022). We took such information into account when assigning identifications and classes to ARTSS1-5 sources.

4. Source catalog

We provide the following information for each source in the ARTSS1-5 catalog:

Column (1) “Id”: The sequence number of the source in the catalog.

Column (2) “Name”: The name of the source in the catalog (prefix “SRGA” followed by the source coordinates).

Columns (3 and 4) “RA, Dec”: The equatorial coordinates (J2000).

Column (5) “R98”: The statistical position uncertainty at 98% confidence.

Columns (6) “S/N”: The significance of the detection.

Column (7) “Flux”: The flux in the 4–12 keV energy band and the corresponding 1σ uncertainty.

Column (8) “Conventional name”: The conventional name of the source, if available.

Column (9) “Redshift”: The cosmological redshift for extragalactic objects if known.

Column (10) “Class”: The astrophysical class of the object: low- or high-mass X-ray binary (LMXB or HMXB); X-ray binary of uncertain type (X-RAY BINARY); cataclysmic variable or symbiotic binary (CV); ultra-luminous X-ray source (ULX); supernova remnant (SNR); supernova remnant with a central pulsar, when both may contribute to the X-ray emission (SNR/Pulsar); magnetar (MAGNETAR); stellar object, excluding the explicitly mentioned types (STAR); star-forming region (SFR), AGN of the Seyfert or, rarely, LINER type (SEYFERT); unclassified AGN (AGN); beamed AGN (BLAZAR); BL Lac or flat-spectrum radio quasar); cluster of galaxies (CLUSTER); and unclassified source (UNIDENT). A question mark indicates that the quoted classification is tentative (see the comments on these cases in Appendix A).

Building on our previous experience of constructing catalogs of sources detected in all-sky X-ray surveys (e.g., Revnivtsev et al. 2004; Krivonos et al. 2022; Pavlinisky et al. 2022), we restricted ourselves to providing a single conventional name for previously known ARTSS1-5 sources. To this end, we prefer to indicate the X-ray observatory and/or survey that discovered a given source (e.g., 4U or 2RXS). However, this is often difficult to do, as two or more

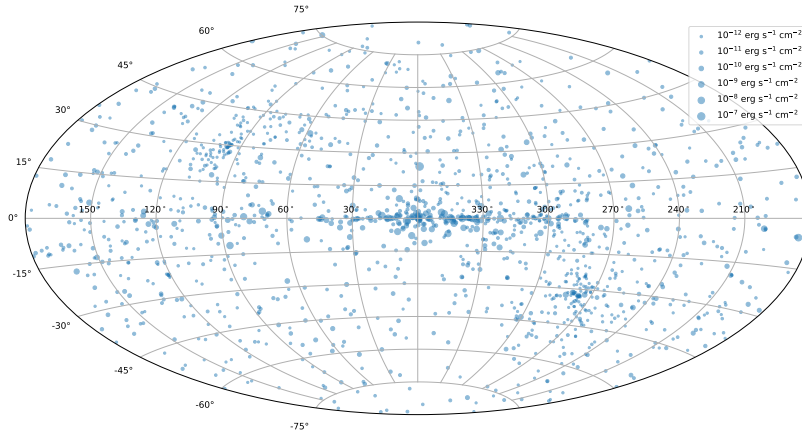


Fig. 6. Positions in Galactic coordinates of the X-ray sources detected by ART-XC in the 4–12 keV energy band during ARTSS1-5. The size of the symbol reflects the X-ray brightness of a source, as indicated in the legend.

surveys and/or teams, for example the Burst Alert Telescope (BAT) on board the *Neil Gehrels Swift* Observatory and the Imager on-Board the INTEGRAL Satellite on board the INTERNational Gamma-Ray Astrophysics Laboratory (INTEGRAL/IBIS), may have reported the detection of the same source at about the same time. Moreover, many objects were originally known from optical or radio observations rather than from X-ray observations, so in such cases we usually use the optical or radio name (e.g., NGC or 3C). There are further subtleties. In particular, when referring to a source discovered during the ROSAT all-sky survey, we prefer to use the name (2RXS) from the (latest) second catalog (Boller et al. 2016). However, occasionally we use a shorter (RX or RBS) name if a source is well known under this name from the literature.

Figure 6 shows the positions of the ARTSS1-5 sources on the sky. The size of the symbols indicates the X-ray brightness of sources.

4.1. Source counts and survey sensitivity

Figure 7 shows the cumulative and differential flux distributions of the ARTSS1-5 sources in the 4–12 keV energy band. The median flux is $4.9 \times 10^{-12} \text{ erg s}^{-1} \text{ cm}^{-2}$.

Figure 8 shows the distribution of the ARTSS1-5 sources on the ecliptic latitude–X-ray flux diagram. This plot highlights how the sensitivity of the ART-XC all-sky survey monotonically increases from $\sim 4 \times 10^{-12} \text{ erg s}^{-1} \text{ cm}^{-2}$ near the ecliptic plane (at $|b_{\text{ecl}}| < 30^\circ$) to $\sim 7 \times 10^{-13} \text{ erg s}^{-1} \text{ cm}^{-2}$ near the ecliptic poles (at $|b_{\text{ecl}}| > 82^\circ$). The quoted values are the median fluxes of the sources detected near the detection threshold, namely at $5.3 < S/N < 6$. An accurate calculation of the sensitivity map of the survey and the completeness of detection of sources as a function of their flux will be presented elsewhere (Burenin et al., in prep.).

4.2. Source classes

Table 1 summarizes the statistics of objects of various classes in the ARTSS1-5 catalog. We have managed to identify 1463 out of the 1545 sources. Of these 1463, 174 are tentative

Table 1. Statistics of the ARTSS1-5 sources by location in the Universe and by type (including tentative classifications).

Category and type	Count
Galactic	469
LMXB	97
HMXB	84
X-ray binary	2
CV	192
magnetar	7
star	66
SNR, SNR/Pulsar	17
star-forming region	2
unclassified	2
The Local Group	30
galaxy	1
LMXB	3
HMXB	19
X-ray binary	1
ULX	1
SNR and SNR/Pulsar	5
Extragalactic	964
galaxy cluster	48
Seyfert or LINER	619
blazar	196
unclassified AGN	96
galaxy	1
ULX	4
unidentified	82

identifications, which is to say that for them there is a likely optical/IR counterpart but follow-up observations are needed to ascertain or improve their classification. The majority of the identified objects (66%) are extragalactic, a small fraction (2%) are located in the Local Group of galaxies (namely, in the Large Magellanic Cloud, the Small Magellanic Cloud, M31, and M33), and 32% are of Galactic origin. The largest groups within the Galactic category are CVs (including symbiotic binaries), LMXBs, and HMXBs. The extragalactic objects are dominated by Seyfert galaxies and blazars.

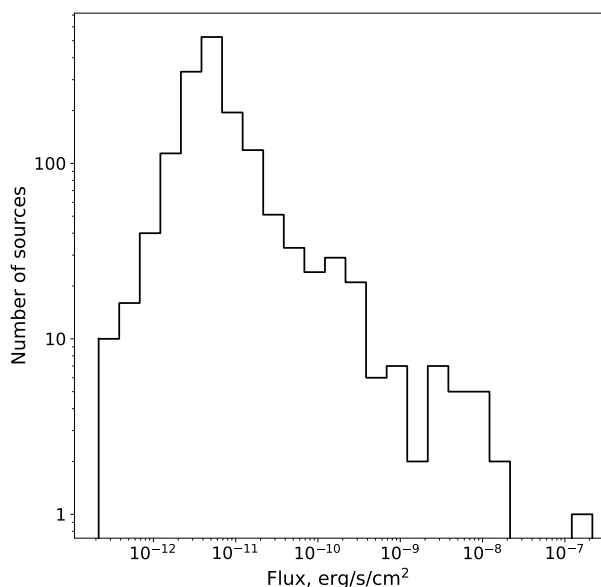
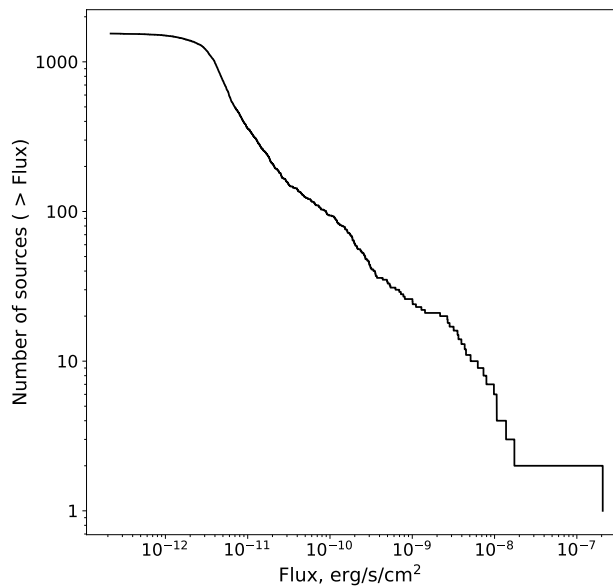


Fig. 7. Cumulative (top) and differential (bottom) flux distributions of the ARTSS1-5 sources.

Extended astrophysical objects such as SNRs and clusters of galaxies are expected to be significantly underrepresented in the ARTSS1-5 catalog (for the adopted flux threshold) because our search algorithm is designed for the detection of point X-ray sources. For example, such famous objects as the Coma and Virgo clusters of galaxies are not present in the catalog due to the huge size they subtend on the sky, despite them being bright X-ray sources.

Eighty-four sources in the catalog, or $\sim 5\%$ of all sources, remain unidentified; of these 84 sources, $\sim 30 \pm 6$ are expected to be spurious X-ray detections. The majority of the unidentified sources (62) were discovered by ART-XC. The

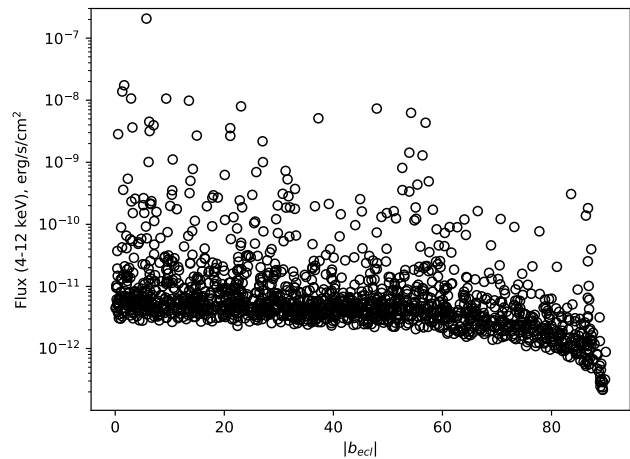


Fig. 8. Fluxes of the ARTSS1-5 sources as a function of ecliptic latitude.

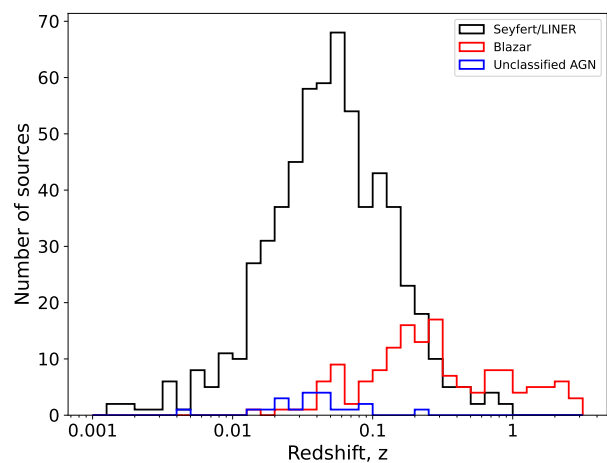


Fig. 9. Redshift distribution of the AGN in the ARTSS1-5 catalog: Seyfert galaxies (black), blazars (red), and unclassified AGN (blue).

total number of new X-ray sources in the ARTSS1-5 catalog (including the identified ones) is 158.

Figure 9 shows the redshift distribution of the AGN. The median redshift of the un-beamed (i.e., excluding blazars) AGN is 0.05, and it is 0.25 for the blazars. The redshifts are still missing for 129 AGN and AGN candidates in the ARTSS1-5 catalog.

4.3. Localization accuracy

As already mentioned, we evaluated the statistical uncertainties of source positions using ML fitting. Figure 10 shows the resulting R_{98} uncertainties as a function of S/N for the ARTSS1-5 sources. There is a clear correlation between these quantities, which can be approximately described as

$$R_{98} \approx 89'' \left(\frac{S}{N} \right)^{-0.84}. \quad (4)$$

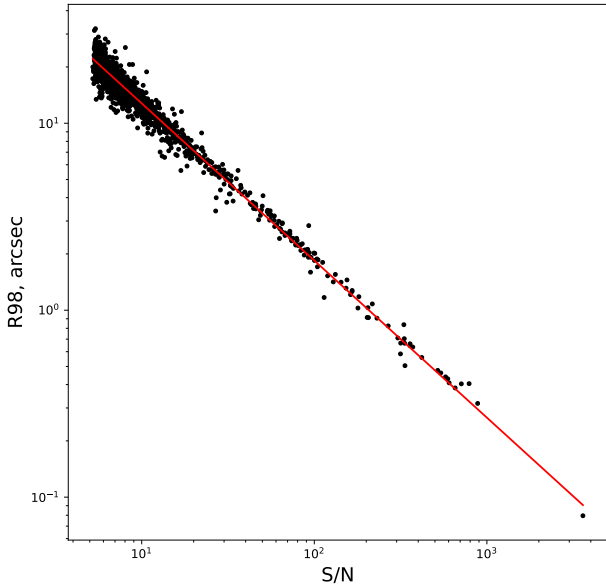


Fig. 10. Statistical position uncertainties of the ARTSS1-5 sources as a function of their detection significance. The solid line shows the approximate relation between these quantities given by Eq. (4).

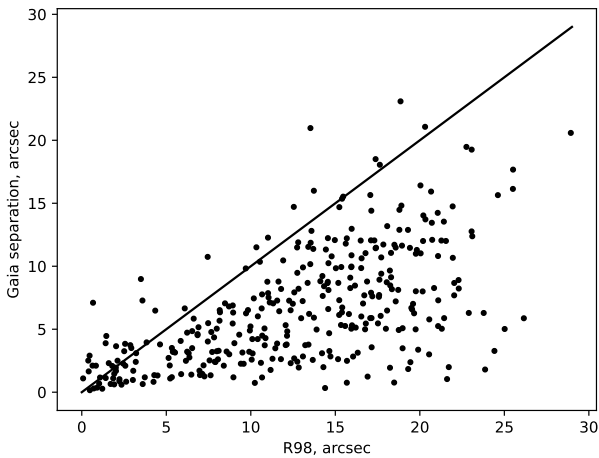


Fig. 11. Offsets between the positions of ARTSS1-5 sources and their *Gaia* DR3 counterparts versus the 98%-confidence statistical error radii of the X-ray positions. The diagonal line shows the 1:1 relation.

The median statistical position uncertainty is $R_{98} = 16.1''$, while for 90% of the ARTSS1-5 sources $R_{98} < 22.3''$.

There can also be some systematic uncertainties associated with the determination of source positions. To estimate these, we selected those ARTSS1-5 sources that can be reliably associated with a point-like Galactic object and have an optical counterpart in the *Gaia* DR3 catalog, and compared their ART-XC and *Gaia* positions. In total, 346 objects were included in this analysis. Figure 11 shows the X-ray–optical offsets versus the 98%-confidence statistical position errors (R_{98}) for the test subsample. The fraction of outliers

($S > R_{98}$), 10%, exceeds the 2% expected for the purely statistical uncertainty. Most of these outliers are associated with bright X-ray sources, for which R_{98} is just a few arcseconds. From this comparison, we can estimate a typical systematic positional uncertainty for the ARTSS1-5 catalog at $R_{\text{syst}} \approx 7''$, so that the total error radii of ARTSS1-5 sources can be crudely estimated as $\sqrt{R_{98}^2 + R_{\text{syst}}^2}$.

4.4. Cross-match with external X-ray and gamma-ray source catalogs

Most of the objects in the ARTSS1-5 catalog were known as X-ray sources before. We cross-correlated the catalog with a number of all-sky or nearly all-sky X-ray and gamma-ray surveys: the second ROSAT all-sky survey (2RXS; [Boller et al. 2016](#)), the *XMM-Newton* slew survey (XMMSL2; [Saxton et al. 2008](#), table XMMSLEWCLN in HEASARC), the combined Monitor of All-sky X-ray Image/Gas Slit Camera (MAXI/GSC) 7-year all-sky source catalog (3MAXI; [Kawamuro et al. 2018](#); [Hori et al. 2018](#), table MAXIGSC7YR in HEASARC), the *Swift*/BAT 105-month all-sky survey (hereafter, Swift105mo; [Oh et al. 2018](#)), the INTEGRAL/IBIS 17-year all-sky survey (hereafter, INT17yr; [Krivonos et al. 2022](#)), and the *Fermi* Gamma-ray Space Telescope/Large Area Telescope (*Fermi*/LAT) 14-year all-sky survey (4FGL-DR4; [Abdollahi et al. 2022](#); [Ballet et al. 2023](#)).

We took into account those matches where the angular separation between an ARTSS1-5 source and a source from an external catalog was less than the sum of the corresponding 98% error radii (R_{98}). For ARTSS1-5, we added in quadrature a systematic error of $10''$ (slightly larger than was estimated in Section 4.3, to be on the safe side) to the statistical errors. The R_{98} values for the external catalogs were computed, assuming a two-dimensional Gaussian probability distribution, from the diverse positional uncertainties provided by these catalogs. Specifically, 2RXS reports 1σ positional errors (σ_x and σ_y) on image coordinates, while XMMSL2 and 3MAXI provide 1σ error radii (R_{68})⁶. For Swift105mo and INT17yr, we estimated R_{68} based on the detection significance of sources, following [Oh et al. \(2018\)](#) and [Krivonos et al. \(2007\)](#), respectively. The 4FGL-DR4 catalog provides the semimajor and semiminor axes of 95%-confidence ellipsoidal localization regions; for simplicity, we converted these into 95%-confidence error radii (R_{95}) corresponding to circles of the same area, and also excluded extended 4FGL-DR4 sources.

We have found 4, 4, and 2 cases where two ART-XC sources are blended into one INT17yr, Swift105mo, and 4FGL-DR2 source, respectively. We counted each of these cases as two matches. All of these associations except for two are located in crowded regions of the sky, such as the Galactic plane, Galactic center, and nearby galaxies (Large Magellanic Cloud, M31, and NGC 4945), where high angular resolution is required to resolve individual X-ray sources. Additionally, there are 98 cases where two or more XMMSL2 sources are found within the match region around an ARTSS1-5 source. We regarded each such group as a single match. Most of these cases appear to be caused by im-

⁶ For a number of 3MAXI sources at low Galactic latitudes without a reported position error in [Hori et al. \(2018\)](#), we estimated R_{68} as $80'/S_{\text{det}, 4-10}$, where $S_{\text{det}, 4-10}$ is the MAXI/GSC source detection significance in the 4–10 keV band.

perfect merging of individual *XMM-Newton* slew detections into “unique sources” in the XMMSL2 catalog.

Table 2 provides the results of the cross-matching analysis. The largest overlap of the ARTSS1-5 catalog is observed with the 2RXS, XMMSL2, and Swift105mo catalogs. The vast majority of these associations must be real. To estimate the number of spurious matches, we shifted the positions of the ART-XC point sources in random directions by $45'$ and repeated the cross-matching analysis; we ran many such simulations for each external catalog. The chosen offset is small compared to both the effective angular scale height of the Galactic population of X-ray sources and the effective size of the ART-XC deep fields near the ecliptic poles. On the other hand, it is much larger than the positional uncertainties of the vast majority of sources in the external catalogs under consideration, except for a few sources in the 3MAXI and 4FGL-DR4 catalogs. To take these exceptional sources into account, we excluded from the count of spurious matches those few cases where an ARTSS1-5 source was linked with the same 3MAXI or 4FGL-DR4 source before and after applying the positional shift (such associations can be real, rather than spurious). In the last column of Table 2, we provide the estimated numbers of spurious matches with the external catalogs.

Of the 1545 ARTSS1-5 sources, 194 have not been detected in any of the six all-sky surveys on our list. Taking into account that the ARTSS1-5 catalog allows for the presence of $\sim 2\%$ of spurious detections (i.e., $\sim 30 \pm 6$ sources), we can conclude that ~ 160 real sources are unique to the ARTSS1-5 catalog among the known all-sky X-ray and gamma-ray catalogs.

No strong trends are apparent in the statistics of cross-identifications with external X-ray source catalogs in terms of celestial position or source class. Specifically, we compared the relative fraction of cross-matches of ARTSS1-5 sources with the 2RXS, XMMSL2, and Swift105mo catalogs (i) near and outside the Galactic plane ($|b| < 10^\circ$ versus $|b| > 10^\circ$) and (ii) for Galactic versus extragalactic sources (according to Table 1), and the resulting numbers differ just by several per cent for each of the mentioned external catalogs. In particular, for 2RXS, the largest difference in the relative (with respect to ARTSS1-5) fraction of cross-matches is found between Galactic and extragalactic sources: 57.4% versus 69.0%, whereas for Swift105mo the largest difference is observed between the $|b| < 10^\circ$ and $|b| > 10^\circ$ samples, namely 61.7% versus 49.8% (for XMMSL2 the variations are yet smaller). It is difficult to interpret this information, because all these surveys differ significantly in their spectral response and coverage of the sky (except for 2RXS, whose exposure map is skewed toward the Ecliptic poles as for SRG/ART-XC) and, moreover, XMMSL2 has not covered the whole sky. However, intrinsic variability, spectral hardness, and line-of-sight absorption (both intrinsic and Galactic) certainly play key roles in this statistics.

We note that all of the surveys considered here, except for 2RXS, were conducted over periods of at least 8 years but some of them (in particular, XMMSL2) are characterized by a low duty cycle. For comparison, the ARTSS1-5 catalog is based on a relatively short period of 2.3 years of nearly continuous scanning of the sky, characterized by a duty cycle of more than 97%.

4.5. Ecliptic poles

Longer exposures were carried out for the regions around the ecliptic poles compared to other fields during the ART-XC all-sky survey (see Fig. 1), and it is interesting to examine the composition of the X-ray source samples detected in these “deep surveys.” Specifically, we focus our attention on the regions $b_{\text{ecl}} > 82^\circ$ and $b_{\text{ecl}} < -82^\circ$, with an area of ≈ 200 square degrees each, around the north and south ecliptic poles (NEP and SEP), respectively. For the adopted detection significance threshold, the expected number of spurious sources in the combined NEP–SEP sample is ~ 0.3 (i.e., this sample is expected to be highly pure).

There are 49 ARTSS1-5 sources, with fluxes down to $\sim 2 \times 10^{-13} \text{ erg s}^{-1} \text{ cm}^{-2}$, in the NEP field. The majority of them (44) were known as X-ray sources before and 5 sources have been discovered by ART-XC. These five sources proved to be AGN, based on our follow-up optical spectroscopy program (in addition, we identified via optical spectroscopy 3 AGN among the previously known X-ray sources). Most of the NEP sample are extragalactic sources: 3 galaxy clusters and 41 AGN (including candidates). There are also 5 Galactic objects: 3 CVs and 2 coronally active stars.

The SEP region contains 60 ARTSS1-5 sources, with fluxes down to $\sim 3 \times 10^{-13} \text{ erg s}^{-1} \text{ cm}^{-2}$, including nine X-ray sources discovered by ART-XC. One-third of the SEP sample (20 objects) are X-ray binaries and SNRs residing in the Large Magellanic Cloud. Most of the remaining sources are extragalactic: one galaxy cluster and 33 AGN (including candidates). There are also five Galactic objects (three CVs and CV candidates, one HMXB, and one star), and one unclassified object. As expected, the AGN detected in the NEP and SEP fields are on average more distant than those found elsewhere, with the most distant un-beamed AGN located at $z \sim 0.9$.

5. Discussion and summary

We have updated the catalog of sources detected by the ART-XC telescope during the SRG all-sky survey by adding data from the third, fourth, and the $\sim 40\%$ complete fifth half-year scans of the sky to the data of the first two scans on which the previous version of the catalog (ARTSS12, Pavlinsky et al. 2022) was based. The new catalog comprises 1545 sources detected in the 4–12 keV energy band. The achieved sensitivity ranges between $\sim 4 \times 10^{-12} \text{ erg s}^{-1} \text{ cm}^{-2}$ near the ecliptic plane and $\sim 7 \times 10^{-13} \text{ erg s}^{-1} \text{ cm}^{-2}$ near the ecliptic poles. The new ART-XC catalog is ~ 1.3 – 1.5 times deeper than the previous one. The sensitivity as a function of celestial coordinates will be evaluated more accurately elsewhere (Burenin et al., in prep.), based on extensive numerical simulations of the survey.

Just a few all-sky or nearly all-sky surveys have been conducted in similar medium X-ray bands (i.e., at energies ~ 2 – 20 keV). In particular, the HEAO-1 experiment A2 performed a survey of the extragalactic sky ($|b| > 20 \text{ deg}$) in the 2–10 keV energy band (Piccinotti et al. 1982), the *Rossini* X-ray Timing Explorer (RXTE) Slew Survey (XSS) covered the $|b| > 10^\circ$ sky in the 3–20 keV band, and the MAXI/GSC all-sky survey (3MAXI) covered the entire sky in the 4–10 keV band (Kawamuro et al. 2018; Hori et al. 2018). All these surveys had much lower angular resolutions ($\sim 1^\circ$) compared to ARTSS1-5, which led to source confusion in crowded regions of the sky and complicated the identification

Table 2. Cross-match of the ARTSS1-5 sources with selected X-ray and gamma-ray source catalogs.

X-ray survey	Energy band	Reference	Cross-matches	Spurious matches ^{a)}
ROSAT (2RXS) 1 year	0.1–2.4 keV	Boller et al. (2016)	960	4.5 (2–7)
<i>XMM-Newton</i> slew	0.2–12 keV	Saxton et al. (2008)	874	1.8 (< 4)
MAXI/GSC 7 years	4–10 keV	Kawamuro et al. (2018); Hori et al. (2018)	286	5.6 (3–9)
<i>Swift</i> /BAT 105 months	14–195 keV	Oh et al. (2018)	785	5.8 (3–8)
INTEGRAL 17 years	17–60 keV	Krivonos et al. (2022)	504	4.5 (2–7)
<i>Fermi</i> /LAT 14 years	50 MeV–1 TeV	Abdollahi et al. (2022)	222	23.8 (18–30)

^{a)} Expected value of spurious matches and the corresponding 90% confidence interval.

of X-ray sources. The median sensitivities of the HEAO-1 A2 survey, XSS, and 3MAXI, converted to the 4–12 keV energy band, are $\sim 1.8 \times 10^{-11}$, $\sim 1.1 \times 10^{-11}$, and $\sim 8 \times 10^{-12} \text{ erg s}^{-1} \text{ cm}^{-2}$ (for spectra not very different from those of the Crab), which is significantly worse than the sensitivity achieved during ARTSS1-5 in its shallowest part near the ecliptic plane.

The *XMM-Newton* slew survey (XMMSL2; Saxton et al. 2008) covered $\sim 84\%$ of the sky⁷. The median flux of the sources detected in its hard band of 2–12 keV is $9.3 \times 10^{-12} \text{ erg s}^{-1} \text{ cm}^{-2}$, which corresponds to $\sim 5.7 \times 10^{-12} \text{ erg s}^{-1} \text{ cm}^{-2}$ in the 4–12 keV band for Crab-like spectra. This should be compared to the median flux of $\sim 4.9 \times 10^{-12} \text{ erg s}^{-1} \text{ cm}^{-2}$ of the ARTSS1-5 sources. Therefore, XMMSL2 (hard band) and ARTSS1-5 are comparable in sensitivity, but the latter provides a more regular coverage of the sky and is done in a slightly harder energy range.

As a result of the increased depth compared to the first year of the ART-XC all-sky survey (Pavlinisky et al. 2022), the dominance of AGN among the classified sources has strengthened, with $\sim 60\%$ of the ARTSS1-5 catalog sources being AGN or AGN candidates. The catalog includes 158 objects that were not known as X-ray sources before. Given that ~ 30 of them are expected to be spurious detections (for the adopted detection significance threshold), there are ~ 130 truly new X-ray sources, which corresponds to $\sim 8\%$ of the entire catalog. This fraction has increased with respect to ARTSS12, as anticipated.

The ARTSS1-5 catalog has a significant added value in terms of the identification and classification of sources. Nearly 83% of the sources are already reliably classified and another $\sim 11\%$ have tentative classifications. We are pursuing the goal of achieving a nearly 100% identification completeness. To this end, we have been carrying out a follow-up optical spectroscopy program, which has already allowed us to identify and classify ~ 60 AGN and ~ 10 Galactic objects (mostly CVs). So far, this campaign has been focused on the northern sky ($\text{Dec} > -25^\circ$), and we urge its extension to the southern hemisphere. Our ultimate objective is to provide statistically complete samples of different classes of objects, in particular AGN and CVs, selected in the 4–12 keV energy band, which is largely unique to the ART-XC survey. The current samples of AGN and CVs in the ARTSS1-5 catalog comprise ~ 900 and ~ 200 objects, respectively. We are now developing an ARTSS1-5 web database⁸ that will provide additional information on the counterparts of the ARTSS1-5 sources.

The SRG/ART-XC all-sky survey has recently been resumed after a 1.5-year pause. Four new scans of the sky are to be conducted by the end of 2025. The next official release of the ART-XC catalog should be based on all eight scans of the sky, and according to our preliminary estimates the final catalog will contain more than 2500 sources.

Acknowledgements. The *Mikhail Pavlinsky* ART-XC telescope is the hard X-ray instrument on board the SRG Observatory, a flagship astrophysical project of the Russian Federal Space Program realized by the Russian Space Agency in the interests of the Russian Academy of Sciences. The ART-XC team thanks the Russian Space Agency, Russian Academy of Sciences, and State Corporation Rosatom for the support of the SRG project and ART-XC telescope. We thank Lavochkin Association (NPOL) with partners for the creation and operation of the SRG spacecraft (Navigator). We thank Acrorad Co., Ltd. (Japan), which manufactured the CdTe dies, and Integrated Detector Electronics AS – IDEAS (Norway), which manufactured the ASICs for the X-ray detectors. SS, RB, EF, RK, IM, GU, EZ, and IZ acknowledge the support of this research by the Russian Science Foundation (grant 19-12-00396). We are grateful to the referee for the helpful comments and suggestions.

References

- Abdollahi, S., Acero, F., Baldini, L., et al. 2022, ApJS, 260, 53
 Ahumada, R., Allende Prieto, C., Almeida, A., et al. 2020, ApJS, 249, 3
 Ajello, M., Angioni, R., Axelsson, M., et al. 2020, ApJ, 892, 105
 Ajello, M., Baldini, L., Ballet, J., et al. 2022, ApJS, 263, 24
 Ajello, M., Ghisellini, G., Paliya, V. S., et al. 2016, ApJ, 826, 76
 An, H., Hascoët, R., Kaspi, V. M., et al. 2013, ApJ, 779, 163
 Angioni, R., Ros, E., Kadler, M., et al. 2020, A&A, 641, A152
 Annuar, A., Alexander, D. M., Gandhi, P., et al. 2020, MNRAS, 497, 229
 Assef, R. J., Stern, D., Kochanek, C. S., et al. 2013, ApJ, 772, 26
 Bahramian, A., Gladstone, J. C., Heinke, C. O., et al. 2014, MNRAS, 441, 640
 Bahramian, A., Heinke, C. O., Maccarone, T. J., Shaw, A. W., & Wijnands, R. 2021, The Astronomer’s Telegram, 14536, 1
 Baldwin, J. A., Phillips, M. M., & Terlevich, R. 1981, PASP, 93, 5
 Ballet, J., Bruel, P., Burnett, T. H., Lott, B., & The Fermi-LAT collaboration. 2023, arXiv e-prints, arXiv:2307.12546
 Barnard, R., Stiele, H., Hatzidimitriou, D., et al. 2008, ApJ, 689, 1215
 Bassani, L., Ursini, F., Malizia, A., et al. 2021, MNRAS, 500, 3111
 Böhringer, H., Burwitz, V., Zhang, Y. Y., Schuecker, P., & Nowak, N. 2005, ApJ, 633, 148
 Boller, T., Freyberg, M. J., Trümper, J., et al. 2016, A&A, 588, A103
 Brandt, W. N. & Yang, G. 2022, in Handbook of X-ray and Gamma-ray Astrophysics, 78
 Britt, C. T., Torres, M. A. P., Hynes, R. I., et al. 2013, ApJ, 769, 120
 Burenin, R. A., Amvrosov, A. L., Eiselevich, M. V., et al. 2016, Astronomy Letters, 42, 295
 Burgess, A. M. & Hunstead, R. W. 2006, AJ, 131, 100
 Callingham, J. R., Tuthill, P. G., Pope, B. J. S., et al. 2019, Nature Astronomy, 3, 82
 Canbay, R., Bilir, S., Özdönmez, A., & Ak, T. 2023, AJ, 165, 163
 Cash, W. F. 1979, ApJ, 228, 939

⁷ <https://www.cosmos.esa.int/web/xmm-newton/xmmsl2-ug>

⁸ to be located at <https://www.srg.cosmos.ru>

- Chang, Y. L., Arsioli, B., Giommi, P., Padovani, P., & Brandt, C. H. 2019, *A&A*, 632, A77
- Chen, S., Berton, M., La Mura, G., et al. 2018, *A&A*, 615, A167
- Chen, Y.-P., Zaw, I., Farrar, G. R., & Elgamal, S. 2022, *ApJS*, 258, 29
- Clavel, M., Tomsick, J. A., Hare, J., et al. 2019, *ApJ*, 887, 32
- Coleiro, A., Chaty, S., Zurita Heras, J. A., Rahoui, F., & Tomsick, J. A. 2013, *A&A*, 560, A108
- Condon, J. J., Cotton, W. D., Greisen, E. W., et al. 1998, *AJ*, 115, 1693
- Cusumano, G., Segreto, A., La Parola, V., et al. 2015, *MNRAS*, 446, 1041
- Cutri, R. M., Wright, E. L., Conrow, T., et al. 2021, *VizieR Online Data Catalog*, II/328
- D’Abrusco, R., Álvarez Crespo, N., Massaro, F., et al. 2019, *ApJS*, 242, 4
- De, K., Daly, F. A., & Soria, R. 2024, *MNRAS*, 528, L38
- de Gasperin, F., Intema, H. T., & Frail, D. A. 2018, *MNRAS*, 474, 5008
- Degenaar, N., Starling, R. L. C., Evans, P. A., et al. 2012, *A&A*, 540, A22
- Doroshenko, V., Staubert, R., Maitra, C., et al. 2022, *A&A*, 661, A21
- Evans, I. N., Primini, F. A., Glotfelty, K. J., et al. 2010, *ApJS*, 189, 37
- Evans, P. A., Page, K. L., Beardmore, A. P., et al. 2023, *MNRAS*, 518, 174
- Frasca, A., Guillout, P., Marilli, E., et al. 2006, *A&A*, 454, 301
- Fratta, M., Scaringi, F., Drew, J. E., et al. 2021, *MNRAS*, 505, 1135
- Gaia Collaboration, Vallenari, A., Brown, A. G. A., et al. 2023, *A&A*, 674, A1
- Geier, S., Raddi, R., Gentile Fusillo, N. P., & Marsh, T. R. 2019, *A&A*, 621, A38
- Goldoni, P., Pita, S., Boisson, C., et al. 2021, *A&A*, 650, A106
- Goodwin, A. J., Galloway, D. K., in’t Zand, J. J. M., et al. 2019, *MNRAS*, 486, 4149
- Gordon, Y. A., Boyce, M. M., O’Dea, C. P., et al. 2021, *ApJS*, 255, 30
- Goulding, A. D. & Alexander, D. M. 2009, *MNRAS*, 398, 1165
- Green, M. J., Maoz, D., Mazeh, T., et al. 2023, *MNRAS*, 522, 29
- Greiner, J., Schwarz, R., Tappert, C., et al. 2010, *Astronomische Nachrichten*, 331, 227
- Haberl, F., Maitra, C., Carpano, S., et al. 2020, *The Astronomer’s Telegram*, 13609, 1
- Halpern, J. P. & Thorstensen, J. R. 2015, *AJ*, 150, 170
- Halpern, J. P., Thorstensen, J. R., Cho, P., et al. 2018, *AJ*, 155, 247
- Healey, S. E., Romani, R. W., Taylor, G. B., et al. 2007, *ApJS*, 171, 61
- Heinze, A. N., Tonry, J. L., Denneau, L., et al. 2018, *AJ*, 156, 241
- Helfand, D. J., White, R. L., & Becker, R. H. 2015, *ApJ*, 801, 26
- Hinkle, J. T., Holoien, T. W. S., Shappee, B. J., et al. 2022, *ApJ*, 930, 12
- Hon, W. J., Wolf, C., Onken, C. A., Webster, R., & Auchettl, K. 2022, *MNRAS*, 511, 54
- Hori, T., Shidatsu, M., Ueda, Y., et al. 2018, *ApJS*, 235, 7
- Itoh, R., Utsumi, Y., Inoue, Y., et al. 2020, *ApJ*, 901, 3
- Jayasinghe, T., Kochanek, C. S., Stanek, K. Z., et al. 2018, *MNRAS*, 477, 3145
- Jayasinghe, T., Stanek, K. Z., Kochanek, C. S., et al. 2019, *MNRAS*, 486, 1907
- Jones, D. H., Read, M. A., Saunders, W., et al. 2009, *MNRAS*, 399, 683
- Karasev, D. I., Lutovinov, A. A., Revnivtsev, M. G., & Krivonos, R. A. 2012, *Astronomy Letters*, 38, 629
- Karasev, D. I., Lutovinov, A. A., Tkachenko, A. Y., et al. 2018, *Astronomy Letters*, 44, 522
- Karasev, D. I., Sazonov, S. Y., Tkachenko, A. Y., et al. 2020, *Astronomy Letters*, 45, 836
- Karasev, D. I., Semena, A. N., Mereminskiy, I. A., et al. 2023, *Astronomy Letters*, 49, 662
- Kawamuro, T., Ueda, Y., Shidatsu, M., et al. 2018, *ApJS*, 238, 32
- Klutsch, A., Frasca, A., Guillout, P., et al. 2020, *A&A*, 637, A43
- Koss, M., Trakhtenbrot, B., Ricci, C., et al. 2017, *ApJ*, 850, 74
- Koss, M. J., Glidden, A., Baloković, M., et al. 2016, *ApJLett*, 824, L4
- Koss, M. J., Ricci, C., Trakhtenbrot, B., et al. 2022a, *ApJS*, 261, 2
- Koss, M. J., Trakhtenbrot, B., Ricci, C., et al. 2022b, *ApJS*, 261, 6
- Krivonos, R., Revnivtsev, M., Lutovinov, A., et al. 2007, *A&A*, 475, 775
- Krivonos, R., Tkachenko, A., Burenin, R., et al. 2017, *Experimental Astronomy*, 44, 147
- Krivonos, R. A., Sazonov, S. Y., Kuznetsova, E. A., et al. 2022, *MNRAS*, 510, 4796
- Krziesinski, J. & Balona, L. A. 2022, *A&A*, 663, A45
- Kumar, H. S., Safi-Harb, S., Slane, P. O., & Gotthelf, E. V. 2014, *ApJ*, 781, 41
- Kuźmicz, A. & Jamroz, M. 2021, *ApJS*, 253, 25
- Landi, R., Masetti, N., Morelli, L., et al. 2007, *ApJ*, 669, 109
- Langer, N., Baade, D., Bodensteiner, J., et al. 2020, *A&A*, 633, A40
- Laurent-Muehleisen, S. A., Kollgaard, R. I., Ciardullo, R., et al. 1998, *ApJS*, 118, 127
- Liu, X., Shen, Y., Strauss, M. A., & Hao, L. 2011, *ApJ*, 737, 101
- Lo, K. K., Farrell, S., Murphy, T., & Gaensler, B. M. 2014, *ApJ*, 786, 20
- Lutovinov, A., Burenin, R., Sazonov, S., et al. 2010, *The Astronomer’s Telegram*, 2759, 1
- Lutovinov, A. A., Tsygankov, S. S., Mereminskiy, I. A., et al. 2022, *A&A*, 661, A28
- Lynx X-ray Observatory Concept Study Report. 2019, <https://wwwastro.msfc.nasa.gov/lynx/docs/LynxConceptStudy.pdf>
- Maccarone, T. J., Yukita, M., Hornschemeier, A., et al. 2016, *MNRAS*, 458, 3633
- Maeda, Y., Mori, H., & Dotani, T. 2013, *Advances in Space Research*, 51, 1278
- Mahony, E. K., Croom, S. M., Boyle, B. J., et al. 2010, *MNRAS*, 401, 1151
- Maitra, C., Kaltenbrunner, D., Haberl, F., et al. 2023, *A&A*, 669, A30
- Malizia, A., Bassani, L., Landi, R., et al. 2023, *A&A*, 671, A152
- Markwardt, C. B., Swank, J. H., Klein-Wolt, M., & Smith, D. M. 2007, *The Astronomer’s Telegram*, 1164, 1
- Marocco, F., Eisenhardt, P. R. M., Fowler, J. W., et al. 2021, *ApJS*, 253, 8
- Maselli, A., Forman, W. R., Jones, C., Kraft, R. P., & Perri, M. 2022, *ApJS*, 262, 51
- Maselli, A., Massaro, F., Cusumano, G., et al. 2016, *MNRAS*, 460, 3829
- Masetti, N., Parisi, P., Jiménez-Bailón, E., et al. 2012, *A&A*, 538, A123
- Masetti, N., Parisi, P., Palazzi, E., et al. 2013, *A&A*, 556, A120
- Massaro, F., Giroletti, M., D’Abrusco, R., et al. 2014, *ApJS*, 213, 3
- Massaro, F., Missaglia, V., Stuardi, C., et al. 2018, *ApJS*, 234, 7
- Mauch, T., Murphy, T., Buttery, H. J., et al. 2003, *MNRAS*, 342, 1117
- Mejía-Restrepo, J. E., Trakhtenbrot, B., Koss, M. J., et al. 2022, *ApJS*, 261, 5
- Mereminskiy, I. A., Dodin, A. V., Lutovinov, A. A., et al. 2022, *A&A*, 661, A32
- Monroe, T. R., Prochaska, J. X., Tejos, N., et al. 2016, *AJ*, 152, 25
- Murphy, T., Mauch, T., Green, A., et al. 2007, *MNRAS*, 382, 382
- Ofek, E. O. & Zackay, B. 2018, *AJ*, 155, 169
- Oh, K., Koss, M., Markwardt, C. B., et al. 2018, *ApJS*, 235, 4
- Osterbrock, D. E. 1981, *ApJ*, 249, 462
- Parisi, P., Masetti, N., Jiménez-Bailón, E., et al. 2012, *A&A*, 545, A101
- Pavlinksky, M., Sazonov, S., Burenin, R., et al. 2022, *A&A*, 661, A38
- Pavlinksky, M., Tkachenko, A., Levin, V., et al. 2021, *A&A*, 650, A42
- Peña-Herazo, H. A., Paggi, A., García-Pérez, A., et al. 2021, *AJ*, 162, 177
- Piccinotti, G., Mushotzky, R. F., Boldt, E. A., et al. 1982, *ApJ*, 253, 485
- Planck Collaboration, Aghanim, N., Arnaud, M., et al. 2011, *A&A*, 536, A9
- Predehl, P., Andritschke, R., Arefiev, V., et al. 2021, *A&A*, 647, A1
- Reig, P., Tzouvanou, A., & Pantoulas, V. 2022, *The Astronomer’s Telegram*, 15612, 1
- Revnivtsev, M., Sazonov, S., Gilfanov, M., Churazov, E., & Sunyaev, R. 2006, *A&A*, 452, 169
- Revnivtsev, M., Sazonov, S., Jahoda, K., & Gilfanov, M. 2004, *A&A*, 418, 927
- Reynolds, C. S., Lohfink, A. M., Babul, A., et al. 2014, *ApJLett*, 792, L41
- Reynolds, M. T., Miller, J. M., Maitra, D., et al. 2012, *The Astronomer’s Telegram*, 3963, 1
- Ricci, F., Treister, E., Bauer, F. E., et al. 2022, *ApJS*, 261, 8
- Ritter, H. & Kolb, U. 2003, *A&A*, 404, 301
- Rojas, A. F., Masetti, N., Minniti, D., et al. 2017, *A&A*, 602, A124
- Russell, H. R., Fabian, A. C., Sanders, J. S., et al. 2010, *MNRAS*, 402, 1561
- Russell, T. D., Del Santo, M., Marino, A., et al. 2022, *MNRAS*, 513, 6196
- Salganik, A., Tsygankov, S. S., Lutovinov, A. A., et al. 2022, *MNRAS*, 514, 4018
- Samus’, N. N., Kazarovets, E. V., Durlevich, O. V., Kireeva, N. N., & Pastukhova, E. N. 2017, *Astronomy Reports*, 61, 80
- Sánchez-Sáez, P., Arredondo, J., Bayo, A., et al. 2023, *A&A*, 675, A195

- Saxton, R. D., Read, A. M., Esquej, P., et al. 2008, *A&A*, 480, 611
- Schlaflly, E. F., Green, G. M., Lang, D., et al. 2018, *ApJS*, 234, 39
- Schmidt, S. J., Shappee, B. J., van Saders, J. L., et al. 2019, *ApJ*, 876, 115
- Schwöpe, A., Buckley, D. A. H., Kawka, A., et al. 2022, *A&A*, 661, A42
- Schwöpe, A., Hasinger, G., Lehmann, I., et al. 2000, *Astronomische Nachrichten*, 321, 1
- Semena, A., Mereminskiy, I., Lutovinov, A., Molkov, S., & Pavlinsky, M. 2020, *The Astronomer's Telegram*, 13415, 1
- Semena, A., Mereminskiy, I., Lutovinov, A., et al. 2024a, *MNRAS*, 529, 941
- Semena, A., Vikhlinin, A., Mereminskiy, I., et al. 2024b, *arXiv e-prints*, arXiv:2404.02061
- Sguera, V., Sidoli, L., Bird, A. J., Paizis, A., & Bazzano, A. 2020, *MNRAS*, 491, 4543
- Shidatsu, M., Pike, S., Mihara, T., et al. 2022, *The Astronomer's Telegram*, 15495, 1
- Sidoli, L., Esposito, P., & Sguera, V. 2020, *The Astronomer's Telegram*, 14039, 1
- Sluse, D., Surdej, J., Claeskens, J. F., et al. 2003, *A&A*, 406, L43
- Smith, L. C., Lucas, P. W., Kurtev, R., et al. 2018, *MNRAS*, 474, 1826
- Sperauskas, J., Deveikis, V., & Tokovinin, A. 2019, *A&A*, 626, A31
- Starling, R. L. C., Wildy, C., Wiersema, K., et al. 2017, *MNRAS*, 468, 378
- Stephen, J. B., Bassani, L., Malizia, A., Masetti, N., & Ubertini, P. 2018, *The Astronomer's Telegram*, 11341, 1
- Stiele, H., Pietsch, W., Haberl, F., et al. 2011, *A&A*, 534, A55
- Sunyaev, R., Arefiev, V., Babyshkin, V., et al. 2021, *A&A*, 656, A132
- Szkody, P., Olde Loohuis, C., Koplitz, B., et al. 2021, *AJ*, 162, 94
- Thorstensen, J. R. 2020, *AJ*, 160, 6
- Thorstensen, J. R., Alvarado-Anderson, C. K., Burrows, A. D., Goebel-Bain, R. M., & Katz, D. C. 2023, *AJ*, 166, 131
- Tomsick, J. A., Bodaghee, A., Chaty, S., et al. 2012, *ApJ*, 754, 145
- Tomsick, J. A., Lansbury, G. B., Rahoui, F., et al. 2017, *ApJS*, 230, 25
- Townsley, L. K., Broos, P. S., Garmire, G. P., et al. 2014, *ApJS*, 213, 1
- Tsujimoto, M., Morihana, K., Hayashi, T., & Kitaguchi, T. 2018, *PASJ*, 70, 109
- Uskov, G. S., Sazonov, S. Y., Zaznobin, I. A., et al. 2023, *Astronomy Letters*, 49, 25
- Uskov, G. S., Sazonov, S. Y., & Zaznobin, I. A. e. a. 2024, *Astronomy Letters*
- Uskov, G. S., Zaznobin, I. A., Sazonov, S. Y., et al. 2022, *Astronomy Letters*, 48, 87
- Vikhlinin, A., McNamara, B. R., Forman, W., et al. 1998, *ApJ*, 502, 558
- Wang, L.-L., Luo, A. L., Shen, S.-Y., et al. 2018, *MNRAS*, 474, 1873
- Webb, N. A., Coriat, M., Traulsen, I., et al. 2020, *A&A*, 641, A136
- Wenger, M., Ochsenbein, F., Egret, D., et al. 2000, *A&AS*, 143, 9
- Wilms, J., Kreykenbohm, I., Weber, P., et al. 2020, *The Astronomer's Telegram*, 13416, 1
- Wils, P., Krajci, T., Hamsch, F.-J., & Muyliaert, E. 2011, *Information Bulletin on Variable Stars*, 5982, 1
- Xu, X., Shao, Y., & Li, X.-D. 2019, *MNRAS*, 489, 3031
- Yao, Y., Kulkarni, S. R., Burdge, K. B., et al. 2021, *ApJ*, 920, 120
- Young, A. J., Wilson, A. S., Terashima, Y., Arnaud, K. A., & Smith, D. A. 2002, *ApJ*, 564, 176
- Zaznobin, I., Sazonov, S., Burenin, R., et al. 2022a, *A&A*, 661, A39
- Zaznobin, I. A., Sazonov, S. Y., Mereminskiy, I. A., et al. 2022b, *The Astronomer's Telegram*, 15582, 1
- Zaznobin, I. A., Uskov, G. S., Sazonov, S. Y., et al. 2021, *Astronomy Letters*, 47, 71
- Zhekov, S. A., Gagné, M., & Skinner, S. L. 2014, *ApJ*, 785, 8

Appendix A: Notes on individual sources

Here⁹, we provide additional comments on the identification and classification of a number of sources from the ARTSS1-5 catalog, namely those with dubious identification or classification as well as recently or newly discovered X-ray sources. In addition to the databases and catalogs already mentioned in Section 3.1, we acquired this information from the literature and from our ongoing follow-up optical spectroscopy campaign.

For a few of the objects discussed below, we obtained a tentative Seyfert classification (class ‘‘Seyfert?’’ in the catalog) by inspecting their optical spectra available from the SDSS or 6dF surveys. To this end, we used the standard criteria based on the widths and intensities of emission lines (Osterbrock 1981; Baldwin et al. 1981) following our previous work on the classification of AGN from the SRG/ART-XC all-sky survey (e.g., Uskov et al. 2023, 2024).

SRGA J000048.1-070914

A Seyfert 1.9 at $z = 0.0375$ (Koss et al. 2022a).

SRGA J000132.9+240237

Associated with 2MASX J00013232+2402304, a Seyfert 1.9 at $z = 0.1048$ (Uskov et al. 2024).

SRGA J001439.6+183500

A Seyfert 2 at $z = 0.0180$ (Uskov et al. 2023).

SRGA J002203.6+254017

A Seyfert 1.2 at $z = 0.1292$ (Starling et al. 2017).

SRGA J002241.4+804348

A Seyfert 1 at $z = 0.1147$ (Uskov et al. 2023).

SRGA J003535.1+462345

Associated with the dwarf nova GALEX J003535.7+462353 (Ritter & Kolb 2003; Wils et al. 2011).

SRGA J003947.5-754949

Likely associated with the galaxy LEDA 242675, $W1 - W2 \sim 1.1$.

SRGA J004142.9+413410

Likely an LMXB in the globular cluster Bol 45 in M31 (Stiele et al. 2011).

SRGA J004223.1+290401

Associated with the known Seyfert galaxy 2MASX J00422385+2903588 at $z = 0.0711$ (Wang et al. 2018), previously undetected in X-rays.

SRGA J004238.9+411603

The central region of M31, unresolved into individual X-ray sources.

SRGA J004313.9+410723

In M31, might be confused with other sources.

SRGA J004505.9+620746

Likely an SNR (Mereminskiy et al., in prep.).

SRGA J004545.6+413956

An X-ray binary in the globular cluster Bo 375 in M31, likely with a neutron star (Barnard et al. 2008; Maccarone et al. 2016).

SRGA J004732.9-251713

A starburst galaxy with many point X-ray sources and hot interstellar gas.

SRGA J004852.9-734945

In the SMC.

SRGA J005456.2-722644

In the SMC.

SRGA J005642.6+604301

The prototype gamma Cas star.

SRGA J010336.0-720135

In the SMC.

SRGA J010430.3-723133

In the SMC.

SRGA J010743.0+574423

A Seyfert 1.9 at $z = 0.0699$ (Uskov et al. 2023).

SRGA J011506.0+882903

Likely associated with the bright star Gaia DR3 576260267526450048, at a distance ~ 400 pc, a spectroscopic binary in a young stellar association (Klutsch et al. 2020). Hence, likely a coronally active star.

SRGA J011630.5-123557

A Seyfert 1.9 at $z = 0.1424$ (Koss et al. 2022a).

SRGA J011704.8-732638

In the SMC.

⁹ <https://zenodo.org/doi/10.5281/zenodo.11191704>

SRGA J011905.4+160504

Associated with 2MASX J01190583+1604550, a Seyfert 2 galaxy at $z = 0.0700$ (Uskov et al., in prep.).

SRGA J012823.7+162743

A Seyfert 2 at $z = 0.0383$.

SRGA J013350.9+303932

In M33.

SRGA J014458.7-023211

Likely associated with the galaxy 2MASX J01445853-0231589, $W1 - W2 \sim 0.7$.

SRGA J015006.8-322444

Possibly associated with the galaxy LEDA 131950 at $z = 0.0384$, $W1 - W2 \sim 0.3$.

SRGA J015440.4-270705

A Seyfert 1 at $z = 0.1510$ (Koss et al. 2022a).

SRGA J015524.4+022825

A Seyfert 1 at $z = 0.0847$ (Koss et al. 2022a).

SRGA J015641.5-835833

Likely associated with the star Gaia DR3 4617143036371460864 at a distance ~ 500 pc.

SRGA J015657.4-530202

The spectroscopic redshift is $z = 0.3043$ (Goldoni et al. 2021).

SRGA J020012.7+065507

Associated with the bright, long-period variable star DE Psc at a distance ~ 700 pc. Hence, possibly a symbiotic star.

SRGA J020639.4-714824

A flat-spectrum radio source (Healey et al. 2007).

SRGA J020749.4+445032

A Seyfert 1.9 at $z = 0.0217$ (Koss et al. 2022a).

SRGA J021643.4+255250

Associated with the galaxy LEDA 1753646, a Seyfert 2 at $z = 0.0663$ (Uskov et al., in prep.).

SRGA J022235.4+250818

A Seyfert 1 at $z = 0.0616$ (Koss et al. 2022a).

SRGA J022625.5+592746

A radio galaxy with unknown AGN optical type and redshift (Bassani et al. 2021).

SRGA J022746.2-693129

A giant star at a distance ~ 240 pc. The exact nature of the X-ray emission is unknown.

SRGA J023800.1+193818

Associated with 2MASS J02375999+1938118, a Seyfert 1 galaxy at $z = 0.0335$ (Uskov et al. 2024).

SRGA J025208.6+482952

A Seyfert 1.9 at $z = 0.0337$ (Uskov et al. 2023).

SRGA J025234.6+431001

A Seyfert 2 at $z = 0.0512$ (Uskov et al. 2022).

SRGA J025900.3+502958

Associated with LEDA 2374943, a Seyfert 1 galaxy at $z = 0.0946$ (Uskov et al. 2024).

SRGA J030536.3+762243

A Seyfert 1 at $z = 0.1966$ (Mejía-Restrepo et al. 2022).

SRGA J030838.7-552042

Associated with LEDA 410289, a Seyfert 2 galaxy at $z = 0.0779$ (Chen et al. 2022).

SRGA J031130.8-315249

A CV (nova-like and/or polar, Ritter & Kolb 2003).

SRGA J031402.8+244442

Also a BL Lac candidate (Laurent-Muehleisen et al. 1998).

SRGA J031415.5-542459

Possibly associated with WISEA J031416.45-542445.3, $W1 - W2 \sim 0.8$.

SRGA J032317.9-481816

There are broad $H\beta$ and $H\gamma$ lines in the optical spectrum, $z = 0.155$ (Monroe et al. 2016).

SRGA J032511.9+404152

A pair of interacting Seyfert 2 galaxies, LEDA 97012 and LEDA 4678815 (Lutovinov et al. 2010; Masetti et al. 2012).

SRGA J032718.6+552032

Unclassified radio-loud AGN (Maselli et al. 2016; Massaro et al. 2018).

SRGA J032846.5-530316

Likely associated with the galaxy 2MASX J03284504-5303273, $W1 - W2 \sim 0.7$.

SRGA J032910.2-220116

A Seyfert 1.8 (Ricci et al. 2022).

SRGA J033203.9-704000

A blazar at $z = 0.277$ (Peña-Herazo et al. 2021).

SRGA J033336.5-370656

The position of the ART-XC source is 44 arcsec away from the position of the Seyfert galaxy CTS 77, but another known Seyfert galaxy, FCC B868 ($z = 0.0656$), located at 93 arcsec from the ART-XC source, may contribute to the X-ray signal.

SRGA J033622.6-605854

A Seyfert 1 at $z = 0.471$ (Monroe et al. 2016).

SRGA J035023.8-501809

A Seyfert 2 (Koss et al. 2022a).

SRGA J035745.5+415457

A Seyfert 2 at $z = 0.0518$ (Koss et al. 2022a).

SRGA J040111.1-535446

Associated with the gamma-ray source 4FGL J0401.0-5353, a blazar candidate of unknown type (Ajello et al. 2020).

SRGA J040335.6+472440

Associated with 2MASS J04033641+4724383, a Seyfert 1 galaxy at $z = 0.0962$ (Uskov et al. 2024).

SRGA J040543.1+570730

An RS CVn variable (Frasca et al. 2006).

SRGA J040551.3+380353

A flat-spectrum radio source (Itoh et al. 2020).

SRGA J040753.2-611607

A Seyfert 2 (Chen et al. 2022).

SRGA J040850.6-791410

Likely associated with the star Gaia DR3 4625832751643853696 at a distance ~ 1300 pc.

SRGA J041108.8-591127

A dwarf nova (Thorstensen et al. 2023).

SRGA J041243.1+582520

A Seyfert 1 at $z = 0.0684$ (Mejía-Restrepo et al. 2022).

SRGA J041328.1-061455

A flat-spectrum radio source (Healey et al. 2007).

SRGA J041733.7-525302

Likely associated with the galaxy 2MASX J04173452-5253070, $W1 - W2 \sim 0.2$.

SRGA J042435.7-754140

Likely associated with the red giant HD 28839 at a distance ~ 190 pc.

SRGA J042616.8-592325

Associated with the galaxy LEDA 371722, $W1 - W2 \sim 0.9$.

SRGA J043008.4+455702

The bright, long-period variable V591 Per at a distance ~ 1000 pc, a candidate binary with an orbital period of 2.48 days (TESS, Green et al. 2023).

SRGA J043208.9+354922

A Seyfert 1 at $z = 0.0506$ (Zaznobin et al. 2021).

SRGA J043510.7-752749

Likely associated with the variable star CRTS J043509.7-752743 at a distance ~ 500 pc.

SRGA J043516.4+512821

Based on the Swift/XRT position (Evans et al. 2023), likely associated with WISEA J043519.72+512833.4, $W1 - W2 \sim 1.2$, also a radio source. A note of caution: the *Swift*/XRT position is 34 arcsec away from the ART-XC position, i.e. significantly outside R_{98} .

SRGA J043523.0+552235

An X-ray transient, SRGA J043520.9+552226 = SRGE J043523.3+552234, discovered by SRG/ART-XC and eROSITA, associated with the optical transient AT2019wey. An LMXB and a black hole candidate (Yao et al. 2021; Mereminskiy et al. 2022).

SRGA J043838.8-661405

Likely associated with the galaxy Fairall 304, $W1 - W2 \sim 0.5$.

SRGA J043943.9-090312

A Seyfert 2 (Chen et al. 2022).

SRGA J044048.9+292443

Associated with the star Gaia DR3 158134751604204416 at a distance of ~ 300 pc.

SRGA J044956.8-642127

Possibly associated with WISEA J044956.29-642136.2, $W1 - W2 \sim 0.9$.

SRGA J045001.1-494525

Possibly associated with WISEA J045001.39-494525.1, $W1 - W2 \sim 0.8$.

SRGA J045001.8-551240

A Seyfert 2 at $z = 0.0216$ (Koss et al. 2022a).

SRGA J045048.9+301443

A Seyfert 1.9 at $z = 0.0331$ (Zaznobin et al. 2021).

SRGA J045253.8-585350

A blazar candidate (D'Abrusco et al. 2019).

SRGA J045424.1-570045

Likely associated with the galaxy WISEA J045424.13-570045.9, $W1 - W2 \sim 0.8$, a radio source.

SRGA J045431.4+524008

A Seyfert 1.9 at $z = 0.0312$ (Uskov et al. 2023).

SRGA J045442.2-431419

A Seyfert 1.9 (Koss et al. 2017).

SRGA J045602.7+273600

An Orion variable.

SRGA J050021.4+523801

Associated with the gamma-ray source 4FGL J0500.2+5237, likely a blazar (Chang et al. 2019).

SRGA J050125.9-703338

In the LMC.

SRGA J050249.5-622749

Associated with WISEA J050250.64-622740.6, $W1 - W2 \sim 1.1$.

SRGA J050434.1-553129

Likely associated with the galaxy ESO 158-17, $W1 - W2 \sim 0.2$.

SRGA J050809.7-660656

A new Be X-ray pulsar (eRASSU J050810.4-660653) discovered by SRG/eROSITA in the LMC (Haberl et al. 2020; Salganik et al. 2022), previously detected during the ROSAT all-sky survey (2RXS J050810.2-660645).

SRGA J050956.7-641743

A BL Lac at $z = 0.271$ (Peña-Herazo et al. 2021).

SRGA J051111.0-110305

A Seyfert 1 at $z = 0.1168$ (Uskov et al., in prep.).

SRGA J051300.0-252322

Possibly associated with the variable star (Jayasinghe et al. 2018; Heinze et al. 2018) Gaia DR3 2956561001583884800, at a distance ~ 600 pc.

SRGA J051313.8+662746

A Seyfert 2 at $z = 0.0148$ (Uskov et al. 2023).

SRGA J051400.8-402723

Likely associated with the galaxy LEDA 586143, $W1 - W2 \sim 0.8$, a radio source.

SRGA J051401.8-504559

Likely associated with WISEA J051401.99-504603.5, $W1 - W2 \sim 1.0$, a radio source.

SRGA J052028.6-715734

In the LMC.

SRGA J052115.1+251331

A CV (Thorstensen 2020).

SRGA J052412.0-662049

In the LMC.

SRGA J052503.0-693848

In the LMC.

SRGA J052602.5-660510

In the LMC.

SRGA J052627.5-211716

A Seyfert 2 (Koss et al. 2022a).

SRGA J052802.4-393451

A Seyfert 1 at $z = 0.0367$ (Koss et al. 2022a).

SRGA J052858.5-670957

In the LMC.

SRGA J052915.0-662447

A new Be X-ray Pulsar, eRASSU J052914.9-662446, discovered by SRG/eROSITA in the LMC (Maitra et al. 2023).

SRGA J052947.7-655645

In the LMC.

SRGA J052959.2-340205

A Seyfert 1.8 (Uskov et al. 2022).

SRGA J053013.2-655127

In the LMC.

SRGA J053043.0-665431

In the LMC.

SRGA J053232.2-655144

In the LMC.

SRGA J053249.5-662217

In the LMC.

SRGA J053322.0-684130

In the LMC.

SRGA J053358.8-714528

Likely associated with the galaxy ESO 56-154, $W1 - W2 \sim 0.1$, a radio source.

SRGA J053411.7-045030

There are two *Chandra* sources within the ART-XC localization region: 2CXO J053412.8-045035 and 2CXO J053410.4-045038, each with an X-ray flux $\sim 3 \times 10^{-13}$ erg s $^{-1}$ cm $^{-2}$ (Evans et al. 2010). Both are associated with Orion variable stars.

SRGA J053526.1-691609

In the LMC.

SRGA J053528.7-050541

Possibly associated with the Orion variable V1740 Ori, but other nearby stars may contribute to the flux.

SRGA J053738.8+210827

A gamma Cas star.

SRGA J053748.0-691021

In the LMC.

SRGA J053856.8-640503

In the LMC.

SRGA J053939.0-694439

In the LMC.

SRGA J054011.1-691956

In the LMC.

SRGA J054023.2-554443

Based on the *Swift*/XRT position (2SXPS J054022.5-554445), likely associated with the galaxy 2MASS J05402254-5544457, $W1 - W2 \sim 0.6$.

SRGA J054134.6-682542

In the LMC.

SRGA J055052.7-621453

A Seyfert 1 (Uskov et al. 2022; Chen et al. 2022).

SRGA J055523.5-765506

Likely associated with the galaxy IC 2160, $W1 - W2 \sim 0.1$, a radio source. Appears to be a Seyfert 2 based on the 6dF spectrum, but the H α region is missing.

SRGA J055805.0-564634

Associated with 2MASX J05580592-5646361, a Seyfert 2 galaxy (Chen et al. 2022).

SRGA J060041.7+000619

A Seyfert 1.9 (Malizia et al. 2023).

SRGA J060045.5-645602

Likely associated with the galaxy ESO 86-49, $W1 - W2 \sim 0.1$, a radio source.

SRGA J060211.3-673802

Possibly associated with WISEA J060211.85-673806.2, $W1 - W2 \sim 1.1$.

SRGA J060241.7-595155

Associated with LEDA 178859, $W1 - W2 \sim 0.7$, which appears to be a Seyfert 2 galaxy based on the 6dF spectrum.

SRGA J060431.7-395014

Likely associated with the galaxy LEDA 593504, $W1 - W2 \sim 0.5$.

SRGA J060650.6-624544

Associated with the galaxy LEDA 340165, $W1 - W2 \sim 0.8$.

SRGA J060729.5-614832

A heavily obscured AGN (Goulding & Alexander 2009; Annuar et al. 2020) in an edge-on galaxy.

SRGA J061035.2-652521

A Seyfert 1 (Chen et al. 2022).

SRGA J061111.1-095612

Possibly associated with the star Gaia DR3 3004437272613544576, at a distance ~ 700 pc.

SRGA J061154.6-435703

Likely associated with the galaxy LEDA 542558, $W1 - W2 \sim 0.6$.

SRGA J061324.1-290027

A Seyfert 2 at $z = 0.0705$ (Uskov et al. 2022).

SRGA J061448.3+093421

Likely associated with the variable star CY Ori, which has been tentatively classified as a dwarf nova¹⁰.

SRGA J061619.0-705229

Based on the XMM-Newton position (4XMM J061617.1-705229, Webb et al. 2020), likely associated with the infrared source WISEA J061617.13-705228.7, $W1 - W2 \sim 0.4$.

SRGA J061903.6-694744

Possibly associated with the galaxy 2MASX J06190057-6947399, $W1 - W2 \sim 0.0$.

SRGA J062040.0+264338

The redshift is $z = 0.134$ (Peña-Herazo et al. 2021).

SRGA J062109.9-680551

Associated with the galaxy LEDA 179145, a Seyfert 2 (Chen et al. 2022).

SRGA J062339.4-265803

Also known as SRGt 062340.2-265751, a novalike CV (Schwope et al. 2022).

SRGA J062627.7+072726

A Seyfert 2 at $z = 0.0425$ (Uskov et al. 2022).

SRGA J062946.0-834423

Likely associated with WISEA J062948.62-834421.6, $W1 - W2 \sim 1.0$.

SRGA J063326.9-561425

A Seyfert 2 (Uskov et al. 2022).

SRGA J063517.1-695405

Associated with the galaxy WISEA J063517.18-695401.4 = 6dFGS gJ063517.2-695402, $W1 - W2 \sim 1.0$, a radio source.

SRGA J063558.5+075525

Associated with the bright star TYC 733-2098-1 at a distance ~ 200 pc, not a CV (Zaznobin et al., in prep.).

SRGA J064151.5-032039

A flat-spectrum radio quasar at $z = 1.196$ (Ajello et al. 2016).

SRGA J064421.9-662623

Associated with the galaxy 6dFGS gJ064421.9-662620, $W1 - W2 \sim 0.8$, a Seyfert 1 galaxy based on the 6dF spectrum (Uskov et al., in prep.).

SRGA J064620.5-692813

Associated with the galaxy 2MASX J06462178-6928111, a Seyfert 2 (Chen et al. 2022).

SRGA J064849.8-694520

A blazar at $z = 0.233$ (Peña-Herazo et al. 2021).

SRGA J065018.7-380522

A narrow-line Seyfert 1 galaxy (Chen et al. 2018).

¹⁰ <https://www.aavso.org/vsx/index.php?view=detail.top&oid=23188>

SRGA J065313.0-673633

Associated with the dwarf nova ASASSN-V J065311.74-673642.9 (Sánchez-Sáez et al. 2023).

SRGA J065316.2-670832

Possibly associated with WISE J065313.86-670811.1, $W1 - W2 \sim 1.1$, a radio source.

SRGA J065513.2-012841

Also known as MAXI J0655-013. A Be HMXB (Zaznobin et al. 2022b; Reig et al. 2022) and an X-ray pulsar (Shidatsu et al. 2022).

SRGA J065638.8-670224

Possibly associated with the star Gaia DR3 5281660651288601472 at a distance ~ 640 pc.

SRGA J065721.8-670549

Possibly associated with the star Gaia DR3 5281647899528664320 at a distance ~ 900 pc.

SRGA J070110.6-323451

Associated with the galaxy 2MASS J07011023-3234529, $W1 - W2 \sim 0.8$.

SRGA J070236.6-704441

Likely associated with the galaxy LEDA 272172, $W1 - W2 \sim 0.1$.

SRGA J070511.2-670531

Possibly associated with WISEA J070508.26-670525.9, $W1 - W2 \sim 1.4$.

SRGA J070637.0+635109

A Seyfert 1.8 at $z = 0.0140$ (Uskov et al. 2022).

SRGA J070932.6-353737

A Seyfert 1.5 at $z = 0.030$ (Rojas et al. 2017).

SRGA J071020.4-241648

Likely associated with the galaxy 2MASX J07102131-2416501, $W1 - W2 \sim 0.5$, a radio source.

SRGA J071029.2-390131

Appears to be a Seyfert 1 galaxy based on the 6dF spectrum.

SRGA J071415.0-262116

Associated with the Be star 27 CMa at ~ 440 pc. Possibly, a gamma Cas star.

SRGA J071740.2-710346

Associated with WISEA J071740.40-710347.3, $W1 - W2 \sim 1.0$.

SRGA J071947.9-753801

Associated with the galaxy 2MASS J07195059-7537573, $W1 - W2 \sim 0.7$.

SRGA J072041.0-552615

Associated with the galaxy LEDA 409410, $W1 - W2 \sim 0.6$.

SRGA J072319.9-732653

A cluster of galaxies discovered via the Sunyaev-Zeldovich effect by the *Planck observatory* and confirmed in X-rays by *XMM-Newton* (Planck Collaboration et al. 2011).

SRGA J072957.0-654331

A Seyfert 1 galaxy (Chen et al. 2022).

SRGA J073022.2-750414

Likely associated with 2MASS J07302521-7504018, $W1 - W2 \sim 1.0$.

SRGA J074343.1+183157

Possibly associated with the galaxy WISEA J074343.10+183143.5, $W1 - W2 \sim 0.2$.

SRGA J074414.2-704131

Likely associated with 2MASS J07441473-7041302, $W1 - W2 \sim 0.8$, a radio source.

SRGA J075808.4+835632

A Seyfert 1 at $z = 0.1340$ (Koss et al. 2022a).

SRGA J080142.6+420013

The known AGN SDSS J080142.58+420019.4, previously undetected in X-rays.

SRGA J080559.6+320605

Likely associated with the galaxy 2MASS J08055841+3205542, $W1 - W2 \sim 1.2$.

SRGA J080917.6+474637

Possibly associated with the extended optical object WISEA J080917.45+474651.8, $W1 - W2 \sim 0.5$.

SRGA J082316.0-632939

The redshift is $z = 0.29$ (Ajello et al. 2022).

SRGA J082623.5-703144

Also known as PBC J0826.3-7033. Likely a non-magnetic CV (Parisi et al. 2012).

SRGA J083126.1-600717

Likely associated with the star Gaia DR3 5302213306753527936, at a roughly estimated distance ~ 7.5 kpc.

SRGA J084433.5-375751

Associated with the star HD 74771, a bright variable star (Samus' et al. 2017).

SRGA J084551.9-272922

Possibly associated with the star Gaia DR3 5645994171436695552, at a distance ~ 600 pc.

SRGA J084937.3-554416

Likely associated with one of two stars: Gaia DR3 5316706343179643904 or Gaia DR3 5316706347473511936, at distances ~ 1.5 and ~ 3 kpc, respectively.

SRGA J085040.9-421155

A red-supergiant HMXB (De et al. 2024).

SRGA J085741.3-554226

Possibly associated with WISEA J085739.32-554258.2, $W1 - W2 \sim 2.1$.

SRGA J090106.7-340025

Likely associated with the galaxy WISEA J090108.25-340024.3, $W1 - W2 \sim 1.0$, a radio source.

SRGA J090305.2+130323

Possibly associated with the star Gaia DR3 605340838251799296, at a distance ~ 1200 pc.

SRGA J091514.0-752345

Associated with the galaxy 2MASS J09151520-7523498, $W1 - W2 \sim 1.1$, a radio source.

SRGA J092014.4-383445

Likely associated with WISEA J092014.24-383450.4, $W1 - W2 \sim 0.7$, a strong radio source.

SRGA J092418.1-314217

A LMXB or CV (Tomsick et al. 2017).

SRGA J092712.2-113828

A Seyfert 2 at $z = 0.0109$ (Uskov et al., in prep.).

SRGA J092841.6-620754

Possibly associated with WISEA J092841.59-620741.4, $W1 - W2 \sim 1.2$.

SRGA J095307.9-765751

A blazar at $z = 0.109$ (Peña-Herazo et al. 2021).

SRGA J095704.9-585317

Possibly associated the radio/IR source RACS-DR1 J095702.6-585317 = CatWISE2020 J095702.71-585318.5, $W1 - W2 \sim 1.1$.

SRGA J100513.7-625209

A Seyfert 1 at $z = 0.0714$ (Mejía-Restrepo et al. 2022).

SRGA J101133.2-442257

Based on the Swift/XRT position, possibly associated with the radio/IR source RACS-DR1 J101132.0-442253 = WISEA J101132.10-442253.5, $W1 - W2 \sim 0.4$.

SRGA J102205.8-353801

Likely associated with the hot subdwarf candidate GALEX J102205.1-353756 at a distance ~ 900 pc.

SRGA J102555.0-574844

A very massive, colliding-wind binary.

SRGA J103915.5-490307

Associated with the star Gaia DR3 5364403368050904576, at a distance ~ 3700 pc.

SRGA J104124.3-692952

Possibly associated with the galaxy 2MASX J10412355-6929560, $W1 - W2 \sim 0.4$.

SRGA J104451.4-602510

A Seyfert 2 at $z = 0.0470$ (Koss et al. 2022a).

SRGA J104834.8-390225

A Seyfert 1.2 at $z = 0.0449$ (Mejía-Restrepo et al. 2022).

SRGA J105452.7+771252

Possibly associated with WISEA J105452.40+771310.0, $W1 - W2 \sim 0.7$.

SRGA J105715.0-473958

A Seyfert 1.9 (Oh et al. 2018).

SRGA J110122.2-514909

Associated with the galaxy 2MASX J11012138-5149100 , $W1 - W2 \sim 0.8$.

SRGA J110946.0+800817

A Seyfert 1 at $z = 0.1888$ (Uskov et al. 2023).

SRGA J111457.3-611449

A massive star-forming region. *Chandra* has registered plenty of point X-ray sources and diffuse X-ray emission (Townesley et al. 2014).

SRGA J111515.8-480620

Possibly associated with WISEA J111515.15-480615.4, $W1 - W2 \sim 1.0$.

SRGA J111820.6-543730

Likely a LMXB, rather than an HMXB (Coleiro et al. 2013).

SRGA J112958.5-655520

Based on the *Swift*/XRT coordinates, likely associated with the star Gaia DR3 5236824109000257920, a long-period variable according to Gaia. The distance is at least several kpc, according to Gaia.

SRGA J113151.7-123151

An AGN at $z = 0.658$ lensed by a galaxy at $z = 0.295$ (Sluse et al. 2003).

SRGA J113257.1-260736

Associated with the galaxy WISEA J113256.57-260735.5, $W1 - W2 \sim 1.3$, a radio source.

SRGA J113850.8-232126

A Seyfert 1.9 (Koss et al. 2022a).

SRGA J114515.2+794100

A Seyfert 1 at $z = 0.0060$ (Koss et al. 2022a).

SRGA J114722.1-495308

Possibly associated with the emission-line star TWA 19B, but there is also another bright star, HD 102458, in the vicinity.

SRGA J114754.6+094554

An AGN in a galaxy pair (Liu et al. 2011).

SRGA J115215.3-510703

Possibly associated with the star Gaia DR3 5369277537456720128 at a distance ~ 660 pc,

SRGA J115223.8-673837

Likely associated with the star Gaia DR3 5235694124616931584 at a distance ~ 1050 pc.

SRGA J115415.6-501801

Possibly associated with the star Gaia DR3 5370642890382757888 at a distance of ~ 310 pc.

SRGA J115730.2-343758

Associated with the CV 6dFGS g1157297-343750 (Mahony et al. 2010).

SRGA J115910.3-532435

Likely associated with the galaxy ESO 171-4, $W1 - W2 \sim 0.1$, a radio source (Murphy et al. 2007).

SRGA J120413.5-294651

Possibly associated with WISEA J120412.71-294709.1, $W1 - W2 \sim 0.9$, a radio source.

SRGA J121053.2-040811

Possibly associated with the star Gaia DR3 3597896582057220096 at a distance ~ 900 pc.

SRGA J122806.9-552242

Likely associated with the rotating variable star ASAS J122810-5523.0 at a distance ~ 110 pc.

SRGA J122809.9-092718

A Seyfert 1.5 at $z = 0.223$ (Rojas et al. 2017).

SRGA J123112.7-423529

Likely associated with the star Gaia DR3 6145666951501477376 at a distance ~ 400 pc.

SRGA J123402.7-614310

A transient hard X-ray source, discovered by *INTEGRAL* and confirmed by *Swift*/XRT, likely a supergiant fast X-ray transient (Sguera et al. 2020; Sidoli et al. 2020).

SRGA J123630.6-664551

Likely associated with the star Gaia DR3 5859908625444588160 at a distance ~ 400 pc.

SRGA J123821.5-253208

A bright, short-duration X-ray transient, SRGt J123822.3-253206, discovered by ART-XC and eROSITA (Semena et al. 2020; Wilms et al. 2020).

SRGA J124248.7-630324

A gamma Cas star (Tsujimoto et al. 2018; Langer et al. 2020).

SRGA J124403.4-632220

An X-ray pulsar with a Be companion, discovered by SRG/ART-XC and eROSITA, also known as SRGA J124404.1-632232 and SRGU J124403.8-632231 (Doroshenko et al. 2022).

SRGA J130522.0-492823

In NGC 4945.

SRGA J131036.8-562654

A Seyfert 2 at $z = 0.1142$.

SRGA J131239.9-624258

A Wolf-Rayet star. The most likely physical picture is that of colliding stellar winds in a wide binary system, with the unseen secondary star being another WR star or a luminous blue variable (Zhekov et al. 2014).

SRGA J132031.7-701443

Associated with the bright star Gaia DR3 5844075864125790464 at a distance ~ 2300 pc. Possibly an HMXB or a symbiotic X-ray binary.

SRGA J132327.2-165810

Associated with the galaxy LEDA 158848, $W1 - W2 \sim 0.3$, a radio source.

SRGA J132532.0-621312

Based on the XMM-Newton position (4XMM J132531.2-621309, Webb et al. 2020), likely associated with the near-IR source VVV 358613430 (Smith et al. 2018).

SRGA J133836.9-352851

Associated with the galaxy 2MASS J13383728-3528517, $W1 - W2 \sim 1.3$.

SRGA J133950.6-643002

Possibly associated with IGR J13402-6428 at 2.8 arcmin from the ART-XC position. However, the latter is inconsistent with the positions of two *Chandra* sources, CXOU J133935.8-642537 and CXOU J133959.2-642444, which have been suggested as possible soft X-ray counterparts of IGR J13402-6428 (Tomsick et al. 2012).

SRGA J134742.7-621356

Likely, a supernova remnant (Reynolds et al. 2012).

SRGA J135418.5-374648

The ART-XC source is $39''$ away from the optical position of the Seyfert 2 galaxy Tol 1351-375 and appears to consist of two sources.

SRGA J135534.4+352045

A Seyfert 2 at $z = 0.1021$ (Koss et al. 2022a).

SRGA J140130.2-493239

An FR II radio galaxy (Burgess & Hunstead 2006).

SRGA J140146.3-501333

Possibly associated with the star Gaia DR3 6090855029847914368, at a distance ~ 1200 pc.

SRGA J140503.9-534130

Likely associated with the galaxy 2MASX J14050398-5341278, $W1 - W2 \sim 0.2$.

SRGA J141249.4-402138

A CV of VY Scl-type (Greiner et al. 2010).

SRGA J142006.2-165410

Likely associated with 2MASS J14200653-1653573 = NVSS J142006-165357 = CatWISE J142006.51-165357.0, $W1 - W2 = 1.2$, a flat-spectrum radio source (Itoh et al. 2020).

SRGA J142543.6-310716

Possibly associated with the galaxy 6dF J1425443-310721, $W1 - W2 \sim 0.5$.

SRGA J143701.5+073508

Associated with SDSS J143701.26+073508.3, a Seyfert 2 galaxy at $z = 0.18305$ (based on visual inspection of the SDSS spectrum), $W1 - W2 \sim 0.7$, a radio source.

SRGA J143739.3-361323

The hot subdwarf OB+ candidate (Geier et al. 2019) CD-359665 at a distance ~ 600 pc.

SRGA J144720.0-581607

Possibly associated with the luminous star Gaia DR3 5879166120570299776 at a distance ~ 3200 pc.

SRGA J144914.1-553620

A Seyfert 2 at $z = 0.0187$.

SRGA J145524.8-645953

Likely associated with WISEA J145523.78-650002.5, $W1 - W2 \sim 1.1$, which seems to be extended in DECaPS images.

SRGA J145532.6-544636

Associated with the galaxy 2MASX J14553197-5446291, $W1 - W2 \sim 0.8$.

SRGA J145738.5-362411

Possibly associated with WISEA J145737.30-362412.9, $W1 - W2 \sim 0.9$.

SRGA J150407.2-024810

There is a weak central AGN, but the X-ray emission from the intracluster gas clearly dominates (Böhlinger et al. 2005).

SRGA J151338.1-344046

Associated with the changing-look Seyfert galaxy 2MASX J15133881-3440408 (Hon et al. 2022).

SRGA J151425.6-545900

Likely associated with the bright star Gaia DR3 5886714375305398656, at a distance ~ 2 kpc, which is an ellipsoidal binary candidate (TESS, Green et al. 2023).

SRGA J151931.6-472604

Likely associated with the edge-on galaxy LEDA 2793198, $W1 - W2 \sim 0.2$.

SRGA J152102.1+320410

A Seyfert 2 at $z = 0.1143$ (Zaznobil et al. 2021).

SRGA J153158.5-293020

A blazar candidate (D'Abrusco et al. 2019).

SRGA J153309.3-522318

Possibly associated with the star Gaia DR3 5888715417783989760, at a distance ~ 850 pc, a hot subdwarf candidate (Geier et al. 2019).

SRGA J153412.6+625855

A Seyfert 1 at $z = 0.2372$ (Mejía-Restrepo et al. 2022).

Article number, page 24 of 67

SRGA J153603.0-574849

Associated with WISEA J153602.80-574853.3, $W1 - W2 \sim 0.8$.

SRGA J153814.2-554215

Likely a LMXB (Degenaar et al. 2012).

SRGA J154426.3-201636

Associated with WISEA J154426.00-201634.3, $W1 - W2 \sim 1.1$.

SRGA J154743.0-442203

Likely associated with WISEA J154743.17-442158.4, $W1 - W2 \sim 0.6$.

SRGA J155432.1-334006

Likely associated with 2MASS J15543155-3340151, $W1 - W2 \sim 1.2$.

SRGA J155603.4-521610

The non-magnetic CV ASASSN-19rc (Canbay et al. 2023).

SRGA J155901.6-733759

Associated with WISEA J155902.56-733748.5, $W1 - W2 \sim 0.8$.

SRGA J160050.8-514300

A colliding-wind Wolf-Rayet binary (Callingham et al. 2019).

SRGA J160455.4-722323

Associated with the flaring M-dwarf ASASSN-16hl (Schmidt et al. 2019).

SRGA J160534.2+164904

Associated with the known Seyfert 2 galaxy 2MASX J16053413+1649078 at $z = 0.141$, previously undetected in X-rays.

SRGA J160947.4-545110

Possibly associated with WISEA J160947.26-545107.8, $W1 - W2 \sim 0.6$.

SRGA J161018.6-634242

A Seyfert 1.5, at $z = 0.2094$ (Stephen et al. 2018).

SRGA J161251.4-052105

A Seyfert 2 at $z = 0.0306$ (Uskov et al. 2023).

SRGA J161537.9+594546

Possibly associated with Gaia DR3 1624769330460296192, $W1 - W2 \sim 0.8$, which can be a galaxy. However, there is also a star, Gaia DR3 1624769330461204096, within 2 arcsec.

SRGA J161728.9-502245

Possibly a CV (Tomsick et al. 2012).

SRGA J161735.5+501447

The known AGN SBS 1616+503, previously undetected in X-rays.

SRGA J161944.1-132618

A Seyfert 1.9 at $z = 0.0789$ (Uskov et al. 2023).

SRGA J161947.6+435849

Possibly associated with the quasar SDSS J161946.29+435915.4, $z = 0.8524$, a giant radio quasar (Kuźmicz & Jamroz 2021). However, the offset (29.5 arcsec) is significantly larger than the error radius ($R_{98} = 19.9$ arcsec).

SRGA J162312.1-260324

Possibly associated with WISEA J162311.77-260338.1, $W1 - W2 \sim 1.2$, and with the strong radio source NVSS J162312-260320.

SRGA J162420.7-331101

A Seyfert 2 at $z = 0.0279$ (Koss et al. 2022b).

SRGA J162618.5-392702

The known optical transient ASASSN-17ep (Jayasinghe et al. 2019), associated with either the star Gaia DR3 6017984243894659840 or with the star Gaia DR3 6017984243877931008, which are within 1 arcsec of each other.

SRGA J163529.1-480606

A bright star at a distance ~ 1100 pc. Possibly an HMXB or a symbiotic X-ray binary.

SRGA J163827.9-441447

Possibly associated with the bright radio source AT20G J163827-441444.

SRGA J164046.2-032813

Possibly associated with the star Gaia DR3 4354844848120561920 at a distance ~ 1200 pc.

SRGA J164050.9+654718

Associated with the edge-on galaxy UGC 10519, an obscured AGN at $z = 0.0244$ (Uskov et al., in prep.).

SRGA J164356.8-321347

Possibly associated with the infrared and radio source WISEA J164356.93-321404.1 = NVSS J164356-321409, $W1 - W2 \sim 0.7$.

SRGA J164433.4-513411

Possibly associated with WISEA J164433.25-513413.2, $W1 - W2 \sim 0.3$ (CatWISE), which appears to be extended in DECaPS images.

SRGA J165143.2+532539

A known X-ray source, 2E 1650.6+5330 = 2RXS J165144.7+532532, associated with SBS 1650+535, a Seyfert 1.8 galaxy at $z = 0.0286$ (Uskov et al. 2024).

SRGA J165251.2+172700

Based on the XMM-Newton coordinates (4XMM J165251.4+172651, Webb et al. 2020), associated with the galaxy 2MASX J16525143+1726514, $W1 - W2 \sim 0.2$.

SRGA J165552.1-495737

A Seyfert 2 at $z = 0.0586$ (Malizia et al. 2023).

SRGA J170025.6-724043

A Seyfert 1 (Chen et al. 2022).

SRGA J170336.8+620130

An ambiguous nuclear transient (has some characteristics seen in both tidal disruption events and active galactic nuclei, Hinkle et al. 2022) in the galaxy NGC 6297.

SRGA J170412.5-443136

Also known as XTE J1704-445, a strongly variable X-ray source (Markwardt et al. 2007).

SRGA J170723.3-194422

Based on the XMM-Newton coordinates (XMMSL2 J170722.0-194429), likely associated with WISEA J170722.22-194426.3, $W1 - W2 \sim 0.3$, a radio source.

SRGA J171115.2+530953

Likely associated with WISEA J171115.73+530948.1, $W1 - W2 = 1.0$.

SRGA J171334.7-252015

Likely associated with WISEA J171334.96-252015.4, $W1 - W2 \sim 0.7$.

SRGA J171544.9-232608

Possibly associated with the star Gaia DR3 4114267164182444032, at a distance ~ 680 pc, $W1 - W2 \sim 0.5$, a radio source.

SRGA J173253.5-440735

Likely associated with the star Gaia DR3 5958345771178324224, at a distance ~ 1650 pc.

SRGA J173338.1+363133

A Seyfert 1.9 at $z = 0.0437$ (Koss et al. 2022a).

SRGA J173918.4-545409

Possibly associated with WISEA J173918.41-545401.2, $W1 - W2 \sim 0.9$.

SRGA J174008.8-284721

Likely an intermediate polar rather than a LMXB (Britt et al. 2013; Lo et al. 2014).

SRGA J174027.1-365542

Intermediate polar (Clavel et al. 2019).

SRGA J174038.1-273658

A new X-ray transient discovered by Swift/XRT on 9 April 2021 (Bahramian et al. 2021).

SRGA J174046.3+060353

A CV (Halpern & Thorstensen 2015).

SRGA J174201.3-605516

A Seyfert 1.5 at $z = 0.152$ (Rojas et al. 2017), a FR II radio galaxy (Maselli et al. 2022).

SRGA J174242.0+184112

A close binary system (Heinze et al. 2018) at a distance ~ 200 pc, with an X-ray luminosity $\sim 2 \times 10^{31}$ erg s $^{-1}$. Hence, possibly an RS CVn type system.

SRGA J174445.6-295046

A symbiotic X-ray binary (Bahramian et al. 2014).

SRGA J174850.6+665403

Associated with 2MASX J17485018+6653544, a Seyfert 2 galaxy at $z = 0.0261$ (Uskov et al., in prep.).

SRGA J175328.6-244632

A gamma Cas star.

SRGA J175340.5+654239

A Seyfert 1.9 at $z = 0.1487$ (Uskov et al., in prep.).

SRGA J175721.0-304409

Likely a LMXB with a giant companion (Maeda et al. 2013).

SRGA J175758.4+042732

Associated with the star Gaia DR3 4472788803304480896, a CV (Zaznobil et al., in prep.).

SRGA J175806.5+660038

Associated with LEDA 2682746, a Seyfert 1.9 galaxy at $z = 0.0871$ (Uskov et al., in prep.).

SRGA J180312.5+045110

Likely associated with the infrared source WISEA J180313.39+045115.4, $W1 - W2 \sim 0.9$.

SRGA J180342.0+615651

Associated with the infrared and radio source WISEA J180341.28+615653.3, a Seyfert 1 galaxy at $z = 0.4178$ (Uskov et al., in prep.).

SRGA J180639.3+663247

Associated with 2MASS J18063992+6632411, a Seyfert 2 galaxy at $z = 0.0867$ (Uskov et al., in prep.).

SRGA J180731.6+662950

Associated with WISEA J180733.80+662941.8, a Seyfert 1.9 galaxy at $z = 0.2615$ (Uskov et al., in prep.).

SRGA J180849.4+663426

A flat-spectrum radio source (Massaro et al. 2014).

SRGA J181227.8-181237

An ultra-compact LMXB and burster (Goodwin et al. 2019).

SRGA J181239.8-221924

An X-ray transient. Likely a black-hole X-ray binary, based on X-ray and radio properties (Russell et al. 2022).

SRGA J181636.0-391251

Likely an intermediate polar associated with the star Gaia DR3 6727363681257990016 (Karasev et al. 2020).

SRGA J181749.5+234311

Associated with LEDA 1692433, a Seyfert 1.9 galaxy at $z = 0.0813$ (Uskov et al. 2024).

SRGA J181815.4-545033

Possibly associated with WISEA J181814.61-545027.2, $W1 - W2 \sim 0.7$.

SRGA J182111.0+765816

A Seyfert 2 at $z = 0.0631$ (Uskov et al. 2023).

SRGA J182156.3+642033

A powerful AGN in the central galaxy of a rich cluster. The X-ray luminosities of the quasar and cluster are comparable, according to previous observations, in particular Chandra (Russell et al. 2010; Reynolds et al. 2014).

SRGA J182510.7+645021

A KO giant star with blended double lines in the optical spectrum (Sperauskas et al. 2019), thus most likely a coronally active binary.

SRGA J182528.9+720905

A Seyfert 2 at $z = 0.1108$ (Koss et al. 2022a).

SRGA J182832.6-592055

A blazar candidate (Chang et al. 2019).

SRGA J183754.5+155436

Possibly associated with the bright variable star ASAS J183754+1554.7 = Gaia DR3 4510001297611019392 at a distance ~ 500 pc,

SRGA J183811.5+655457

A Seyfert 1 at $z = 0.2301$ (Uskov et al., in prep.).

SRGA J183906.5-571501

Associated with the infrared source WISEA J183905.95-571505.1, $W1 - W2 \sim 1.8$; suggested to be a BL Lac based on the featureless optical spectrum (Malizia et al. 2023). However, the optical counterpart (Gaia DR3 6637527637032850176) appears to have a large proper motion.

SRGA J184006.8+592011

Likely associated with the galaxy NGC 6696, $W1 - W2 \sim 0.3$.

SRGA J184119.5-045617

The magnetar 1E 1841-045 in the supernova remnant Kes 73, which are both bright in X-rays (An et al. 2013; Kumar et al. 2014) and consistent with the ART-XC position.

SRGA J185421.6+083842

Based on the position of the soft X-ray counterpart determined with *Swift*/XRT (Karasev et al. 2018), the object is likely associated with the infrared source CatWISE J185422.29+083846.1, $W1 - W2 \sim 1.0$, which is likely a star (Zaznubin et al., in prep.).

SRGA J190140.6+012628

An LMXB (Karasev et al. 2012).

SRGA J190308.3+733241

Likely associated with the galaxy WISEA J190306.44+733246.0, $W1 - W2 \sim 0.8$.

SRGA J190529.2-263916

Likely associated with WISEA J190528.57-263915.0, $W1 - W2 \sim 1.1$, a radio source.

SRGA J190629.4-044655

Possibly associated with WISEA J190628.35-044655.2, $W1 - W2 \sim 0.7$.

SRGA J190722.1-204641

Likely an intermediate polar (Xu et al. 2019).

SRGA J191438.9+502846

Associated with the galaxy WISEA J191437.56+502854.6, $W1 - W2 \sim 0.9$, a radio source.

SRGA J191456.9+103641

Likely a HMXB (Cusumano et al. 2015).

SRGA J191628.1+711619

Associated with WISEA J191629.25+711616.4, a Seyfert 1 galaxy at $z = 0.0984$ (Uskov et al. 2024).

SRGA J192413.0+665631

Likely associated with WISEA J192408.23+665624.1, $W1 - W2 \sim 0.8$, a radio source.

SRGA J192501.9+504316

A Seyfert 1.2 at $z = 0.068$ (Masetti et al. 2013).

SRGA J193346.0+325424

A Seyfert 1.2 at $z = 0.063$ (Landi et al. 2007).

SRGA J193707.1+660811

A narrow-line Seyfert 1 galaxy at $z = 0.0714$ (Uskov et al. 2023).

SRGA J194412.5-243619

Associated with 2MASX J19441243-2436217, a Seyfert 2 galaxy at $z = 0.1402$ (Uskov et al. 2024).

SRGA J194438.6-043223

Possibly associated with the star Gaia DR3 4209574176412222336, at a distance ~ 1200 pc.

SRGA J194638.0+704554

An intermediate polar (Zaznobin et al. 2022a).

SRGA J195226.6+380011

Associated with 2MASS J19522509+3800269, a Seyfert 1 galaxy at $z = 0.0767$ (Uskov et al. 2024).

SRGA J195702.7+615028

A Seyfert 1 at $z = 0.0586$ (Uskov et al. 2022).

SRGA J195815.6+194141

A Seyfert 1 at $z = 0.0310$ (Burenin et al. 2016).

SRGA J195927.9+404358

A significant contribution of the central AGN to the X-ray luminosity of the cluster is expected (Young et al. 2002).

SRGA J200206.8+413240

Associated with the strong, flat-spectrum (de Gasperin et al. 2018) radio source NVSS J200206+413243.

SRGA J200331.8+701331

A Seyfert 1 at $z = 0.0976$ (Uskov et al. 2023).

SRGA J200431.2+610218

A Seyfert 2 at $z = 0.05866$ (Zaznobin et al. 2021).

SRGA J201116.5+600418

A CV (Zaznobin et al., in prep.).

SRGA J201633.2+705525

Associated with WISEA J201632.61+705527.2, a Seyfert 1 galaxy at $z = 0.2579$ (Uskov et al. 2024).

SRGA J201921.1+300257

Likely associated with the star Gaia DR3 1861455769748627584, at a distance ~ 900 pc, which is an ellipsoidal binary candidate (TESS, Green et al. 2023).

SRGA J202835.2+254401

A Compton-thick AGN, MCG +04-48-002, at $z = 0.0136$ in a galaxy pair with another Compton-thick AGN, NGC 6921, at $z = 0.0147$. The ART-XC source is associated with MCG +04-48-002, since NGC 6921 is 91" away (Koss et al. 2016).

SRGA J202931.7-614911

A Seyfert 2 at $z = 0.1243$ (Koss et al. 2022a).

SRGA J203515.3+220628

Likely associated with the star Gaia DR3 1818529770639712384 at a distance ~ 800 pc. Suggested to be a pulsating hot subdwarf based on TESS photometry (Krzyszinski & Balona 2022).

SRGA J204149.7-373346

A blazar candidate (Chang et al. 2019) or a cluster of galaxies (Schwope et al. 2000).

SRGA J204318.6+443820

An X-ray pulsar in a Be HMXB system, discovered by SRG/ART-XC and eROSITA (Lutovinov et al. 2022), also known as SRGA J204318.2+443815 = SRGe J204319.0+443820.

SRGA J204547.9+672640

A magnetic CV (Zaznobin et al. 2022a).

SRGA J205522.2+401808

Likely associated with the Be star HD 199356 at a distance ~ 700 pc. Hence, possibly a gamma Cas star.

SRGA J210501.3-353121

Likely associated with WISEA J210500.56-353141.7, W1 – W2 ~ 1.0 , a radio source.

SRGA J210906.7+480643

Likely associated with the star Gaia DR3 2165328756082487168 at a distance ~ 1200 pc, which is an H α -excess source (FratTA et al. 2021) and has been tentatively classified as a dwarf nova¹¹.

¹¹ <https://www.aavso.org/vsx/index.php?view=detail.top&oid=686625>

SRGA J211148.9+722812

A Seyfert 2 at $z = 0.1061$ (Uskov et al. 2023).

SRGA J211644.6+533408

An eclipsing CV with an orbital period of 0.2731 days (Halpern et al. 2018).

SRGA J211703.9-485605

Associated with the galaxy 2MASX J21170265-4856128, $W1 - W2 \sim 0.3$.

SRGA J211747.2+513848

A blazar at $z = 0.0533$ (Koss et al. 2022a).

SRGA J212901.0+363110

Non-magnetic CV (Canbay et al. 2023).

SRGA J213152.0+491400

Associated with the optical transient AT 2019weg = Gaia19fd = ZTF19acfixfe, a CV (Szkody et al. 2021).

SRGA J214331.7+102854

Possibly associated with the star Gaia DR3 1765516439542838272, at a distance ~ 1600 pc.

SRGA J214503.7+634527

Possibly associated with WISEA J214505.18+634541.2, $W1 - W2 \sim 1.3$, which is also a radio source. In the optical, confusion of several objects.

SRGA J215706.5-694132

A broad-line radio galaxy (Angioni et al. 2020; Koss et al. 2022a).

SRGA J220355.8+613222

Likely associated with the star Gaia DR3 2203373473312011008 at ~ 400 pc, which is an H α -excess source (Fratta et al. 2021) and has been classified as a CV based on variability¹².

SRGA J220706.9+360935

Likely associated with WISEA J220707.91+360933.7, $W1 - W2 \sim 0.5$, also a radio source.

SRGA J221913.5+362004

A Seyfert 2 at $z = 0.14667$ (Uskov et al. 2022).

SRGA J222516.9+012242

A gamma Cas star.

SRGA J223132.7-750114

Possibly associated with the star Gaia DR3 6357827237727811712, at a distance ~ 1800 pc.

SRGA J223453.0-843445

A Seyfert 1 at $z = 0.1630$ (Mejía-Restrepo et al. 2022).

SRGA J223715.8+402944

A Seyfert 1 at $z = 0.0582$ (Uskov et al. 2022).

SRGA J225413.1+690700

A CV (Zaznobilin et al. 2022a).

SRGA J230338.2+465214

Associated with WISEA J230338.31+465159.5, a Seyfert 2 galaxy at $z = 0.0460$ (Uskov et al., in prep.).

SRGA J230631.0+155633

Associated with SDSS J230630.38+155620.4, a radio-loud Seyfert 2 galaxy at $z = 0.439$ (Uskov et al., in prep.).

SRGA J230641.7+550827

An intermediate polar (Halpern et al. 2018).

SRGA J230821.7-782225

Likely associated with the galaxy IRAS 23047-7838 = 6dFGSgJ230828.1-782223, $W1 - W2 \sim 1.4$, a radio source.

SRGA J231951.5+564446

Possibly associated with WISEA J231950.48+564444.4, $W1 - W2 \sim 1.0$.

SRGA J232038.1+482320

A Seyfert 2 at $z = 0.04197$ (Uskov et al. 2022).

SRGA J234620.9+812214

Possibly associated with the star Gaia DR3 2286390896172757760, at a distance ~ 1.3 kpc.

SRGA J235250.7-170448

A Seyfert 1 at $z = 0.055$ (Uskov et al. 2022; Koss et al. 2022a).

¹² <https://www.aavso.org/vsx/index.php?view=detail.top&oid=844414>

SRGA J235335.2-454210

Likely associated with the galaxy LEDA 523799, $W1 - W2 \sim 1.4$.

Table A.1. Catalog of sources^{a)} detected during the first five surveys of the *SRG/ART-XC*.

Id	Name SRGA	RA (J2000)	Dec (J2000)	R98 (")	S/N	Flux (10^{-12} erg s $^{-1}$ cm $^{-2}$)	Conventional name	Redshift	Class
N001	J000048.1-070914	0.2005	-7.1539	20.5	6.36	5.69 ± 1.74	SWIFT J0001.0-0708	0.0375	SEYFERT ^{c)}
N002	J000132.9+240237 ^{b)}	0.3869	24.0435	21.1	5.57	3.96 ± 1.36		0.1045	SEYFERT ^{c)}
N003	J000148.6-765739	0.4526	-76.9607	17.9	5.57	3.85 ± 1.22	SWIFT J0001.6-7701	0.0585	SEYFERT
N004	J000310.3+215744	0.7931	21.9622	21.5	5.81	3.58 ± 1.23	Mrk 334	0.0219	SEYFERT
N005	J000359.1+701922	0.9962	70.3227	18.7	6.21	2.19 ± 0.62	IGR J00040+7020	0.0960	SEYFERT
N006	J000549.7+102227	1.4571	10.3742	20.4	5.62	4.38 ± 1.47	RX J0005.8+1022	0.0948	SEYFERT
N007	J000632.6-690026	1.6357	-69.0071	15.4	8.17	5.63 ± 1.47	CTCV J0006-6900		CV
N008	J000636.0+434219	1.6499	43.7052	19.7	6.67	3.61 ± 0.99	2RXS J000637.0+434223	0.1660	SEYFERT
N009	J001030.5+105836	2.6269	10.9767	14.4	7.79	6.20 ± 1.62	Mrk 1501	0.0872	BLAZAR
N010	J001123.9-112850	2.8496	-11.4805	12.5	10.55	11.16 ± 2.26	WW Cet		CV
N011	J001439.6+183500	3.6649	18.5833	17.6	7.01	4.99 ± 1.42	XMMSL2 J001439.6+183450	0.0180	SEYFERT ^{c)}
N012	J001706.1+813458	4.2754	81.5828	13.2	8.73	3.69 ± 0.81	6C 001403+811827	3.3660	BLAZAR
N013	J002052.7+554212	5.2197	55.7034	26.2	6.03	3.62 ± 1.02	V592 Cas		CV
N014	J002107.1-191005	5.2797	-19.1681	23.2	5.38	4.94 ± 1.76	2RXS J002108.2-190950	0.0956	SEYFERT
N015	J002203.6+254017	5.5150	25.6713	17.3	7.89	5.57 ± 1.49	XMMSL1 J002202.9+254004	0.1292	SEYFERT ^{c)}
N016	J002241.4+804348	5.6723	80.7299	17.7	6.83	2.97 ± 0.75	2RXS J002247.6+804418	0.1147	SEYFERT ^{c)}
N017	J002256.9+614101	5.7372	61.6837	11.0	10.91	6.30 ± 1.18	V1033 Cas		CV
N018	J002314.4-152032 ^{b)}	5.8100	-15.3422	21.3	5.44	3.55 ± 1.32			UNIDENT
N019	J002848.1+591719	7.2004	59.2885	4.3	36.56	40.45 ± 2.84	V709 Cas		CV
N020	J002913.8+131610	7.3074	13.2695	23.3	5.52	4.23 ± 1.40	PG 0026+129	0.1420	SEYFERT
N021	J003418.8-790528	8.5782	-79.0912	14.2	7.69	4.42 ± 1.15	RBS 78	0.0741	SEYFERT
N022	J003512.1-450330 ^{b)}	8.8005	-45.0584	23.7	5.41	3.79 ± 1.50			UNIDENT
N023	J003535.1+462345 ^{b)}	8.8963	46.3960	18.3	5.86	3.63 ± 1.11			CV ^{c)}
N024	J003552.3+595003	8.9678	59.8341	5.6	26.25	25.22 ± 2.28	1ES 0033+59.5	0.0860	BLAZAR
N025	J003620.5+454004	9.0853	45.6677	19.4	5.60	2.66 ± 0.89	2MASX J00362092+4539532	0.0476	SEYFERT
N026	J003708.9+612142	9.2872	61.3617	10.2	12.69	8.49 ± 1.38	IGR J00370+6122		HMXB
N027	J003734.3-083620 ^{b)}	9.3927	-8.6054	19.7	5.37	3.24 ± 1.20			UNIDENT
N028	J003746.2-304828	9.4425	-30.8077	21.4	5.59	4.52 ± 1.55	2MASX J00374706-3048335	0.0608	SEYFERT
N029	J003834.0+412837	9.6417	41.4770	24.0	6.16	3.44 ± 1.06	2MASX J00383316+4128509	0.0725	SEYFERT
N030	J003947.5-754949 ^{b)}	9.9479	-75.8304	22.2	5.70	2.96 ± 1.02			AGN? ^{c)}
N031	J004013.0+405009	10.0542	40.8360	14.7	7.28	4.90 ± 1.25	5C 3.76		BLAZAR
N032	J004042.3-791427	10.1763	-79.2410	19.1	6.60	4.01 ± 1.14	ESO 12-21	0.0300	SEYFERT
N033	J004050.1+100324	10.2089	10.0566	16.4	7.62	5.89 ± 1.62	3C 18.0	0.1877	SEYFERT
N034	J004142.9+413410	10.4288	41.5694	16.8	7.18	4.30 ± 1.18	2RXS J004143.4+413423		LMXB? ^{c)}
N035	J004150.4-091819	10.4600	-9.3053	16.5	9.19	9.50 ± 2.11	Abell 85	0.0556	CLUSTER
N036	J004217.0+401944	10.5709	40.3288	17.7	6.30	3.15 ± 1.00	2E 0039.5+4003	0.1027	SEYFERT
N037	J004223.1+290401 ^{b)}	10.5961	29.0668	18.4	6.14	3.30 ± 1.07		0.0711	SEYFERT ^{c)}
N038	J004238.9+411603	10.6621	41.2676	22.2	5.80	3.55 ± 1.14	M31		GALAXY ^{c)}
N039	J004313.9+410723	10.8080	41.1231	19.3	5.61	2.95 ± 0.99	CXOM31 J004314.3+410721		LMXB ^{c)}
N040	J004505.9+620746	11.2747	62.1295	20.9	5.64	2.28 ± 0.76	2RXS J004504.6+620757		SNR? ^{c)}
N041	J004519.8+212744	11.3325	21.4621	21.2	5.81	3.59 ± 1.23	RX J0045.3+2127	2.0700	BLAZAR

Table A.1. continued.

Id	Name SRGA	RA (J2000)	Dec (J2000)	R98 (")	S/N	Flux (10^{-12} erg s $^{-1}$ cm $^{-2}$)	Conventional name	Redshift	Class
N042	J004545.6+413956	11.4400	41.6657	19.8	5.64	2.56 ± 0.90	2E 0042.9+4123		X-RAY BINARY ^{c)}
N043	J004732.9-251713	11.8871	-25.2870	21.9	5.65	4.75 ± 1.64	NGC 253	0.0008	GALAXY ^{c)}
N044	J004752.7+544746	11.9696	54.7962	14.7	6.70	3.77 ± 1.05	4FGL J0047.9+5448		BLAZAR
N045	J004846.7+315729	12.1945	31.9579	5.7	26.01	31.11 ± 2.92	NGC 262	0.0153	BLAZAR
N046	J004852.9-734945	12.2204	-73.8290	19.6	5.95	4.00 ± 1.21	SXP 15.6		HMXB ^{c)}
N047	J005123.4+073033	12.8476	7.5092	22.1	5.82	4.02 ± 1.37	2RXS J005124.4+073043	0.6468	SEYFERT
N048	J005155.3+172604	12.9805	17.4344	12.9	10.27	9.04 ± 1.89	Mrk 1148	0.0645	SEYFERT
N049	J005451.9+252539	13.7161	25.4276	17.0	6.66	4.29 ± 1.18	PG 0052+251	0.1545	SEYFERT
N050	J005456.2-722644	13.7342	-72.4456	10.4	12.28	9.44 ± 1.67	2E 0053.2-7242		HMXB ^{c)}
N051	J005519.3+453026 ^{b)}	13.8304	45.5072	18.6	5.63	2.63 ± 0.89			UNIDENT
N052	J005519.9+461256	13.8330	46.2155	7.6	18.75	18.37 ± 2.24	V515 And		CV
N053	J005642.6+604301	14.1773	60.7169	2.3	73.91	131.45 ± 5.16	gam Cas		STAR ^{c)}
N054	J005720.2-222302	14.3343	-22.3838	18.9	6.77	4.85 ± 1.44	Ton S180	0.0620	SEYFERT
N055	J005953.1+314939	14.9713	31.8276	9.1	13.83	11.43 ± 1.89	Mrk 352	0.0149	SEYFERT
N056	J010332.9-643900	15.8872	-64.6501	18.3	5.92	3.54 ± 1.20	PKS 0101-649	0.1630	BLAZAR
N057	J010336.0-720135	15.8999	-72.0265	13.0	8.35	2.77 ± 0.64	SXP 1323		HMXB ^{c)}
N058	J010430.3-723133	16.1264	-72.5260	19.1	5.96	3.43 ± 1.07	SXP 164		HMXB ^{c)}
N059	J010545.9-343153	16.4411	-34.5313	18.9	7.30	6.28 ± 1.61	HE 0103-3447	0.0571	SEYFERT
N060	J010649.2-225128	16.7050	-22.8579	19.5	6.45	5.48 ± 1.56	CS Cet		STAR
N061	J010743.0+574423 ^{b)}	16.9290	57.7396	17.3	7.20	3.51 ± 0.98		0.0699	SEYFERT ^{c)}
N062	J010744.6+540742	16.9358	54.1284	27.7	5.40	3.11 ± 1.01	RXC J0107.7+5408	0.1066	CLUSTER
N063	J010942.0+731156	17.4250	73.1990	13.0	9.40	5.10 ± 1.05	3C 33.1	0.1810	SEYFERT
N064	J011322.0+251853	18.3418	25.3146	18.5	6.26	4.12 ± 1.27	SWIFT J0113.8+2515	1.5893	BLAZAR
N065	J011350.3-145049	18.4594	-14.8469	22.2	6.11	3.79 ± 1.27	Mrk 1152	0.0527	SEYFERT
N066	J011506.0+882903	18.7748	88.4843	22.8	5.50	2.34 ± 0.77	2RXS J011522.7+882921		STAR? ^{c)}
N067	J011630.5-123557	19.1272	-12.5992	22.8	5.57	3.16 ± 1.18	SWIFT J0116.5-1235	0.1424	SEYFERT ^{c)}
N068	J011704.8-732638	19.2701	-73.4440	1.3	152.79	163.61 ± 3.41	SMC X-1		HMXB ^{c)}
N069	J011802.8+651730	19.5118	65.2915	2.2	83.09	163.28 ± 5.84	4U 0114+65		HMXB
N070	J011832.3+634434	19.6345	63.7428	1.6	95.08	151.86 ± 4.66	4U 0115+63		HMXB
N071	J011905.4+160504	19.7727	16.0845	21.3	5.99	3.29 ± 1.10	SWIFT J0119.2+1604	0.0700	SEYFERT ^{c)}
N072	J012256.5+072508	20.7354	7.4189	15.2	7.66	4.36 ± 1.17	HD 8357		STAR
N073	J012308.4+342050	20.7849	34.3473	8.3	15.56	15.47 ± 2.26	1ES 0120+34.0	0.2700	BLAZAR
N074	J012337.9-231104	20.9079	-23.1844	18.2	6.09	4.23 ± 1.31	RBS 193	0.4040	BLAZAR
N075	J012345.8-584813	20.9408	-58.8037	7.5	20.83	22.77 ± 2.58	Fairall 9	0.0461	SEYFERT
N076	J012354.3-350400	20.9762	-35.0668	6.6	22.60	29.07 ± 3.04	NGC 526	0.0192	SEYFERT
N077	J012427.0+334757	21.1124	33.7991	11.3	11.13	8.65 ± 1.64	NGC 513	0.0195	SEYFERT
N078	J012531.4+320806	21.3809	32.1350	10.8	11.59	8.88 ± 1.66	Mrk 993	0.0155	SEYFERT
N079	J012750.9+380800	21.9622	38.1334	20.7	5.66	3.41 ± 1.10	2MASS J01275053+3808120		CV
N080	J012806.3-184824	22.0262	-18.8068	17.2	7.05	4.54 ± 1.30	MCG -03-04-072	0.0460	SEYFERT
N081	J012823.7+162743	22.0986	16.4621	22.8	5.53	3.13 ± 1.13	SWIFT J0128.4+1631	0.0383	SEYFERT ^{c)}
N082	J013053.9-060547 ^{b)}	22.7244	-6.0965	24.4	5.39	3.89 ± 1.33			UNIDENT
N083	J013350.9+303932	23.4619	30.6588	15.0	8.60	6.02 ± 1.42	M33 X-8		ULX ^{c)}

Table A.1. continued.

Id	Name SRGA	RA (J2000)	Dec (J2000)	R98 (")	S/N	Flux (10^{-12} erg s $^{-1}$ cm $^{-2}$)	Conventional name	Redshift	Class
N084	J013500.8-295441	23.7535	-29.9114	21.1	5.47	2.80 ± 0.99	HD 9770		STAR
N085	J013521.7+062554	23.8405	6.4316	21.9	6.01	3.05 ± 1.02	RX J0135.3+0625	0.1480	SEYFERT
N086	J013631.8+390601	24.1325	39.1003	22.0	5.96	3.85 ± 1.18	RX J0136.4+3905	0.7500	BLAZAR
N087	J013709.3+505724	24.2886	50.9567	16.2	6.19	3.49 ± 1.02	KT Per		CV
N088	J013749.2+581409	24.4550	58.2358	10.7	10.29	5.54 ± 1.10	RX J0137.7+5814		BLAZAR
N089	J013836.0-400048	24.6500	-40.0133	13.0	8.35	5.56 ± 1.32	ESO 297-18	0.0252	SEYFERT
N090	J013957.7+013206	24.9903	1.5349	21.8	5.41	3.52 ± 1.19	ICRF J013957.3+013146	0.2600	SEYFERT
N091	J014347.9-584558	25.9496	-58.7662	14.4	8.29	7.09 ± 1.69	4FGL J0143.7-5846		BLAZAR
N092	J014458.7-023211 ^{b)}	26.2445	-2.5364	21.3	5.59	3.23 ± 1.07		0.0957	AGN? ^{c)}
N093	J014621.8+614500	26.5907	61.7501	8.8	14.93	12.41 ± 1.79	4U 0142+61		MAGNETAR
N094	J014700.8+612129	26.7534	61.3580	6.1	23.98	23.87 ± 2.36	RX J0146.9+6121		HMXB
N095	J015006.8-322444 ^{b)}	27.5284	-32.4122	18.1	5.59	2.83 ± 0.97		0.0384	AGN? ^{c)}
N096	J015141.9-361109	27.9247	-36.1859	22.8	5.57	3.10 ± 1.03	ESO 354-4	0.0335	SEYFERT
N097	J015248.6-032652	28.2024	-3.4477	15.0	8.55	4.69 ± 1.17	IGR J01528-0326	0.0167	SEYFERT
N098	J015400.2-594750	28.5009	-59.7972	21.1	5.89	3.81 ± 1.22	RX J0154.0-5947		CV
N099	J015440.4-270705	28.6683	-27.1181	15.3	8.08	5.90 ± 1.44	Ton S233	0.1510	SEYFERT ^{c)}
N100	J015524.4+022825	28.8519	2.4735	15.5	6.85	5.09 ± 1.39	1ES 0152+02.2	0.0847	SEYFERT ^{c)}
N101	J015641.5-835833	29.1729	-83.9757	15.4	9.07	5.30 ± 1.16	2RXS J015633.8-835835		CV? ^{c)}
N102	J015657.4-530202	29.2393	-53.0339	11.2	11.06	8.22 ± 1.61	RBS 259	0.3043	BLAZAR ^{c)}
N103	J015709.6+471550	29.2901	47.2638	23.5	5.50	2.48 ± 0.91	PBC J0157.3+4715	0.0490	SEYFERT
N104	J020012.7+065507	30.0531	6.9185	18.2	5.61	2.81 ± 1.01	RX J0200.2+0655		CV? ^{c)}
N105	J020300.5-240211	30.7520	-24.0363	19.6	6.47	4.68 ± 1.39	RBS 273	0.1780	SEYFERT
N106	J020457.4-170123	31.2391	-17.0231	19.5	6.51	3.96 ± 1.10	PKS 0202-17	1.7395	BLAZAR
N107	J020540.0+644937	31.4166	64.8270	20.6	8.85	6.08 ± 1.32	3C 58		SNR / PULSAR
N108	J020639.4-714824	31.6640	-71.8066	22.4	5.62	2.86 ± 0.93	PKS 0205-720	0.2600	BLAZAR? ^{c)}
N109	J020653.7+151745	31.7238	15.2958	9.7	14.40	14.57 ± 2.20	TT Ari		CV
N110	J020749.4+445032	31.9556	44.8422	22.3	5.70	2.95 ± 1.01	SWIFT J0208.2+4452	0.0217	SEYFERT ^{c)}
N111	J020835.4-173931	32.1475	-17.6587	22.1	5.44	2.56 ± 0.88	IGR J02086-1742	0.1290	SEYFERT
N112	J020916.8+444933	32.3199	44.8258	17.0	7.65	5.10 ± 1.32	2RXS J020917.8+444946		BLAZAR
N113	J020926.0-295350	32.3584	-29.8974	21.0	5.75	2.77 ± 0.97	RBS 286	0.1749	SEYFERT
N114	J020934.3-742717	32.3927	-74.4548	8.1	16.68	13.19 ± 1.77	RX J0209.6-7427		HMXB
N115	J020937.8+522645	32.4076	52.4460	6.3	23.38	21.60 ± 2.21	2E 0206.3+5212	0.0492	SEYFERT
N116	J020950.1-631843	32.4590	-63.3118	13.0	11.16	7.22 ± 1.36	WX Hyi		CV
N117	J021052.5-494155	32.7188	-49.6986	15.6	7.65	4.47 ± 1.13	ESO 197-27	0.0481	SEYFERT
N118	J021412.4-353738	33.5517	-35.6271	19.1	5.53	2.79 ± 0.95	2RXS J021411.8-353747		BLAZAR
N119	J021417.4+514444	33.5727	51.7456	15.9	8.18	5.24 ± 1.24	RX J0214.2+5144	0.0490	BLAZAR
N120	J021434.5-004558	33.6437	-0.7660	22.0	5.50	3.44 ± 1.17	NGC 863	0.0261	SEYFERT
N121	J021435.8-643002	33.6490	-64.5005	16.3	7.27	4.67 ± 1.22	RBS 295	0.0739	SEYFERT
N122	J021643.4+255250 ^{b)}	34.1806	25.8805	23.1	5.60	3.08 ± 1.08		0.0663	SEYFERT ^{c)}
N123	J021722.4+382454	34.3435	38.4151	18.5	7.00	4.76 ± 1.31	Ark 79	0.0175	SEYFERT
N124	J021731.8+734936	34.3826	73.8266	14.0	9.41	4.24 ± 0.94	6C 021252+733537	2.3462	BLAZAR
N125	J022207.0+522119	35.5293	52.3553	19.1	5.68	3.37 ± 1.08	RX J0222.1+5221	0.2000	SEYFERT

Table A.1. continued.

Id	Name SRGA	RA (J2000)	Dec (J2000)	R98 (")	S/N	Flux (10^{-12} erg s $^{-1}$ cm $^{-2}$)	Conventional name	Redshift	Class
N126	J022235.4+250818	35.6474	25.1383	14.6	9.04	6.25 ± 1.46	SWIFT J0222.3+2509	0.0616	SEYFERT ^{c)}
N127	J022332.6+454922	35.8860	45.8229	14.7	7.84	4.69 ± 1.14	SWIFT J0223.4+4551	0.0620	SEYFERT
N128	J022431.7-654413 ^{b)}	36.1319	-65.7368	23.7	5.59	2.77 ± 0.91			UNIDENT
N129	J022441.1-190834	36.1713	-19.1427	18.4	6.43	3.38 ± 1.03	ESO 545-13	0.0337	SEYFERT
N130	J022503.5-231242	36.2646	-23.2118	22.7	5.38	2.42 ± 0.83	PKS 0222-23	0.2322	SEYFERT
N131	J022507.9-631310	36.2828	-63.2195	23.3	5.99	3.30 ± 1.06	Fairall 296	0.0572	SEYFERT
N132	J022625.5+592746	36.6064	59.4628	18.2	6.95	4.13 ± 1.12	SWIFT J0225.8+5946		SEYFERT ^{c)}
N133	J022746.2-693129	36.9427	-69.5248	9.3	15.10	10.80 ± 1.62	CL Hyi		STAR? ^{c)}
N134	J022814.6+311843	37.0609	31.3120	6.4	21.11	24.03 ± 2.75	NGC 931	0.0166	SEYFERT
N135	J023005.4-085952	37.5226	-8.9978	10.5	12.60	10.77 ± 1.86	Mrk 1044	0.0164	SEYFERT
N136	J023053.7-684157	37.7238	-68.6993	17.1	6.47	3.31 ± 0.95	CW Hyi		CV
N137	J023150.4-364027	37.9598	-36.6741	19.1	6.12	3.30 ± 0.99	IC 1816	0.0169	SEYFERT
N138	J023231.4+383938 ^{b)}	38.1307	38.6607	20.9	5.46	2.32 ± 0.84			UNIDENT
N139	J023247.8+201719	38.1994	20.2887	13.9	7.71	5.39 ± 1.40	1ES 0229+20.0	0.1390	BLAZAR
N140	J023347.9+022927	38.4496	2.4908	20.0	6.07	3.65 ± 1.16	PKS 0231+022	0.3208	BLAZAR
N141	J023420.3+323026	38.5847	32.5073	7.1	22.69	27.81 ± 2.95	NGC 973	0.0162	SEYFERT
N142	J023438.0-084716	38.6583	-8.7878	13.2	10.51	8.52 ± 1.67	NGC 985	0.0431	SEYFERT
N143	J023800.1+193818	39.5005	19.6384	26.7	5.39	3.32 ± 1.17	2RXS J023759.4+193802	0.0335	SEYFERT ^{c)}
N144	J023808.0-310624 ^{b)}	39.5332	-31.1066	23.3	5.39	2.40 ± 0.86			UNIDENT
N145	J023820.5-521144	39.5853	-52.1954	14.8	7.58	3.37 ± 0.87	ESO 198-24	0.0456	SEYFERT
N146	J023832.0-311700	39.6335	-31.2831	8.9	13.95	10.68 ± 1.63	RBS 337	0.2329	BLAZAR
N147	J023842.2-611725	39.6758	-61.2902	11.3	10.58	6.17 ± 1.20	SWIFT J0238.5-6119	0.0544	SEYFERT
N148	J023848.7-403835	39.7029	-40.6432	15.6	6.62	3.37 ± 0.97	CTS B21.06	0.0612	SEYFERT
N149	J024032.0+611348	40.1334	61.2301	13.4	9.56	6.68 ± 1.35	LS I +61 303		HMXB
N150	J024134.4+071115	40.3934	7.1876	18.5	5.89	3.93 ± 1.21	Mrk 595	0.0270	SEYFERT
N151	J024240.7-000054	40.6694	-0.0149	13.4	9.50	7.69 ± 1.64	NGC 1068	0.0038	SEYFERT
N152	J024251.5+564132	40.7145	56.6922	7.6	17.72	15.64 ± 2.03	PT Per		CV
N153	J024457.8+622807	41.2408	62.4687	5.3	26.79	29.40 ± 2.65	4U 0241+61	0.0448	SEYFERT
N154	J024844.0+310655	42.1832	31.1153	14.2	9.05	5.97 ± 1.38	VY Ari		STAR
N155	J024859.5+263041	42.2478	26.5113	17.7	6.64	3.99 ± 1.14	SWIFT J0249.1+2627	0.0580	SEYFERT
N156	J025027.3+464734	42.6139	46.7927	13.5	8.65	6.68 ± 1.52	SWIFT J0250.2+4650	0.0219	SEYFERT
N157	J025208.6+482952	43.0358	48.4978	19.0	6.03	3.47 ± 1.09	2RXS J025208.8+482956	0.0337	SEYFERT ^{c)}
N158	J025223.3-083042	43.0969	-8.5117	16.7	8.27	5.69 ± 1.39	IGR J02524-0829	0.0168	SEYFERT
N159	J025234.6+431001	43.1443	43.1670	16.4	6.39	3.38 ± 1.06	2SXPS J025233.8+431001	0.0512	SEYFERT ^{c)}
N160	J025431.4+413519	43.6310	41.5887	18.7	6.71	4.80 ± 1.31	2A 0251+413	0.0172	CLUSTER
N161	J025608.0+192636	44.0334	19.4433	13.0	9.58	7.91 ± 1.67	XY Ari		CV
N162	J025621.2-321104	44.0883	-32.1844	10.7	12.28	8.61 ± 1.45	ESO 417-6	0.0163	SEYFERT
N163	J025854.9+133415	44.7287	13.5709	18.1	7.18	6.27 ± 1.63	Abell 401	0.0737	CLUSTER
N164	J025900.3+502958 ^{b)}	44.7512	50.4993	24.1	5.79	3.45 ± 1.09		0.0946	SEYFERT ^{c)}
N165	J030003.9-104928	45.0164	-10.8246	7.1	19.69	20.34 ± 2.43	MCG -02-08-038	0.0326	SEYFERT
N166	J030008.1+163030	45.0339	16.5082	16.0	8.22	5.48 ± 1.35	RX J0300.1+1630	0.0350	SEYFERT
N167	J030536.3+762243	46.4013	76.3786	20.1	6.42	3.29 ± 0.96	2RXS J030536.9+762258	0.1966	SEYFERT ^{c)}

Table A.1. continued.

Id	Name SRGA	RA (J2000)	Dec (J2000)	R98 (")	S/N	Flux (10^{-12} erg s $^{-1}$ cm $^{-2}$)	Conventional name	Redshift	Class
N168	J030605.9-390219	46.5246	-39.0385	18.5	6.24	2.37 ± 0.74	NGC 1217	0.0210	SEYFERT
N169	J030735.2-725008	46.8965	-72.8355	10.7	10.64	5.86 ± 1.09	1H 0307-722	0.0276	SEYFERT
N170	J030810.8+405719	47.0449	40.9552	10.8	12.09	12.72 ± 2.15	bet Per		STAR
N171	J030838.7-552042 ^{b)}	47.1613	-55.3450	17.9	6.18	2.29 ± 0.67		0.0779	SEYFERT ^{c)}
N172	J031103.3-440228	47.7639	-44.0411	17.6	6.47	2.65 ± 0.73	1BIGB J031103.1-440227		BLAZAR
N173	J031118.1-204618	47.8253	-20.7718	15.1	7.93	4.72 ± 1.16	RX J0311.3-2046	0.0670	SEYFERT
N174	J031130.8-315249	47.8783	-31.8804	9.4	13.66	9.06 ± 1.45	2QZ J031130.9-315250		CV ^{c)}
N175	J031202.1+502911	48.0087	50.4864	15.4	8.08	5.47 ± 1.33	2RXS J031202.6+502922	0.0619	SEYFERT
N176	J031324.7-350643	48.3528	-35.1120	19.4	5.66	3.10 ± 0.93	CTS 76	0.1149	SEYFERT
N177	J031402.8+244442	48.5116	24.7451	19.4	6.06	4.29 ± 1.35	IRAS 03110+2433	0.0558	SEYFERT ^{c)}
N178	J031415.5-542459	48.5648	-54.4164	18.3	5.67	1.97 ± 0.63	2RXS J031412.7-542519		AGN? ^{c)}
N179	J031757.9-441434	49.4914	-44.2427	20.6	8.49	5.02 ± 1.06	Abell 3112	0.0759	CLUSTER
N180	J031819.5-662903	49.5813	-66.4842	19.0	5.66	1.83 ± 0.60	NGC 1313 X-1		ULX
N181	J031819.6+682920	49.5816	68.4889	15.3	7.68	3.88 ± 0.99	SWIFT J0318.7+6828	0.0901	SEYFERT
N182	J031948.8+413042	49.9532	41.5115	5.6	36.15	86.01 ± 5.42	Perseus Cluster	0.0176	CLUSTER
N183	J031952.1+184536	49.9670	18.7600	8.3	17.61	19.42 ± 2.61	1E 0317.0+1835	0.1900	BLAZAR
N184	J032317.9-481816	50.8244	-48.3045	19.4	5.61	1.85 ± 0.56	2RXS J032320.6-481809	0.1550	SEYFERT ^{c)}
N185	J032440.7+341046	51.1698	34.1794	15.7	8.71	6.40 ± 1.51	1H 0323+342	0.0629	BLAZAR
N186	J032503.0-415412	51.2625	-41.9033	17.5	6.66	2.97 ± 0.81	Fairall 1106	0.0578	SEYFERT
N187	J032511.9+404152	51.2997	40.6979	16.8	7.52	4.46 ± 1.24	IGR J03249+4041	0.0475	SEYFERT ^{c)}
N188	J032523.9-563550	51.3498	-56.5972	9.0	12.71	5.97 ± 0.96	2RXS J032522.4-563545	0.0602	BLAZAR
N189	J032635.5+284246	51.6480	28.7128	8.2	16.77	18.72 ± 2.56	UX Ari		STAR
N190	J032718.6+552032	51.8274	55.3422	21.6	5.44	2.93 ± 1.00	3C 86		AGN? ^{c)}
N191	J032846.5-530316	52.1936	-53.0545	21.6	5.57	1.88 ± 0.60	2SXPS J032845.3-530331	0.0771	AGN? ^{c)}
N192	J032910.2-220116	52.2925	-22.0211	18.9	6.29	3.20 ± 0.99	SWIFT J0329.4-2157	0.0349	SEYFERT ^{c)}
N193	J033052.0+053817	52.7167	5.6380	19.8	6.86	4.13 ± 1.22	1ES 0328+054	0.0460	SEYFERT
N194	J033111.9+435417	52.7996	43.9047	8.4	17.10	16.60 ± 2.25	GK Per		CV
N195	J033203.9-704000	53.0162	-70.6665	20.1	5.78	2.42 ± 0.72	4FGL J0331.8-7040	0.2770	BLAZAR ^{c)}
N196	J033319.0+371812	53.3291	37.3032	14.8	8.35	6.21 ± 1.48	IGR J03334+3718	0.0550	SEYFERT
N197	J033336.4-360827	53.4015	-36.1407	7.3	19.19	14.42 ± 1.69	NGC 1365	0.0055	SEYFERT
N198	J033336.5-370656	53.4022	-37.1155	22.9	6.09	2.94 ± 0.84	CTS 77	0.0640	SEYFERT ^{c)}
N199	J033354.0+201438	53.4751	20.2438	21.5	5.41	3.03 ± 1.10	2RXS J033354.1+201457		UNIDENT
N200	J033622.6-605854	54.0943	-60.9817	20.8	5.52	1.42 ± 0.47	2RXS J033624.4-605849	0.4710	SEYFERT ^{c)}
N201	J033624.0-034729	54.0998	-3.7913	21.2	5.53	2.77 ± 0.99	2RXS J033623.3-034728	0.1618	BLAZAR
N202	J033630.0+321818	54.1248	32.3050	19.8	7.06	4.89 ± 1.37	4C 32.14	1.2594	BLAZAR
N203	J033647.5+003513	54.1979	0.5870	10.8	12.26	10.95 ± 1.91	HD 22468		STAR
N204	J033840.0+095826	54.6665	9.9738	20.5	6.78	6.60 ± 1.73	2A 0335+096	0.0350	CLUSTER
N205	J034114.2+045325	55.3093	4.8903	19.4	5.66	3.23 ± 1.10	RX J0341.2+0453	0.0840	SEYFERT
N206	J034203.7-211448	55.5153	-21.2465	11.2	11.42	8.02 ± 1.45	ESO 548-81	0.0145	SEYFERT
N207	J034208.7+633930	55.5363	63.6584	20.9	5.65	2.89 ± 0.95	RX J0342.0+6339	0.1280	SEYFERT
N208	J034209.2+631301	55.5384	63.2171	15.7	7.24	4.30 ± 1.11	BD Cam		CV
N209	J034305.8-533753	55.7741	-53.6315	20.9	5.90	2.27 ± 0.67	Abell 3158	0.0597	CLUSTER

Table A.1. continued.

Id	Name SRGA	RA (J2000)	Dec (J2000)	R98 (")	S/N	Flux (10^{-12} erg s $^{-1}$ cm $^{-2}$)	Conventional name	Redshift	Class
N210	J034511.1-393427	56.2961	-39.5743	14.5	7.29	3.31 ± 0.83	TOL 0343-397	0.0430	SEYFERT
N211	J034838.2-274912	57.1593	-27.8199	18.7	6.14	2.65 ± 0.83	PKS 0346-27	0.9910	BLAZAR
N212	J034849.9+482738 ^{b)}	57.2078	48.4606	22.6	5.49	3.38 ± 1.10			UNIDENT
N213	J034923.4-115925	57.3475	-11.9903	10.8	11.92	9.97 ± 1.74	1ES 0347-121	0.1850	BLAZAR
N214	J035023.8-501809	57.5991	-50.3026	13.7	8.14	3.31 ± 0.73	ESO 201-4	0.0359	SEYFERT ^{c)}
N215	J035103.2-502830	57.7634	-50.4750	15.3	6.63	2.44 ± 0.65	RBS 480	0.2671	SEYFERT
N216	J035128.5-142909	57.8689	-14.4858	20.4	5.42	2.87 ± 0.96	3C 95	0.6140	SEYFERT
N217	J035141.5-402755	57.9228	-40.4653	15.3	7.94	3.88 ± 0.90	Fairall 1116	0.0586	SEYFERT
N218	J035256.9-683122	58.2370	-68.5229	8.1	14.63	7.56 ± 1.07	PKS 0352-686	0.0870	BLAZAR
N219	J035409.6+024926	58.5399	2.8240	19.3	6.25	4.17 ± 1.26	2E 0351.5+0240	0.0360	SEYFERT
N220	J035410.3-165257	58.5428	-16.8824	18.8	5.78	2.72 ± 0.91	RBS 490		CV
N221	J035522.9+310244	58.8456	31.0455	1.8	111.80	353.45 ± 9.99	X Per		HMXB
N222	J035558.3-610436	58.9931	-61.0766	13.3	7.93	2.42 ± 0.56	1ES 0355-61.2	0.2266	SEYFERT
N223	J035657.2-404134	59.2385	-40.6928	16.0	7.18	3.04 ± 0.81	SWIFT J0356.9-4041	0.0748	SEYFERT
N224	J035745.5+415457	59.4397	41.9159	18.9	6.80	4.15 ± 1.22	SWIFT J0357.6+4153	0.0518	SEYFERT ^{c)}
N225	J035758.2-001112	59.4926	-0.1865	23.3	5.47	3.21 ± 1.11	RX J0357.9-0011	0.0139	SEYFERT
N226	J035930.2+505751	59.8756	50.9643	12.7	9.59	7.06 ± 1.46	4C 50.11	1.5187	BLAZAR
N227	J040111.1-535446	60.2962	-53.9127	23.1	5.74	1.88 ± 0.54	2RXS J040111.3-535457		BLAZAR? ^{c)}
N228	J040225.5-180253	60.6064	-18.0481	14.3	8.58	5.11 ± 1.19	ESO 549-49	0.0263	SEYFERT
N229	J040335.6+472440	60.8983	47.4112	23.3	5.37	3.18 ± 1.06	2RXS J040337.5+472432	0.0962	SEYFERT ^{c)}
N230	J040502.0-371110	61.2582	-37.1861	9.3	14.67	9.39 ± 1.36	ESO 359-19	0.0552	SEYFERT
N231	J040533.7-130819	61.3903	-13.1386	19.9	5.85	3.23 ± 1.05	PKS 0403-13	0.5706	BLAZAR
N232	J040543.1+570730	61.4296	57.1250	18.2	6.73	4.33 ± 1.22	RX J0405.6+5707		STAR ^{c)}
N233	J040551.3+380353	61.4639	38.0648	21.0	6.67	4.34 ± 1.30	4C 37.11	0.0551	BLAZAR ^{c)}
N234	J040749.5-121126	61.9561	-12.1906	15.9	8.31	5.55 ± 1.34	PKS 0405-123	0.5726	BLAZAR
N235	J040753.2-611607	61.9717	-61.2686	17.1	6.55	1.86 ± 0.49	SWIFT J0407.8-6116	0.0214	SEYFERT ^{c)}
N236	J040850.6-791410	62.2108	-79.2362	14.6	8.01	3.52 ± 0.83	2SXPS J040848.1-791405		CV? ^{c)}
N237	J040912.5-711736	62.3020	-71.2932	12.3	9.24	3.66 ± 0.76	VW Hyi		CV
N238	J040941.0-075334	62.4210	-7.8929	6.2	25.49	35.27 ± 3.22	EI Eri		STAR
N239	J041108.8-591127	62.7867	-59.1907	16.8	5.49	1.47 ± 0.44	2RXS J041110.1-591111		CV ^{c)}
N240	J041241.4-471243	63.1723	-47.2120	10.2	12.32	5.44 ± 0.89	RBS 518	0.1320	SEYFERT
N241	J041243.1+582520	63.1797	58.4223	24.6	5.60	3.28 ± 1.11	SWIFT J0412.8+5842	0.0684	SEYFERT ^{c)}
N242	J041325.1+102747	63.3546	10.4631	11.5	16.99	25.28 ± 3.08	Abell 478	0.0881	CLUSTER
N243	J041328.1-061455	63.3670	-6.2486	23.2	5.60	2.98 ± 1.05	ICRF J041328.2-061501	0.1586	BLAZAR ^{c)}
N244	J041452.6-075537	63.7193	-7.9270	10.5	12.65	10.76 ± 1.81	2E 0412.4-0802	0.0384	SEYFERT
N245	J041456.6-533940	63.7357	-53.6611	15.2	7.24	2.23 ± 0.55	RBS 526		BLAZAR
N246	J041733.7-525302 ^{b)}	64.3903	-52.8840	18.4	5.66	1.58 ± 0.47		0.0456	AGN? ^{c)}
N247	J041821.3+380136	64.5889	38.0268	6.4	24.08	28.83 ± 2.95	3C 111	0.0488	SEYFERT
N248	J042000.8-545615	65.0032	-54.9376	8.3	15.14	5.89 ± 0.79	NGC 1566	0.0050	SEYFERT
N249	J042201.0+485608	65.5044	48.9356	22.4	6.79	4.75 ± 1.29	IGR J04221+4856	0.1140	SEYFERT
N250	J042202.4-415331	65.5099	-41.8920	16.0	7.06	2.52 ± 0.67	CTS B26.08	0.0621	SEYFERT
N251	J042223.3-561338	65.5973	-56.2272	11.8	8.23	2.42 ± 0.52	ESO 157-23	0.0435	SEYFERT

Table A.1. continued.

Id	Name SRGA	RA (J2000)	Dec (J2000)	R98 (")	S/N	Flux (10^{-12} erg s $^{-1}$ cm $^{-2}$)	Conventional name	Redshift	Class
N252	J042316.3-012036	65.8179	-1.3434	15.9	7.18	5.25 ± 1.36	PKS 0420-01	0.9161	BLAZAR
N253	J042340.2+040757	65.9173	4.1325	18.9	6.70	4.54 ± 1.27	IRAS 04210+0400	0.0461	SEYFERT
N254	J042435.7-754140	66.1487	-75.6945	18.6	5.54	2.17 ± 0.65	2RXS J042441.4-754115		STAR? ^{c)}
N255	J042533.8+344728	66.3910	34.7912	19.4	6.34	4.35 ± 1.29	2RXS J042533.0+344715	0.0578	SEYFERT
N256	J042554.9-194540	66.4787	-19.7611	13.1	9.53	5.55 ± 1.22	IW Eri		CV
N257	J042600.5-571200	66.5021	-57.2001	5.4	22.86	10.62 ± 0.98	1H 0419-577	0.1040	SEYFERT
N258	J042608.9+354143	66.5372	35.6953	19.0	6.56	4.94 ± 1.42	2RXS J042608.9+354149		CV
N259	J042616.8-592325	66.5702	-59.3902	12.7	7.66	1.61 ± 0.37	XMMSL2 J042617.5-592334		AGN? ^{c)}
N260	J042917.0-265430	67.3207	-26.9084	14.5	7.12	3.31 ± 0.90	HE 0427-27	0.0640	SEYFERT
N261	J043008.4+455702	67.5352	45.9506	17.5	6.85	4.44 ± 1.27	XMMSL2 J043008.4+455656		CV? ^{c)}
N262	J043041.9-533654	67.6745	-53.6149	17.0	6.14	1.70 ± 0.47	Fairall 303	0.0400	SEYFERT
N263	J043125.8-612530	67.8574	-61.4250	17.4	9.06	1.49 ± 0.27	Abell 3266	0.0589	CLUSTER
N264	J043136.8-024122	67.9034	-2.6895	20.3	5.95	3.42 ± 1.08	RBS 550	0.0420	SEYFERT
N265	J043208.9+354922	68.0369	35.8226	9.7	13.68	11.92 ± 2.01	XMMSL2 J043208.2+354924	0.0506	SEYFERT ^{c)}
N266	J043311.1+052116	68.2963	5.3546	5.0	31.44	40.81 ± 3.43	3C 120	0.0330	SEYFERT
N267	J043353.7+643803	68.4739	64.6341	19.9	6.17	4.07 ± 1.25	MS Cam		STAR
N268	J043510.7-752749	68.7946	-75.4637	10.6	10.53	4.78 ± 0.87	2RXS J043510.3-752731		CV? ^{c)}
N269	J043516.4+512821	68.8185	51.4725	20.7	5.87	4.81 ± 1.54	LSXPS J043519.8+512833		AGN? ^{c)}
N270	J043517.3-780155	68.8222	-78.0320	16.8	6.47	2.43 ± 0.66	ESO 15-11	0.0612	SEYFERT
N271	J043523.0+552235 ^{b)}	68.8457	55.3764	1.3	165.73	372.27 ± 7.87			LMXB ^{c)}
N272	J043554.1-363638	68.9754	-36.6106	16.6	6.74	2.76 ± 0.77	CTS A29.15	0.1410	SEYFERT
N273	J043622.0-102241	69.0915	-10.3781	10.9	11.61	8.43 ± 1.57	Mrk 618	0.0355	SEYFERT
N274	J043728.9-471130	69.3706	-47.1917	13.6	7.92	2.84 ± 0.66	1ES 0435-472	0.0530	SEYFERT
N275	J043814.2-104746	69.5590	-10.7960	17.4	7.78	5.25 ± 1.30	MCG -02-12-050	0.0364	SEYFERT
N276	J043828.0-614803	69.6167	-61.8009	12.5	9.16	2.32 ± 0.46	RBS 563	0.0690	SEYFERT
N277	J043838.8-661405	69.6616	-66.2347	18.8	5.50	1.33 ± 0.40	Fairall 304	0.0489	AGN? ^{c)}
N278	J043858.5+071638	69.7437	7.2773	21.7	5.35	3.23 ± 1.11	RXC J0439.0+0715	0.2450	CLUSTER
N279	J043930.0-043556	69.8752	-4.5988	16.8	7.75	5.42 ± 1.37	BF Eri		CV
N280	J043943.9-090312	69.9328	-9.0534	22.6	6.20	3.38 ± 1.07	2RXS J043944.4-090331	0.0518	SEYFERT ^{c)}
N281	J043958.9-594100	69.9954	-59.6833	13.3	8.85	2.13 ± 0.43	ESO 118-33	0.0580	SEYFERT
N282	J044017.9-433306	70.0745	-43.5516	12.5	9.40	3.95 ± 0.83	PKS 0438-43	2.8630	BLAZAR
N283	J044048.9+292443	70.2037	29.4120	18.5	6.46	3.85 ± 1.23	2RXS J044047.9+292441		STAR ^{c)}
N284	J044058.8+443154	70.2452	44.5317	11.6	11.60	11.29 ± 2.17	RX J0440.9+4431		HMXB
N285	J044122.5-270818	70.3438	-27.1383	11.2	9.73	5.57 ± 1.13	H 0439-272	0.0835	SEYFERT
N286	J044153.9-082635	70.4746	-8.4432	19.3	5.39	2.66 ± 0.94	1ES 0439-085	0.0410	SEYFERT
N287	J044321.0+472121	70.8375	47.3558	23.8	5.63	4.18 ± 1.46	V392 Per		CV
N288	J044345.8+285807	70.9410	28.9686	22.1	5.82	4.74 ± 1.44	UGC 3142	0.0217	SEYFERT
N289	J044408.0+281300	71.0335	28.2165	18.7	7.14	5.41 ± 1.51	SWIFT J0444.1+2813	0.0113	SEYFERT
N290	J044437.4-280949	71.1559	-28.1636	15.4	7.25	3.37 ± 0.88	PKS 0442-28	0.1475	SEYFERT
N291	J044657.2-030518	71.7383	-3.0883	20.9	6.07	3.48 ± 1.10	2RXS J044656.8-030514	0.0313	SEYFERT
N292	J044721.1-050812	71.8378	-5.1368	20.1	6.49	4.18 ± 1.19	2RXS J044720.3-050813	0.0449	SEYFERT
N293	J044925.4-435007	72.3557	-43.8353	10.5	10.43	4.45 ± 0.83	PKS 0447-439	0.1070	BLAZAR

Table A.1. continued.

Id	Name SRGA	RA (J2000)	Dec (J2000)	R98 (")	S/N	Flux (10^{-12} erg s $^{-1}$ cm $^{-2}$)	Conventional name	Redshift	Class
N294	J044942.5-391122	72.4269	-39.1893	14.1	7.56	3.09 ± 0.76	PKS 0448-392	1.2995	BLAZAR
N295	J044942.6-643628	72.4276	-64.6079	15.4	6.79	1.34 ± 0.33	IRAS 04493-6441	0.0600	SEYFERT
N296	J044956.8-642127 ^{b)}	72.4868	-64.3575	19.4	5.74	1.04 ± 0.29			AGN? ^{c)}
N297	J045001.1-494525	72.5044	-49.7570	18.9	5.55	1.53 ± 0.46	XMMSL2 J045000.1-494522		AGN? ^{c)}
N298	J045001.8-551240	72.5076	-55.2111	16.4	6.34	1.37 ± 0.38	SWIFT J0449.6-5515	0.0216	SEYFERT ^{c)}
N299	J045048.9+301443	72.7037	30.2454	22.0	5.99	4.78 ± 1.53	SWIFT J0450.6+3015	0.0331	SEYFERT ^{c)}
N300	J045142.2-034840	72.9259	-3.8110	21.8	5.57	2.85 ± 1.00	MCG-01-13-025	0.0154	SEYFERT
N301	J045143.8-581057	72.9325	-58.1825	7.8	14.86	4.54 ± 0.58	RBS 594	0.0910	SEYFERT
N302	J045204.3+493243	73.0179	49.5453	12.0	11.15	11.72 ± 2.27	RX J0452.0+4932	0.0277	SEYFERT
N303	J045253.8-585350	73.2242	-58.8973	11.4	9.20	2.07 ± 0.40	2RXS J045253.9-585349		BLAZAR? ^{c)}
N304	J045411.4-664334	73.5475	-66.7261	17.5	5.55	1.14 ± 0.33	RX J0454.1-6643	0.2280	SEYFERT
N305	J045424.1-570045 ^{b)}	73.6003	-57.0125	15.6	5.94	1.22 ± 0.34			AGN? ^{c)}
N306	J045431.0+171229 ^{b)}	73.6291	17.2081	23.4	5.49	4.32 ± 1.52			UNIDENT
N307	J045431.4+524008 ^{b)}	73.6307	52.6688	14.1	8.08	6.60 ± 1.69		0.0312	SEYFERT ^{c)}
N308	J045442.2-431419	73.6760	-43.2386	12.4	8.46	3.14 ± 0.71	2RXS J045444.3-431427	0.0877	SEYFERT ^{c)}
N309	J045550.7-461554	73.9614	-46.2651	16.0	6.30	1.88 ± 0.53	PKS 0454-46	0.8528	BLAZAR
N310	J045600.1-753228	74.0004	-75.5412	13.6	8.67	2.98 ± 0.62	ESO 033-2	0.0181	SEYFERT
N311	J045602.7+273600	74.0113	27.6000	14.3	7.91	6.81 ± 1.83	V721 Tau		STAR? ^{c)}
N312	J045609.3-215904	74.0386	-21.9844	16.7	5.86	2.45 ± 0.78	PKS 0454-22	0.5340	SEYFERT
N313	J045708.1+452747	74.2838	45.4630	11.6	11.75	12.39 ± 2.33	2RXS J045707.2+452751		CV
N314	J045817.7-751643	74.5738	-75.2786	8.0	15.79	6.36 ± 0.83	YY Men		STAR
N315	J045957.7-611506	74.9906	-61.2517	12.3	8.55	1.74 ± 0.34	RBS 607	0.0860	SEYFERT
N316	J050021.4+523801	75.0890	52.6335	13.2	8.81	7.74 ± 1.84	XMMSL2 J050021.4+523801		BLAZAR ^{c)}
N317	J050125.9-703338	75.3579	-70.5606	16.9	6.19	1.51 ± 0.41	2E 0501.8-7037		HMXB ^{c)}
N318	J050209.3+033139	75.5385	3.5274	14.5	8.95	7.48 ± 1.86	2E 0459.5+0327	0.0160	SEYFERT
N319	J050227.3+244519	75.6137	24.7552	10.0	13.63	15.21 ± 2.64	V1062 Tau		CV
N320	J050249.5-622749	75.7061	-62.4637	17.0	6.33	0.98 ± 0.25	EC 05023-6231		AGN? ^{c)}
N321	J050259.0+225943	75.7456	22.9954	15.1	9.56	9.51 ± 2.24	RX J0502.9+2259	0.0555	SEYFERT
N322	J050303.5-663356	75.7648	-66.5654	12.4	8.38	1.69 ± 0.35	CAL F	0.0640	SEYFERT
N323	J050434.1-553129 ^{b)}	76.1419	-55.5246	20.0	5.56	1.23 ± 0.36		0.0221	AGN? ^{c)}
N324	J050434.1-734930	76.1423	-73.8250	10.0	10.58	3.90 ± 0.68	IGR J05053-7343	0.0452	SEYFERT
N325	J050441.0-423225 ^{b)}	76.1708	-42.5403	20.5	5.42	1.69 ± 0.54			UNIDENT
N326	J050643.9-610946	76.6830	-61.1629	17.6	5.39	0.91 ± 0.26	PKS 0506-61	1.0930	BLAZAR
N327	J050648.3-193651	76.7013	-19.6142	16.6	6.79	4.20 ± 1.16	2RXS J050648.3-193650	0.0941	SEYFERT
N328	J050755.6+673721	76.9818	67.6226	16.0	7.91	5.31 ± 1.40	1ES 0502+675	0.3140	BLAZAR
N329	J050809.7-660656	77.0405	-66.1155	4.4	28.58	8.90 ± 0.65	2RXS J050810.2-660645		HMXB ^{c)}
N330	J050956.7-641743	77.4863	-64.2953	8.4	14.08	3.07 ± 0.39	RBS 625	0.2710	BLAZAR ^{c)}
N331	J051045.5+162955	77.6897	16.4985	9.2	17.19	25.71 ± 3.52	4U 0517+17	0.0179	SEYFERT
N332	J051111.0-110305 ^{b)}	77.7960	-11.0514	22.1	6.16	3.37 ± 1.17		0.1168	SEYFERT ^{c)}
N333	J051157.7-182935	77.9905	-18.4932	19.6	6.29	3.98 ± 1.22	ESO 553-22	0.0421	SEYFERT
N334	J051300.0-252322 ^{b)}	78.2501	-25.3895	18.5	6.76	4.28 ± 1.25			CV? ^{c)}

Table A.1. continued.

Id	Name SRGA	RA (J2000)	Dec (J2000)	R98 (")	S/N	Flux (10^{-12} erg s $^{-1}$ cm $^{-2}$)	Conventional name	Redshift	Class
N335	J051313.8+662746	78.3077	66.4627	16.1	7.62	5.30 ± 1.39	2SXPS J051316.0+662750	0.0148	SEYFERT ^{c)}
N336	J051327.8-654718	78.3656	-65.7884	7.7	14.64	3.00 ± 0.36	SWIFT J0513.4-6547		HMXB
N337	J051400.8-402723 ^{b)}	78.5033	-40.4564	20.0	5.48	1.88 ± 0.62			AGN? ^{c)}
N338	J051401.8-504559	78.5076	-50.7664	18.6	5.71	1.48 ± 0.43	2RXS J051400.7-504606		AGN ^{c)}
N339	J051406.6-400237	78.5276	-40.0437	2.6	67.60	89.93 ± 3.68	4U 0513-40		LMXB
N340	J051611.3-000900	79.0470	-0.1497	9.4	15.27	18.93 ± 2.82	Ark 120	0.0327	SEYFERT
N341	J051620.9-103344	79.0873	-10.5622	16.0	7.07	4.85 ± 1.42	MCG -02-14-009	0.0284	SEYFERT
N342	J051638.7-514648	79.1613	-51.7801	10.9	12.56	4.48 ± 0.67	RBS 635	0.2220	SEYFERT
N343	J051903.6+630347	79.7650	63.0630	17.1	8.34	5.84 ± 1.51	2RXS J051905.0+630333		STAR
N344	J051935.3-323924	79.8971	-32.6565	9.4	14.54	10.66 ± 1.66	ESO 362-18	0.0124	SEYFERT
N345	J051949.9-454643	79.9577	-45.7787	5.6	24.53	16.55 ± 1.48	Pictor A	0.0350	SEYFERT
N346	J052028.6-715734	80.1190	-71.9595	0.9	206.01	307.86 ± 4.67	LMC X-2		LMXB ^{c)}
N347	J052101.4-252154	80.2556	-25.3650	21.3	5.69	3.57 ± 1.17	IRAS 05189-2524	0.0428	SEYFERT
N348	J052115.1+251331	80.3130	25.2253	16.0	7.41	6.85 ± 1.87	ASASSN-15pq		CV ^{c)}
N349	J052257.6-362738	80.7401	-36.4604	8.2	14.40	10.00 ± 1.51	PKS 0521-36	0.0566	BLAZAR
N350	J052412.0-662049	81.0501	-66.3470	10.8	8.34	1.28 ± 0.24	RX J0524.2-6620		HMXB ^{c)}
N351	J052430.1+424457	81.1252	42.7492	12.8	9.44	8.78 ± 1.99	Paloma		CV
N352	J052503.0-693848	81.2624	-69.6467	14.3	7.79	1.74 ± 0.37	SNR J052501-693842		SNR ^{c)}
N353	J052523.5+241328	81.3478	24.2244	12.8	11.18	13.11 ± 2.53	RX J0525.3+2413		CV
N354	J052602.5-660510	81.5106	-66.0862	15.3	5.77	0.64 ± 0.17	N49/SGR 0526-66		SNR / PULSAR ^{c)}
N355	J052627.5-211716	81.6148	-21.2879	13.2	9.74	6.67 ± 1.48	SWIFT J0526.2-2118	0.0278	SEYFERT ^{c)}
N356	J052802.4-393451	82.0098	-39.5808	17.7	6.58	3.06 ± 0.86	2RXS J052802.3-393450	0.0367	SEYFERT ^{c)}
N357	J052832.9+283827	82.1372	28.6409	13.5	10.82	10.80 ± 2.26	2RXS J052832.2+283821		CV
N358	J052844.5-652655	82.1853	-65.4487	3.8	33.85	6.57 ± 0.40	AB Dor		STAR
N359	J052858.5-670957	82.2436	-67.1658	13.7	6.44	0.95 ± 0.23	4XMM J052858.4-670946		HMXB ^{c)}
N360	J052915.0-662447 ^{b)}	82.3125	-66.4131	11.7	8.49	1.14 ± 0.21			HMXB ^{c)}
N361	J052925.4-324903	82.3560	-32.8176	4.5	33.99	43.85 ± 3.24	TV Col		CV
N362	J052947.7-655645	82.4488	-65.9460	3.8	31.09	6.12 ± 0.39	RX J0529.8-6556		HMXB ^{c)}
N363	J052959.2-340205	82.4966	-34.0346	18.6	6.69	3.42 ± 0.99	XMMSL2 J052958.9-340159	0.0790	SEYFERT ^{c)}
N364	J053013.2-655127	82.5551	-65.8575	19.2	5.27	0.56 ± 0.15	XMMU J053011.3-655123		HMXB ^{c)}
N365	J053043.0-665431	82.6790	-66.9085	8.7	11.49	2.08 ± 0.30	SWIFT J053041.9-665426		HMXB ^{c)}
N366	J053231.9+624752	83.1330	62.7977	20.3	6.41	4.71 ± 1.38	V391 Cam		CV
N367	J053232.2-655144	83.1343	-65.8622	9.8	11.35	1.38 ± 0.20	RX J0532.5-6551		HMXB ^{c)}
N368	J053249.5-662217	83.2062	-66.3713	1.2	114.03	39.75 ± 0.89	LMC X-4		HMXB ^{c)}
N369	J053322.0-684130	83.3419	-68.6918	15.2	6.34	1.09 ± 0.26	SWIFT J053321.3-684121		HMXB ^{c)}
N370	J053358.8-714528	83.4951	-71.7577	10.1	10.20	2.75 ± 0.47	2SXPS J053359.1-714523	0.0242	AGN? ^{c)}
N371	J053411.7-045030	83.5486	-4.8417	18.8	6.05	3.81 ± 1.31	2E 0531.7-0452		STAR? ^{c)}
N372	J053431.1-601614	83.6298	-60.2704	9.4	10.87	2.02 ± 0.32	2RXS J053431.6-601612	0.0570	SEYFERT
N373	J053431.5+220102	83.6311	22.0173	0.4	788.86	13790.05 ± 75.98	Crab		SNR / PULSAR
N374	J053450.5-580142	83.7106	-58.0284	3.0	47.61	20.70 ± 1.01	TW Pic		CV
N375	J053457.0+282840	83.7377	28.4779	17.1	7.33	5.64 ± 1.67	SWIFT J0535.2+2830		CV

Table A.1. continued.

Id	Name SRGA	RA (J2000)	Dec (J2000)	R98 (")	S/N	Flux (10^{-12} erg s $^{-1}$ cm $^{-2}$)	Conventional name	Redshift	Class
N376	J053515.2-052256	83.8132	-5.3821	8.9	22.24	39.97 ± 4.09	Orion Nebula Cluster		SFR
N377	J053526.1-691609	83.8589	-69.2691	10.9	8.73	1.53 ± 0.29	SN 1987A		SNR ^{c)}
N378	J053528.7-050541	83.8697	-5.0947	21.6	5.54	3.62 ± 1.30	4XMM J053529.0-050604		STAR? ^{c)}
N379	J053532.1+401121	83.8836	40.1892	18.0	6.39	4.92 ± 1.55	PBC J0535.6+4011	0.0200	SEYFERT
N380	J053600.6+502412 ^{b)}	84.0023	50.4035	19.0	5.84	4.25 ± 1.40			UNIDENT
N381	J053738.8+210827	84.4116	21.1408	9.7	14.14	18.68 ± 2.95	zet Tau		STAR ^{c)}
N382	J053748.0-691021	84.4501	-69.1725	6.7	16.05	3.30 ± 0.38	PSR J0537-6910		SNR / PULSAR ^{c)}
N383	J053854.4+261854	84.7266	26.3150	2.6	72.22	233.76 ± 9.78	A 0535+26		HMXB
N384	J053856.8-640503	84.7368	-64.0840	0.6	315.71	182.64 ± 1.73	LMC X-3		HMXB ^{c)}
N385	J053939.0-694439	84.9125	-69.7441	0.9	202.44	138.43 ± 2.06	LMC X-1		HMXB ^{c)}
N386	J054011.1-691956	85.0464	-69.3323	2.4	62.85	25.41 ± 0.96	PSR B0540-69		SNR / PULSAR ^{c)}
N387	J054023.2-554443	85.0967	-55.7454	19.0	6.38	1.44 ± 0.40	2RXS J054023.2-554448		AGN? ^{c)}
N388	J054134.6-682542	85.3943	-68.4284	11.6	8.38	1.33 ± 0.25	XMMU J054134.7-682550		HMXB ^{c)}
N389	J054248.0+605131	85.6999	60.8585	7.5	20.46	25.72 ± 3.04	BY Cam		CV
N390	J054320.1-410158	85.8335	-41.0327	6.5	19.58	14.16 ± 1.66	TX Col		CV
N391	J054356.6-553210	85.9860	-55.5362	7.9	15.66	6.13 ± 0.79	RBS 679	0.2730	BLAZAR
N392	J054423.0+590750	86.0958	59.1305	19.7	6.21	3.99 ± 1.27	SWIFT J0544.4+5909	0.0676	SEYFERT
N393	J054641.3-641520	86.6723	-64.2557	7.1	14.34	1.63 ± 0.19	RBS 681	0.3230	BLAZAR
N394	J054828.5-474533	87.1187	-47.7592	18.1	6.17	2.24 ± 0.64	ESO 205-3	0.0505	SEYFERT
N395	J054843.8+322907 ^{b)}	87.1826	32.4853	25.5	5.42	3.75 ± 1.39			UNIDENT
N396	J054921.3-620520	87.3387	-62.0889	9.9	12.35	2.48 ± 0.35	2RXC J0549.2-6205	0.3760	CLUSTER
N397	J054958.5+072518 ^{b)}	87.4937	7.4218	23.1	5.55	4.44 ± 1.53			UNIDENT
N398	J055033.9-663657	87.6412	-66.6159	11.4	7.10	0.45 ± 0.09	CAL 91	0.0752	SEYFERT
N399	J055040.7-321620	87.6695	-32.2721	7.1	19.40	17.27 ± 2.09	PKS 0548-322	0.0690	BLAZAR
N400	J055052.7-621453	87.7194	-62.2480	12.5	8.14	1.24 ± 0.25	2RXS J055054.2-621454	0.0587	SEYFERT ^{c)}
N401	J055211.3-072726	88.0469	-7.4573	5.3	30.27	53.53 ± 4.60	NGC 2110	0.0076	SEYFERT
N402	J055224.6-640214	88.1024	-64.0372	9.1	11.77	1.38 ± 0.19	PKS 0552-640	0.6800	BLAZAR
N403	J055228.1+592837	88.1171	59.4768	11.4	12.14	12.70 ± 2.33	2RXS J055229.4+592842	0.0581	SEYFERT
N404	J055329.9-815658	88.3746	-81.9494	21.4	5.48	1.61 ± 0.53	HD 42270		STAR
N405	J055453.4+462620	88.7226	46.4388	6.2	24.96	45.20 ± 4.60	MCG +08-11-11	0.0205	SEYFERT
N406	J055523.5-765506	88.8480	-76.9184	17.6	6.26	1.76 ± 0.47	XMMSL2 J055526.8-765509	0.0158	SEYFERT? ^{c)}
N407	J055646.5-331029	89.1939	-33.1746	7.5	19.38	19.81 ± 2.34	MAXI J0556-332		LMXB
N408	J055759.1+535342	89.4964	53.8950	10.1	14.40	17.15 ± 2.80	V405 Aur		CV
N409	J055801.5-382008	89.5063	-38.3355	8.2	14.43	11.19 ± 1.68	4U 0557-38	0.0339	SEYFERT
N410	J055805.0-564634 ^{b)}	89.5209	-56.7760	13.5	7.32	1.82 ± 0.44			SEYFERT ^{c)}
N411	J055807.3-383835	89.5303	-38.6432	18.9	6.11	3.16 ± 0.96	EXO 0556.4-3838	0.3020	BLAZAR
N412	J055947.3-502652	89.9470	-50.4477	7.5	17.58	10.71 ± 1.29	PKS 0558-504	0.1372	BLAZAR
N413	J060041.7+000619	90.1737	0.1052	23.5	5.44	5.08 ± 1.74	IRAS 05581+0006	0.1147	SEYFERT ^{c)}
N414	J060045.5-645602 ^{b)}	90.1895	-64.9338	15.7	5.64	0.47 ± 0.12			AGN ^{c)}
N415	J060210.6+282816	90.5443	28.4710	9.7	14.83	22.78 ± 3.74	RX J0602.1+2828	0.0330	SEYFERT
N416	J060211.3-673802	90.5470	-67.6340	20.0	5.21	0.29 ± 0.07	2RXS J060211.5-673811		AGN? ^{c)}

Table A.1. continued.

Id	Name SRGA	RA (J2000)	Dec (J2000)	R98 (")	S/N	Flux (10^{-12} erg s $^{-1}$ cm $^{-2}$)	Conventional name	Redshift	Class
N417	J060241.7-595155	90.6738	-59.8654	10.1	10.83	2.86 ± 0.48	XMMSL2 J060241.6-595149	0.1005	SEYFERT? ^{c)}
N418	J060431.7-395014 ^{b)}	91.1323	-39.8373	21.2	5.53	2.26 ± 0.82			AGN? ^{c)}
N419	J060533.9-640053	91.3913	-64.0147	12.4	8.15	1.19 ± 0.23	2RXS J060534.3-640051		UNIDENT
N420	J060548.9-275440	91.4537	-27.9111	17.6	7.72	5.98 ± 1.55	IGR J06058-2755	0.0892	SEYFERT
N421	J060650.6-624544	91.7109	-62.7622	8.1	13.04	2.62 ± 0.36	XMMSL2 J060649.4-624543		AGN? ^{c)}
N422	J060729.5-614832	91.8728	-61.8089	13.4	8.68	1.85 ± 0.37	ESO 121-6	0.0040	AGN ^{c)}
N423	J060917.4-560658	92.3227	-56.1161	11.9	9.36	3.20 ± 0.64	CTS H34.06	0.0318	SEYFERT
N424	J061006.7-624319	92.5278	-62.7220	10.1	10.95	2.39 ± 0.37	2RXS J061006.6-624312	0.1570	SEYFERT
N425	J061035.2-652521	92.6466	-65.4226	11.6	7.26	0.79 ± 0.16	2RXS J061036.9-652508	0.0367	SEYFERT ^{c)}
N426	J061111.1-095612 ^{b)}	92.7964	-9.9366	20.2	5.50	4.21 ± 1.45			CV? ^{c)}
N427	J061144.5-814925	92.9356	-81.8235	7.9	14.32	7.29 ± 1.04	AH Men		CV
N428	J061148.4-662434	92.9518	-66.4094	4.0	27.02	3.17 ± 0.21	IGR J06117-6625	0.2300	SEYFERT
N429	J061154.6-435703	92.9776	-43.9509	15.8	6.95	3.20 ± 0.91	2RXS J061154.0-435705		AGN? ^{c)}
N430	J061317.4-181228 ^{b)}	93.3226	-18.2078	22.2	5.62	4.17 ± 1.44			UNIDENT
N431	J061322.8+474419	93.3450	47.7386	8.5	16.67	21.12 ± 2.99	SS Aur		CV
N432	J061324.1-290027	93.3504	-29.0075	10.7	11.27	11.10 ± 2.06	2RXS J061324.1-290029	0.0705	SEYFERT ^{c)}
N433	J061351.3-074248 ^{b)}	93.4636	-7.7134	22.6	5.51	4.92 ± 1.72			UNIDENT
N434	J061448.3+093421 ^{b)}	93.7014	9.5725	22.3	6.07	5.48 ± 1.81			CV? ^{c)}
N435	J061538.6+710219	93.9109	71.0385	17.6	7.88	6.52 ± 1.66	Mrk 3	0.0135	SEYFERT
N436	J061547.9+094101 ^{b)}	93.9497	9.6837	22.7	6.09	5.70 ± 1.94			UNIDENT
N437	J061619.0-705229	94.0793	-70.8746	14.3	6.76	0.81 ± 0.19	2RXS J061617.5-705236		AGN? ^{c)}
N438	J061707.4+090814	94.2810	9.1371	1.4	128.80	779.22 ± 20.77	4U 0614+09		LMXB
N439	J061903.6-694744 ^{b)}	94.7652	-69.7957	19.3	5.27	0.52 ± 0.14			AGN? ^{c)}
N440	J062040.0+264338	95.1666	26.7271	24.8	5.60	5.87 ± 2.09	RX J0620.6+2644	0.1340	BLAZAR ^{c)}
N441	J062109.9-680551 ^{b)}	95.2913	-68.0974	7.0	12.78	1.35 ± 0.17		0.0651	SEYFERT ^{c)}
N442	J062308.1-643630	95.7837	-64.6085	8.9	10.84	1.98 ± 0.31	PMN J0623-6436	0.1289	BLAZAR
N443	J062339.4-265803	95.9140	-26.9674	18.9	6.41	5.32 ± 1.58	2RXS J062339.8-265744		CV ^{c)}
N444	J062345.4-605842	95.9393	-60.9784	6.8	15.75	5.13 ± 0.64	IGR J06239-6052	0.0405	SEYFERT
N445	J062405.6-093900	96.0233	-9.6500	13.5	9.59	9.56 ± 2.30	2MAXI J0623-095		CV
N446	J062516.2+733438	96.3175	73.5773	10.2	12.90	11.55 ± 1.96	MU Cam		CV
N447	J062627.7+072726	96.6153	7.4572	16.8	7.21	6.69 ± 2.00	SWIFT J0626.6+0729	0.0425	SEYFERT ^{c)}
N448	J062946.0-834423	97.4415	-83.7397	20.2	5.62	1.91 ± 0.60	SWIFT J0628.7-8346		AGN? ^{c)}
N449	J062952.9-113457 ^{b)}	97.4705	-11.5826	22.3	5.41	4.35 ± 1.63			UNIDENT
N450	J063107.8+112735	97.7823	11.4596	26.7	5.74	6.02 ± 2.11	SWIFT J0630.9+1129		UNIDENT
N451	J063200.6-540458	98.0027	-54.0828	12.7	8.55	3.49 ± 0.78	1ES 0630-540	0.2036	BLAZAR
N452	J063245.7+634017	98.1904	63.6713	21.2	5.63	4.00 ± 1.44	IRAS 06280+6342	0.0128	SEYFERT
N453	J063326.9-561425	98.3620	-56.2403	11.6	11.15	4.38 ± 0.76	2RXS J063326.4-561427	0.0478	SEYFERT ^{c)}
N454	J063403.2-744639	98.5133	-74.7775	16.9	7.19	1.74 ± 0.40	PBC J0635.0-7441	0.1120	SEYFERT
N455	J063517.1-695405	98.8214	-69.9013	13.2	7.52	0.89 ± 0.18	XMMSL2 J063516.4-695401	0.0803	AGN ^{c)}
N456	J063544.3-751615	98.9345	-75.2707	8.1	13.65	4.44 ± 0.60	PKS 0637-75	0.6530	BLAZAR
N457	J063558.5+075525	98.9937	7.9237	13.7	9.98	12.88 ± 2.83	2E 0633.2+0757		STAR ^{c)}

Table A.1. continued.

Id	Name SRGA	RA (J2000)	Dec (J2000)	R98 (")	S/N	Flux (10^{-12} erg s $^{-1}$ cm $^{-2}$)	Conventional name	Redshift	Class
N458	J063631.3+353557	99.1305	35.5992	28.9	5.61	6.47 ± 2.17	V647 Aur		CV
N459	J063845.1-535839	99.6881	-53.9776	17.9	7.41	3.22 ± 0.76	RXC J0638.7-5358	0.2245	CLUSTER
N460	J064005.0-125310	100.0207	-12.8860	22.7	5.71	4.23 ± 1.53	2RXS J064007.4-125316	0.1350	BLAZAR
N461	J064011.4-255341	100.0474	-25.8949	14.8	8.41	7.88 ± 1.86	2RXS J064011.5-255337	0.0249	SEYFERT
N462	J064038.0-432122	100.1585	-43.3561	15.9	7.34	3.62 ± 1.01	SWIFT J0640.1-4328	0.0610	SEYFERT
N463	J064046.4-242314	100.1932	-24.3873	25.5	5.37	4.17 ± 1.47	PU CMa		CV
N464	J064117.6+324929	100.3233	32.8248	11.6	11.21	16.17 ± 3.25	SWIFT J0641.3+3257	0.0486	SEYFERT
N465	J064151.5-032039	100.4644	-3.3442	20.0	6.07	5.22 ± 1.80	PMN J0641-0320	1.1960	BLAZAR ^{c)}
N466	J064421.9-662623	101.0913	-66.4398	11.9	7.76	1.20 ± 0.25	2RXS J064422.7-662623	0.0784	SEYFERT ^{c)}
N467	J064517.4-165136	101.3226	-16.8599	9.9	13.88	18.65 ± 3.04	HL CMa		CV
N468	J064529.3-541417	101.3720	-54.2380	23.9	5.49	2.78 ± 0.82	Abell 3404	0.1630	CLUSTER
N469	J064620.5-692813 ^{b)}	101.5853	-69.4704	14.0	7.45	0.90 ± 0.20		0.0612	SEYFERT ^{c)}
N470	J064709.9-513600	101.7911	-51.5999	13.2	8.64	4.25 ± 0.95	1ES 0646-51.5		BLAZAR
N471	J064846.6+151621	102.1944	15.2725	21.3	5.97	5.95 ± 1.97	RX J0648.7+1516	0.1790	BLAZAR
N472	J064849.8-694520	102.2076	-69.7557	12.8	7.37	0.98 ± 0.21	2RXS J064850.8-694520	0.2330	BLAZAR ^{c)}
N473	J064932.9-313922	102.3869	-31.6561	19.2	6.52	4.23 ± 1.35	2RXS J064933.7-313913		BLAZAR
N474	J065018.7-380522	102.5777	-38.0895	20.7	6.65	4.23 ± 1.22	2RXS J065017.7-380509	0.0300	SEYFERT ^{c)}
N475	J065047.6+250250	102.6985	25.0473	14.7	8.82	10.84 ± 2.68	1ES 0647+250	0.2030	BLAZAR
N476	J065213.0+742536	103.0542	74.4267	11.3	11.87	11.24 ± 2.09	Mrk 6	0.0195	SEYFERT
N477	J065313.0-673633	103.3044	-67.6091	15.7	6.04	0.91 ± 0.23	2RXS J065313.9-673638		CV ^{e)}
N478	J065316.2-670832	103.3174	-67.1423	17.7	5.48	0.82 ± 0.22	2RXS J065316.6-670818		AGN? ^{e)}
N479	J065434.1+070321	103.6421	7.0559	15.9	8.77	10.66 ± 2.61	RX J0654.5+0703	0.0232	SEYFERT
N480	J065513.2-012841	103.8048	-1.4781	20.0	6.77	6.90 ± 2.07	2SXPS J065512.4-012855		HMXB ^{c)}
N481	J065549.4+400001	103.9558	40.0003	10.2	13.31	16.73 ± 3.08	SWIFT J0655.8+3957	0.0171	SEYFERT
N482	J065638.8-670224 ^{b)}	104.1617	-67.0400	12.6	8.70	1.46 ± 0.28			CV? ^{c)}
N483	J065721.8-670549 ^{b)}	104.3407	-67.0968	12.1	7.74	1.34 ± 0.28			CV? ^{c)}
N484	J065806.4-174424	104.5265	-17.7401	12.5	9.32	9.21 ± 2.12	2RXS J065806.3-174427		CV
N485	J065826.4-555818	104.6100	-55.9717	20.1	5.48	1.92 ± 0.64	Bullet Cluster	0.2960	CLUSTER
N486	J070110.6-323451	105.2940	-32.5810	21.0	5.73	4.41 ± 1.42	2RXS J070110.5-323449	0.0438	AGN ^{c)}
N487	J070236.6-704441	105.6525	-70.7448	16.8	5.34	0.75 ± 0.22	XMMSL2 J070236.8-704425	0.0379	AGN ^{c)}
N488	J070511.2-670531 ^{b)}	106.2965	-67.0918	14.2	7.05	1.29 ± 0.30			AGN? ^{c)}
N489	J070637.0+635109 ^{b)}	106.6540	63.8526	21.9	5.75	4.42 ± 1.53		0.0140	SEYFERT ^{c)}
N490	J070649.5+032450	106.7062	3.4138	16.2	8.20	8.28 ± 2.28	PBC J0706.7+0327		CV
N491	J070713.3+643557	106.8054	64.5991	21.1	5.70	3.98 ± 1.43	VII Zw 118	0.0797	SEYFERT
N492	J070842.8-464245	107.1784	-46.7125	10.8	10.20	6.50 ± 1.34	SWIFT J0709.0-4642	0.0469	SEYFERT
N493	J070913.7-360125	107.3070	-36.0235	17.7	8.23	6.53 ± 1.61	PKS 0707-35	0.1108	SEYFERT
N494	J070932.6-353737	107.3858	-35.6270	18.5	6.71	5.05 ± 1.48	2RXS J070931.8-353735	0.0300	SEYFERT ^{c)}
N495	J071020.4-241648 ^{b)}	107.5849	-24.2801	20.0	5.78	3.70 ± 1.26			AGN? ^{c)}
N496	J071029.2-390131	107.6218	-39.0254	19.4	6.64	4.65 ± 1.35	2RXS J071029.8-390142	0.1629	SEYFERT ^{c)}
N497	J071029.6+590823	107.6235	59.1398	12.9	9.55	9.65 ± 2.23	EXO 0706.1+5913	0.1200	BLAZAR
N498	J071415.0-262116 ^{b)}	108.5623	-26.3544	14.3	8.52	6.56 ± 1.70			STAR? ^{c)}

Table A.1. continued.

Id	Name SRGA	RA (J2000)	Dec (J2000)	R98 (")	S/N	Flux (10^{-12} erg s $^{-1}$ cm $^{-2}$)	Conventional name	Redshift	Class
N499	J071740.2-710346	109.4175	-71.0627	8.0	14.22	3.30 ± 0.43	2E 0718.2-7057		AGN? ^{c)}
N500	J071801.5+440533	109.5061	44.0926	15.3	8.17	9.58 ± 2.40	RX J0718.0+4405	0.0614	SEYFERT
N501	J071947.9-753801	109.9498	-75.6336	17.3	5.53	1.03 ± 0.30	2RXS J071949.0-753757		AGN? ^{c)}
N502	J072041.0-552615	110.1708	-55.4374	19.1	5.68	2.07 ± 0.68	XMMSL2 J072041.2-552616		AGN? ^{c)}
N503	J072319.9-732653	110.8329	-73.4482	19.6	6.10	1.41 ± 0.36	PLCK G285.0-23.7	0.3900	CLUSTER ^{c)}
N504	J072529.9-050333	111.3748	-5.0592	24.4	5.47	5.42 ± 1.81	2RXS J072528.9-050327		BLAZAR?
N505	J072635.8+370011	111.6491	37.0032	18.7	7.17	7.72 ± 2.33	2RXS J072635.2+370006	0.1900	SEYFERT
N506	J072820.3-490845	112.0847	-49.1457	17.6	5.69	2.70 ± 0.92	XMMSL2 J072822.1-490836		STAR
N507	J072853.8-260629	112.2242	-26.1081	8.0	17.89	26.08 ± 3.49	3A 0726-260		HMXB
N508	J072957.0-654331	112.4874	-65.7252	9.9	10.29	2.64 ± 0.46	2RXS J072956.6-654326	0.0796	SEYFERT ^{c)}
N509	J073022.2-750414	112.5924	-75.0706	21.2	5.75	1.28 ± 0.36	2RXS J073023.8-750352		AGN? ^{c)}
N510	J073128.7+095621	112.8698	9.9392	10.9	12.74	18.17 ± 3.39	BG CMi		CV
N511	J073219.7+313754	113.0820	31.6315	21.8	5.78	5.93 ± 2.10	Abell 586	0.1702	CLUSTER
N512	J073237.8-133105	113.1575	-13.5181	10.8	12.06	15.34 ± 2.90	SWIFT J0732.5-1331		CV
N513	J074233.7+494842	115.6404	49.8118	12.1	11.73	14.75 ± 2.94	Mrk 79	0.0222	SEYFERT
N514	J074319.3+285304	115.8303	28.8844	14.2	8.35	8.60 ± 2.32	sig Gem		STAR
N515	J074324.7+303552 ^{b)}	115.8529	30.5978	23.5	5.53	4.77 ± 1.82			UNIDENT
N516	J074328.8-672616	115.8700	-67.4378	18.1	5.72	1.27 ± 0.36	PKS 0744-67	1.5110	BLAZAR
N517	J074343.1+183157 ^{b)}	115.9295	18.5325	27.0	5.36	5.30 ± 1.91			AGN? ^{c)}
N518	J074414.2-704131	116.0594	-70.6918	18.9	5.26	0.96 ± 0.29	2RXS J074411.3-704150		AGN ^{c)}
N519	J074458.6-525716	116.2443	-52.9543	12.4	8.49	4.58 ± 1.07	V436 Car		CV
N520	J074730.4-191746	116.8769	-19.2962	18.8	10.68	16.88 ± 3.24	4U 0739-19	0.1028	CLUSTER
N521	J074737.9-732604	116.9078	-73.4345	14.7	6.34	1.21 ± 0.31	PBC J0747.7-7326	0.0360	SEYFERT
N522	J074905.4-233348	117.2726	-23.5633	23.1	5.48	4.16 ± 1.52	BV Pup		CV
N523	J075051.8-863204	117.7160	-86.5345	15.3	7.43	3.11 ± 0.77	PBC J0749.2-8634	0.1090	SEYFERT
N524	J075117.8+144423	117.8244	14.7398	10.7	12.44	19.33 ± 3.60	PQ Gem		CV
N525	J075151.5+494838	117.9647	49.8106	15.3	8.90	10.38 ± 2.49	MCG +08-15-009	0.0244	SEYFERT
N526	J075504.7+220012	118.7694	22.0033	14.8	9.43	13.14 ± 3.10	U Gem		CV
N527	J075808.4+835632	119.5352	83.9423	18.2	6.32	3.81 ± 1.17	2RXS J075813.0+835636	0.1340	SEYFERT ^{c)}
N528	J075852.2+161649	119.7174	16.2804	19.3	7.16	9.50 ± 2.71	DW Cnc		CV
N529	J075942.0-384357	119.9249	-38.7326	9.1	15.58	17.59 ± 2.60	IGR J07597-3842	0.0405	SEYFERT
N530	J075953.9+232329	119.9745	23.3913	20.5	6.08	6.77 ± 2.30	SWIFT J0800.5+2327	0.0291	SEYFERT
N531	J080021.4+263659	120.0890	26.6163	19.5	6.04	6.30 ± 2.13	IC 486	0.0267	SEYFERT
N532	J080040.3-431104	120.1680	-43.1846	18.0	6.44	3.89 ± 1.20	SWIFT J080040.2-431107		CV
N533	J080142.6+420013 ^{b)}	120.4274	42.0035	19.2	7.65	7.95 ± 2.15		0.0317	SEYFERT ^{c)}
N534	J080158.4-494640	120.4933	-49.7779	12.6	10.09	6.91 ± 1.43	ESO 209-12	0.0405	SEYFERT
N535	J080326.5+084151	120.8603	8.6976	26.0	5.42	6.38 ± 2.29	PBC J0803.4+0840	0.0467	SEYFERT
N536	J080406.7+050700	121.0278	5.1164	14.9	9.69	13.19 ± 2.99	Mrk 1210	0.0135	SEYFERT
N537	J080527.5+753427	121.3647	75.5740	15.9	8.81	7.53 ± 1.76	RX J0805.4+7534	0.1200	BLAZAR
N538	J080532.4-132011 ^{b)}	121.3850	-13.3365	25.2	5.31	5.61 ± 2.04			UNIDENT
N539	J080559.6+320605	121.4985	32.1014	24.7	5.42	5.28 ± 2.05	2RXS J080558.0+320558		AGN ^{c)}
N540	J080913.6-164709 ^{b)}	122.3069	-16.7859	22.0	5.32	4.55 ± 1.71			UNIDENT

Table A.1. continued.

Id	Name SRGA	RA (J2000)	Dec (J2000)	R98 (")	S/N	Flux (10^{-12} erg s $^{-1}$ cm $^{-2}$)	Conventional name	Redshift	Class
N541	J080917.6+474637 ^{b)}	122.3234	47.7769	31.4	5.32	4.48 ± 1.69			AGN ^{c)}
N542	J080949.8+521834	122.4576	52.3094	22.6	5.84	4.54 ± 1.66	RX J0809.8+5218	0.1380	BLAZAR
N543	J081054.4+760249	122.7268	76.0469	16.6	6.97	4.64 ± 1.37	PG 0804+761	0.1000	SEYFERT
N544	J081231.5−571445	123.1315	−57.2457	26.7	5.46	3.35 ± 1.03	CIZA J0812.5-5714	0.0620	CLUSTER
N545	J081506.5−190334	123.7771	−19.0594	24.6	5.57	3.97 ± 1.56	VV Pup		CV
N546	J081724.1−073030	124.3503	−7.5083	28.2	6.15	8.02 ± 2.67	Abell 644	0.0704	CLUSTER
N547	J081748.2+025047	124.4509	2.8464	22.1	5.55	4.40 ± 1.74	2RXS J081748.9+025104	0.1060	SEYFERT
N548	J081820.4−142539	124.5850	−14.4275	18.2	6.99	7.44 ± 2.15	2RXS J081820.4-142554	0.1070	SEYFERT
N549	J081856.9−225248	124.7370	−22.8799	24.0	5.83	4.30 ± 1.59	RX J0818.9-2252	0.0346	SEYFERT
N550	J082316.0−632939	125.8166	−63.4943	19.1	6.36	1.93 ± 0.54	4FGL J0823.1-6330	0.2900	BLAZAR ^{c)}
N551	J082612.7−373712	126.5530	−37.6199	20.0	6.62	5.48 ± 1.62	IGR J08262-3736		HMXB
N552	J082623.5−703144	126.5979	−70.5290	6.5	19.09	7.63 ± 0.81	1ES 0826-703		CV ^{c)}
N553	J082628.0−640417	126.6168	−64.0715	10.9	10.07	3.65 ± 0.68	2RXS J082626.7-640421		BLAZAR
N554	J082943.2+415427	127.4299	41.9075	20.5	6.60	7.38 ± 2.34	RX J0829.7+4154	0.1263	SEYFERT
N555	J083016.5−672535	127.5687	−67.4264	17.5	6.36	1.71 ± 0.45	2RXS J083016.8-672520	0.0348	SEYFERT
N556	J083126.1−600717	127.8588	−60.1213	19.3	5.68	2.33 ± 0.72	XMMSL2 J083125.5-60072		CV? ^{c)}
N557	J083520.7−451030	128.8362	−45.1749	6.0	29.41	44.63 ± 3.69	Vela Pulsar		SNR / PULSAR
N558	J083538.7−040518	128.9112	−4.0882	14.7	8.74	9.70 ± 2.49	NGC 2617	0.0142	SEYFERT
N559	J083821.8+483803	129.5908	48.6341	12.8	11.15	14.78 ± 2.95	EI UMa		CV
N560	J083830.6−355925	129.6277	−35.9902	16.2	7.44	6.14 ± 1.71	Fairall 1146	0.0316	SEYFERT
N561	J083849.2−483126	129.7049	−48.5238	16.9	7.01	4.13 ± 1.20	IGR J08390-4833		CV
N562	J083950.7−121435	129.9612	−12.2432	12.2	12.01	15.55 ± 3.08	3C 206	0.1979	SEYFERT
N563	J084026.1+220436	130.1086	22.0766	17.7	6.72	7.48 ± 2.30	2RXS J084025.0+220428		CV
N564	J084124.4+705336	130.3515	70.8934	10.8	13.24	14.25 ± 2.48	4C 71.07	2.1720	BLAZAR
N565	J084219.5+022011 ^{b)}	130.5811	2.3364	21.7	5.37	4.49 ± 1.80			UNIDENT
N566	J084433.5−375751	131.1395	−37.9641	8.9	15.59	18.37 ± 2.81	2RXS J084433.6-375745		CV ^{c)}
N567	J084518.6+142050	131.3275	14.3473	20.9	7.12	8.37 ± 2.49	PBC J0845.3+1421	0.0605	SEYFERT
N568	J084521.2−353026	131.3382	−35.5071	22.9	5.58	4.47 ± 1.57	SWIFT J0845.0-3531	0.1370	SEYFERT
N569	J084551.9−272922 ^{b)}	131.4664	−27.4893	21.9	5.37	3.52 ± 1.40			CV? ^{c)}
N570	J084701.5−233657	131.7561	−23.6157	23.1	5.95	5.48 ± 1.87	4FGL J0847.0-2336	0.0590	BLAZAR
N571	J084712.7+113349	131.8031	11.5635	22.4	5.72	5.51 ± 1.96	RX J0847.2+1133	0.1984	BLAZAR
N572	J084937.3−554416	132.4056	−55.7378	20.8	5.72	2.79 ± 0.92	2SXPS J084937.6-554419		CV? ^{c)}
N573	J085040.9−421155	132.6702	−42.1987	12.8	9.32	8.44 ± 1.89	SWIFT J0850.8-4219		HMXB ^{c)}
N574	J085741.3−554226 ^{b)}	134.4221	−55.7072	16.5	7.07	2.92 ± 0.84			AGN? ^{c)}
N575	J090106.7−340025	135.2781	−34.0069	24.7	5.45	4.82 ± 1.60	XMMSL2 J090107.5-340035		AGN? ^{c)}
N576	J090207.0−403317	135.5290	−40.5547	1.1	216.85	1428.05 ± 23.76	Vela X-1		HMXB
N577	J090218.2+103542 ^{b)}	135.5760	10.5949	22.3	5.40	6.01 ± 2.15			UNIDENT
N578	J090236.7−481327	135.6528	−48.2242	11.0	12.27	10.32 ± 1.92	IGR J09026-4812	0.0391	SEYFERT
N579	J090305.2+130323 ^{b)}	135.7718	13.0564	23.1	5.29	4.80 ± 1.91			CV? ^{c)}
N580	J090507.5−533024	136.2811	−53.5067	3.6	45.88	67.49 ± 3.98	MAXI J0903-531		HMXB
N581	J090704.9+470920	136.7702	47.1554	19.4	6.63	6.20 ± 1.99	RX J0907.0+4708		STAR
N582	J090802.0−095937	137.0083	−9.9937	24.9	5.32	4.64 ± 1.84	2RXS J090802.0-095929	0.0535	BLAZAR

Table A.1. continued.

Id	Name SRGA	RA (J2000)	Dec (J2000)	R98 (")	S/N	Flux (10^{-12} erg s $^{-1}$ cm $^{-2}$)	Conventional name	Redshift	Class
N583	J091202.5-645207	138.0104	-64.8687	1.5	119.46	122.05 \pm 3.09	MAXI J0911-655		LMXB
N584	J091301.1-210309	138.2545	-21.0524	21.2	6.14	6.15 \pm 2.02	RX J0913.0-2103	0.1980	BLAZAR
N585	J091514.0-752345	138.8083	-75.3958	14.8	8.37	2.48 \pm 0.53	2RXS J091514.2-752354		AGN? ^{c)}
N586	J091609.9-621927	139.0414	-62.3241	7.0	20.20	13.22 \pm 1.42	IRAS 09149-6206	0.0573	SEYFERT
N587	J091727.1-645634	139.3630	-64.9427	15.8	6.13	2.08 \pm 0.58	2RXS J091727.6-645630	0.0859	SEYFERT
N588	J091804.9-120556	139.5205	-12.0990	24.2	7.02	9.89 \pm 2.79	Hydra A Cluster	0.0522	CLUSTER
N589	J091830.7+530251 ^{b)}	139.6278	53.0474	26.9	5.45	6.09 \pm 2.05			UNIDENT
N590	J091953.4-073535	139.9726	-7.5931	21.4	5.75	5.05 \pm 1.86	EXO 0917.3-0722	0.1691	SEYFERT
N591	J092014.4-383445	140.0598	-38.5792	19.5	5.61	3.98 \pm 1.29	2RXS J092013.1-383452		AGN? ^{c)}
N592	J092027.7-551224	140.1153	-55.2066	2.4	74.27	119.83 \pm 4.62	4U 0919-54		LMXB
N593	J092045.8-080317	140.1907	-8.0549	11.2	12.60	18.16 \pm 3.40	MCG -01-24-012	0.0197	SEYFERT
N594	J092133.3-593911	140.3886	-59.6530	17.6	5.46	2.07 \pm 0.66	2RXS J092133.7-593845		CV
N595	J092235.1-631742	140.6462	-63.2951	3.2	48.70	45.88 \pm 2.47	2S 0921-630		LMXB
N596	J092339.7-213554	140.9155	-21.5983	23.0	5.38	3.97 \pm 1.59	PKS 0921-213	0.0528	BLAZAR
N597	J092343.2+225441	140.9301	22.9115	12.6	8.99	11.70 \pm 2.89	RX J0923.7+2254	0.0331	SEYFERT
N598	J092418.1-314217	141.0756	-31.7046	4.3	39.56	97.10 \pm 6.93	NuSTAR J092418-3142.2		LMXB? ^{c)}
N599	J092513.7+521700	141.3071	52.2834	12.0	11.62	14.22 \pm 2.86	Mrk 110	0.0353	SEYFERT
N600	J092547.3+692747	141.4472	69.4630	18.4	6.64	5.29 \pm 1.59	IGR J09253+6929	0.0396	SEYFERT
N601	J092603.1+124408	141.5130	12.7355	14.4	9.31	12.22 \pm 3.03	Mrk 705	0.0288	SEYFERT
N602	J092615.0-842133	141.5624	-84.3591	11.6	10.09	4.62 \pm 0.89	IRAS 09305-8408	0.0632	SEYFERT
N603	J092712.2-113828 ^{b)}	141.8009	-11.6412	21.4	6.25	5.88 \pm 2.04		0.0109	SEYFERT ^{c)}
N604	J092753.0-694441	141.9708	-69.7447	10.7	10.40	3.84 \pm 0.70	PBC J0927.8-6945		CV
N605	J092841.6-620754 ^{b)}	142.1733	-62.1316	22.8	5.55	1.72 \pm 0.56			AGN? ^{c)}
N606	J093035.3+495029	142.6472	49.8415	23.2	5.62	4.70 \pm 1.74	1ES 0927+500	0.1868	BLAZAR
N607	J093527.3+261712	143.8640	26.2867	25.2	5.47	5.92 \pm 2.15	2RXS J093527.3+261721	0.1222	SEYFERT
N608	J093605.5-654849	144.0228	-65.8135	16.9	6.26	1.95 \pm 0.53	SWIFT J0936.2-6553	0.0392	SEYFERT
N609	J094542.1-141940	146.4256	-14.3277	8.3	17.58	31.04 \pm 4.39	NGC 2992	0.0077	SEYFERT
N610	J094634.2+135050	146.6424	13.8473	22.0	5.42	5.17 \pm 2.02	HY Leo		CV
N611	J094740.0-305654	146.9168	-30.9482	4.9	32.95	63.99 \pm 5.12	ESO 434-40	0.0085	SEYFERT
N612	J095155.0-064920	147.9793	-6.8222	16.1	8.09	9.74 \pm 2.65	NGC 3035	0.0145	SEYFERT
N613	J095220.9-623233	148.0869	-62.5424	14.7	7.03	2.79 \pm 0.73	IGR J09522-6231	0.2520	SEYFERT
N614	J095307.9-765751	148.2831	-76.9642	22.8	5.75	1.73 \pm 0.52	RX J0953.1-7657	0.1090	BLAZAR ^{c)}
N615	J095418.7-410820	148.5781	-41.1389	24.0	5.73	3.88 \pm 1.32	PMN J0954-4108		BLAZAR?
N616	J095534.0+690353	148.8918	69.0648	13.9	9.52	8.88 \pm 2.05	M81		SEYFERT
N617	J095549.9+694046	148.9579	69.6794	10.8	12.63	13.85 \pm 2.54	M82 X-1		ULX
N618	J095704.9-585317 ^{b)}	149.2703	-58.8880	18.9	5.40	2.00 \pm 0.66			AGN? ^{c)}
N619	J095717.2-755432	149.3215	-75.9089	19.8	6.28	2.28 \pm 0.61	2RXS J095720.0-755440		UNIDENT
N620	J095754.3+690352	149.4761	69.0646	18.3	6.05	4.04 \pm 1.38	Holmberg IX X-1		ULX
N621	J095838.4-411042	149.6600	-41.1784	21.2	6.51	4.60 \pm 1.41	ICRF J095838.2-411033	2.9340	BLAZAR
N622	J095929.9-224927	149.8746	-22.8240	15.2	8.49	7.67 \pm 1.97	NGC 3081	0.0080	SEYFERT
N623	J100149.2+284701	150.4548	28.7835	21.4	5.60	5.46 \pm 2.04	3C 234.0	0.1849	SEYFERT
N624	J100513.7-625209	151.3071	-62.8692	16.5	6.62	2.48 \pm 0.67	SWIFT J1005.3-6289	0.0714	SEYFERT ^{c)}

Table A.1. continued.

Id	Name SRGA	RA (J2000)	Dec (J2000)	R98 (")	S/N	Flux (10^{-12} erg s $^{-1}$ cm $^{-2}$)	Conventional name	Redshift	Class
N625	J100622.0–701404	151.5916	–70.2345	14.4	7.86	3.04 ± 0.69	OY Car		CV
N626	J100641.4+401737 ^{b)}	151.6723	40.2935	25.6	5.36	5.81 ± 2.04			UNIDENT
N627	J100715.0–731442	151.8124	–73.2449	15.3	7.43	2.84 ± 0.66	XMMSL2 J100713.8-731448		UNIDENT
N628	J100947.1–581737	152.4461	–58.2935	1.9	92.44	90.49 ± 2.85	GRO J1008-57		HMXB
N629	J101011.9–565526	152.5494	–56.9238	9.0	13.74	8.73 ± 1.36	IGR J10100-5655		HMXB
N630	J101016.7–311912	152.5694	–31.3200	16.1	7.78	7.79 ± 1.96	2RXS J101015.8-311909	0.1426	BLAZAR
N631	J101103.6–574814	152.7650	–57.8039	8.9	14.79	9.59 ± 1.38	IGR J10109-5746		CV
N632	J101133.2–442257	152.8883	–44.3826	15.7	7.44	4.36 ± 1.16	2SXPS J101132.0-442255		AGN? ^{c)}
N633	J101416.2–635142	153.5675	–63.8616	22.7	5.52	1.55 ± 0.51	IGR J10147-6354	0.2020	SEYFERT
N634	J101505.3+492607	153.7719	49.4353	16.8	7.69	8.64 ± 2.35	1ES 1011+496	0.2120	BLAZAR
N635	J102140.3–032717	155.4178	–3.4546	18.2	5.89	6.77 ± 2.23	Ark 241	0.0409	SEYFERT
N636	J102205.8–353801 ^{b)}	155.5240	–35.6337	18.3	6.57	4.19 ± 1.35			CV? ^{c)}
N637	J102330.4+195157	155.8766	19.8657	8.5	17.47	30.37 ± 4.41	NGC 3227	0.0038	SEYFERT
N638	J102347.1+003838	155.9464	0.6438	14.5	8.13	10.00 ± 2.74	PSR J1023+0038		LMXB
N639	J102555.0–574844	156.4793	–57.8123	18.9	5.41	2.32 ± 0.75	WR 21a		STAR ^{c)}
N640	J103119.1+505339	157.8295	50.8940	24.6	5.68	4.35 ± 1.61	1ES 1028+511	0.3604	BLAZAR
N641	J103120.6+744206	157.8358	74.7016	19.1	6.03	3.71 ± 1.25	RX J1031.3+7442	0.1230	BLAZAR
N642	J103151.9–345113	157.9664	–34.8536	15.4	8.02	6.83 ± 1.73	NGC 3281	0.0107	SEYFERT
N643	J103154.5–141648	157.9773	–14.2801	17.9	7.74	9.45 ± 2.60	HE 1029-1401	0.0858	SEYFERT
N644	J103735.7–564754	159.3989	–56.7985	4.6	32.70	35.65 ± 2.67	4U 1036-56		HMXB
N645	J103845.6–494652	159.6898	–49.7811	14.8	9.45	5.90 ± 1.27	SWIFT J1038.8-4942	0.0600	SEYFERT
N646	J103915.5–490307	159.8145	–49.0518	16.3	6.46	3.98 ± 1.10	XMMSL2 J103915.1-490301		CV? ^{c)}
N647	J103946.4–050706	159.9435	–5.1182	22.0	5.92	5.90 ± 2.12	RX J1039.7-0507		CV
N648	J104021.9–462521	160.0911	–46.4224	19.4	5.42	2.87 ± 0.97	IGR J10404-4625	0.0238	SEYFERT
N649	J104124.3–692952 ^{b)}	160.3515	–69.4977	17.5	5.83	1.87 ± 0.58			AGN? ^{c)}
N650	J104145.0–474008	160.4373	–47.6690	21.5	5.57	2.88 ± 0.96	IVS B1039-474	2.5580	BLAZAR
N651	J104451.4–602510	161.2141	–60.4195	18.0	7.50	3.37 ± 0.83	IGR J10447-6027	0.0470	SEYFERT ^{c)}
N652	J104503.8–594106	161.2659	–59.6851	2.5	67.63	83.30 ± 3.39	eta Car		STAR
N653	J104651.8–253550	161.7160	–25.5971	19.6	6.56	5.84 ± 1.75	2RXS J104651.9-253545	0.2500	BLAZAR
N654	J104834.8–390225	162.1450	–39.0402	20.7	6.49	4.11 ± 1.22	SWIFT J1048.6-3901	0.0449	SEYFERT ^{c)}
N655	J105452.7+771252 ^{b)}	163.7198	77.2144	20.7	5.49	3.18 ± 1.13			AGN? ^{c)}
N656	J105551.4+215404 ^{b)}	163.9641	21.9011	23.2	5.46	6.17 ± 2.27			UNIDENT
N657	J105715.0–473958	164.3125	–47.6662	17.8	7.23	4.46 ± 1.18	SWIFT J1057.6-4765	0.0156	SEYFERT ^{c)}
N658	J105918.2–512631	164.8257	–51.4420	13.0	8.53	4.87 ± 1.15	ESO 215-14	0.0190	SEYFERT
N659	J105945.0+650405	164.9374	65.0680	18.4	6.26	5.52 ± 1.71	PBC J1059.9+6505	0.0836	SEYFERT
N660	J110019.8–073853	165.0825	–7.6482	23.4	6.16	5.43 ± 1.89	RX J1100.3-0738	0.0655	SEYFERT
N661	J110122.2–514909	165.3425	–51.8191	22.1	5.53	3.03 ± 0.98	SWIFT J1101.4-5152		AGN? ^{c)}
N662	J110221.7–732227 ^{b)}	165.5906	–73.3743	18.4	5.75	1.65 ± 0.50			UNIDENT
N663	J110337.3–232931	165.9056	–23.4919	11.9	11.51	13.92 ± 2.65	2A 1058-226	0.1860	BLAZAR
N664	J110414.6+765900	166.0610	76.9831	22.2	5.90	4.64 ± 1.43	3C 249.1	0.3115	SEYFERT
N665	J110427.6+381234	166.1150	38.2094	4.1	41.02	121.35 ± 8.49	Mrk 421	0.0300	BLAZAR
N666	J110538.8+020252	166.4117	2.0477	20.6	5.96	5.98 ± 2.13	PMN J1105+0202	0.1056	BLAZAR

Table A.1. continued.

Id	Name SRGA	RA (J2000)	Dec (J2000)	R98 (")	S/N	Flux (10^{-12} erg s $^{-1}$ cm $^{-2}$)	Conventional name	Redshift	Class
N667	J110647.3+723407	166.6969	72.5687	8.8	15.67	18.16 \pm 2.67	NGC 3516	0.0088	SEYFERT
N668	J110709.5-444902	166.7894	-44.8173	18.7	6.26	3.65 \pm 1.11	PKS 1104-445	1.5980	BLAZAR
N669	J110946.0+800817 ^{b)}	167.4416	80.1381	22.0	6.17	3.35 \pm 1.09		0.1888	SEYFERT ^{c)}
N670	J111359.5-374047	168.4978	-37.6798	20.6	5.88	2.94 \pm 1.01	V436 Cen		CV
N671	J111418.8-670224	168.5782	-67.0401	20.0	6.05	1.84 \pm 0.58	XMMSL2 J111420.0-670223		UNIDENT
N672	J111457.3-611449	168.7388	-61.2469	22.4	5.70	2.22 \pm 0.72	NGC 3603		SFR ^{c)}
N673	J111515.8-480620	168.8160	-48.1057	19.3	5.78	3.29 \pm 1.03	2RXS J111515.1-480619		AGN? ^{c)}
N674	J111538.8-591714 ^{b)}	168.9117	-59.2871	23.2	5.40	2.30 \pm 0.77			UNIDENT
N675	J111820.6-543730	169.5860	-54.6249	16.0	6.77	2.60 \pm 0.73	IGR J11187-5438		LMXB? ^{c)}
N676	J112048.3-431540	170.2013	-43.2610	14.6	8.40	5.51 \pm 1.33	ESO 265-23	0.0566	SEYFERT
N677	J112115.1-603725	170.3128	-60.6237	0.7	304.55	1291.04 \pm 14.78	Cen X-3		HMXB
N678	J112437.5-591612	171.1561	-59.2700	14.5	10.28	5.68 \pm 1.13	PSR J1124-5916		SNR / PULSAR
N679	J112536.1+542303	171.4004	54.3842	16.6	7.64	7.11 \pm 1.92	Mrk 40	0.0207	SEYFERT
N680	J112549.8-763012	171.4575	-76.5033	17.4	6.03	2.07 \pm 0.60	RX J1125.7-7629		STAR
N681	J112958.5-655520	172.4939	-65.9222	16.0	6.79	3.25 \pm 0.82	2E 1127.7-6538		UNIDENT? ^{c)}
N682	J113033.0-780101	172.6376	-78.0168	10.6	11.23	4.93 \pm 0.86	4FGL J1130.5-7801		BLAZAR
N683	J113151.7-123151	172.9653	-12.5307	22.3	5.40	3.74 \pm 1.32	RXS J1131-1231	0.6580	SEYFERT ^{c)}
N684	J113155.3-343639	172.9805	-34.6108	17.4	6.37	3.74 \pm 1.17	2RXS J113155.6-343632		STAR
N685	J113257.1-260736	173.2381	-26.1267	23.2	5.52	3.62 \pm 1.27	2SXPS J113256.4-260735		AGN? ^{c)}
N686	J113601.0-650624	174.0044	-65.1066	13.5	9.14	3.83 \pm 0.85	2RXS J113601.2-650631		UNIDENT
N687	J113629.8+673704	174.1241	67.6179	14.5	8.81	6.63 \pm 1.65	RX J1136.5+6737	0.1342	BLAZAR
N688	J113641.7-600302	174.1737	-60.0504	19.7	6.53	2.96 \pm 0.85	IGR J11366-6002	0.0149	SEYFERT
N689	J113736.0+005809 ^{b)}	174.4000	0.9690	21.5	5.34	3.28 \pm 1.38			UNIDENT
N690	J113850.8-232126	174.7115	-23.3572	19.4	6.84	5.59 \pm 1.61	HE 1136-2304	0.0270	SEYFERT ^{c)}
N691	J113902.3-374419	174.7598	-37.7387	4.6	33.32	47.99 \pm 3.79	NGC 3783	0.0097	SEYFERT
N692	J113909.2+591204	174.7882	59.2012	20.8	6.96	6.34 \pm 1.93	SBS 1136+594	0.0612	SEYFERT
N693	J113930.2-652352	174.8758	-65.3977	7.8	17.95	11.94 \pm 1.45	GT Mus		STAR
N694	J114122.6-641018	175.3444	-64.1716	5.4	26.28	21.37 \pm 1.93	V1033 Cen		CV
N695	J114338.8+714126	175.9119	71.6905	6.9	20.08	25.61 \pm 3.06	DO Dra		CV
N696	J114357.1-690508	175.9878	-69.0854	26.5	5.53	2.12 \pm 0.69	PSZ2 G296.91-07.00	0.3100	CLUSTER
N697	J114400.0-610736	175.9996	-61.1266	6.4	22.08	18.54 \pm 1.89	IGR J11435-6109		HMXB
N698	J114429.9+365313	176.1248	36.8869	16.5	7.17	5.83 \pm 1.63	KUG 1141+371	0.0382	SEYFERT
N699	J114515.2+794100	176.3134	79.6832	11.1	11.06	6.57 \pm 1.30	1ES 1141+79.9	0.0060	SEYFERT ^{c)}
N700	J114541.2-182712	176.4219	-18.4535	8.8	15.02	17.22 \pm 2.60	H 1143-182	0.0330	SEYFERT
N701	J114554.2-695400	176.4758	-69.8998	13.3	8.80	3.95 \pm 0.86	PKS 1143-696	0.2434	BLAZAR
N702	J114633.0+742116	176.6377	74.3543	22.2	5.51	3.24 \pm 1.18	IRAS 11436+7438	0.0560	SEYFERT
N703	J114722.1-495308	176.8419	-49.8857	9.4	12.52	7.21 \pm 1.24	2RXS J114724.2-495257		UNIDENT ^{c)}
N704	J114728.6-615713	176.8690	-61.9535	1.9	95.74	187.29 \pm 5.85	1E 1145.1-6141		HMXB
N705	J114754.6+094554	176.9777	9.7650	26.0	5.34	3.28 \pm 1.38	SDSS J114753.62+094552.0	0.0951	SEYFERT ^{c)}
N706	J114759.6-621229	176.9985	-62.2081	9.9	12.67	8.44 \pm 1.33	4U 1145-619		HMXB
N707	J114845.8+293827	177.1910	29.6408	18.1	7.45	7.92 \pm 2.30	SWIFT J1148.7+2941	0.0225	SEYFERT
N708	J115215.3-510703 ^{b)}	178.0636	-51.1175	17.6	5.63	2.47 \pm 0.78			CV? ^{c)}

Table A.1. continued.

Id	Name SRGA	RA (J2000)	Dec (J2000)	R98 (")	S/N	Flux (10^{-12} erg s $^{-1}$ cm $^{-2}$)	Conventional name	Redshift	Class
N709	J115223.8–673837	178.0991	–67.6437	15.9	7.98	3.62 ± 0.85	2RXS J115223.8-673809		CV? ^c
N710	J115415.6–501801 ^b	178.5648	–50.3003	11.8	10.18	5.31 ± 1.08			CV? ^c
N711	J115526.5–564150	178.8603	–56.6971	7.0	17.80	14.07 ± 1.75	V1040 Cen		CV
N712	J115722.6–120637 ^b	179.3442	–12.1104	23.5	5.35	3.97 ± 1.40			UNIDENT
N713	J115730.2–343758	179.3760	–34.6329	17.8	6.55	3.99 ± 1.23	2RXS J115730.6-343744		CV ^c
N714	J115755.7+552722	179.4820	55.4561	15.2	9.11	9.15 ± 2.16	NGC 3998	0.0035	SEYFERT
N715	J115910.3–532435 ^b	179.7929	–53.4097	20.0	5.82	2.22 ± 0.76		0.0144	AGN? ^c
N716	J120059.0+064826	180.2458	6.8072	18.7	5.67	3.97 ± 1.41	SWIFT J1200.8+0650	0.0360	SEYFERT
N717	J120248.5–535004	180.7020	–53.8343	9.6	15.92	12.99 ± 1.76	IGR J12026-5349	0.0280	SEYFERT
N718	J120309.7+443155	180.7905	44.5319	14.8	10.00	10.52 ± 2.36	NGC 4051	0.0023	SEYFERT
N719	J120413.5–294651 ^b	181.0564	–29.7809	17.4	6.90	4.11 ± 1.21			AGN ^c
N720	J120628.1–221817 ^b	181.6172	–22.3049	20.1	5.35	3.34 ± 1.18			UNIDENT
N721	J120915.6+470329	182.3149	47.0582	18.2	7.36	6.06 ± 1.75	Mrk 198	0.0243	SEYFERT
N722	J121033.2+392419	182.6382	39.4052	3.4	55.49	195.73 ± 10.43	NGC 4151	0.0033	SEYFERT
N723	J121053.2–040811 ^b	182.7218	–4.1365	21.7	5.52	4.07 ± 1.41			CV? ^c
N724	J121115.4–393328	182.8140	–39.5578	18.3	7.01	4.29 ± 1.21	PBC J1211.3-3933	0.0610	SEYFERT
N725	J121225.6–580026	183.1066	–58.0073	11.1	11.98	7.13 ± 1.27	IGR J12123-5802		CV
N726	J121314.9–645230	183.3122	–64.8750	2.2	78.01	123.11 ± 4.59	4U 1210-64		HMXB
N727	J121324.3–261807	183.3514	–26.3020	15.4	7.99	6.90 ± 1.74	RBS 1080	0.2780	BLAZAR
N728	J121710.1+071129	184.2920	7.1914	18.2	7.56	7.24 ± 2.00	NGC 4235	0.0076	SEYFERT
N729	J121826.8+294847	184.6115	29.8131	11.4	11.18	13.25 ± 2.67	NGC 4253	0.0129	SEYFERT
N730	J121858.2+471809	184.7424	47.3024	20.8	5.87	4.11 ± 1.31	NGC 4258	0.0015	SEYFERT
N731	J122011.7+020346	185.0486	2.0627	19.2	6.50	6.37 ± 1.80	2E 1217.6+0220	0.2402	BLAZAR
N732	J122024.0–585053 ^b	185.0999	–58.8482	20.5	6.52	2.71 ± 0.83			UNIDENT
N733	J122122.8+301035	185.3451	30.1765	16.3	7.86	7.62 ± 2.01	3A 1218+303	0.1836	BLAZAR
N734	J122145.8+751833	185.4407	75.3093	12.2	10.41	7.33 ± 1.57	Mrk 205	0.0708	SEYFERT
N735	J122323.8+024045	185.8490	2.6792	20.0	6.29	4.91 ± 1.52	Mrk 50	0.0239	SEYFERT
N736	J122547.2+123943	186.4467	12.6620	7.4	18.91	32.38 ± 4.14	NGC 4388	0.0084	SEYFERT
N737	J122557.8–642602 ^b	186.4910	–64.4339	16.4	7.49	3.34 ± 0.86			UNIDENT
N738	J122637.6–624613	186.6566	–62.7703	0.9	230.62	811.59 ± 11.99	GX 301-2		HMXB
N739	J122806.9–552242	187.0288	–55.3784	13.5	8.96	5.33 ± 1.19	2RXS J122810.2-552304		STAR? ^c
N740	J122809.9–092718	187.0414	–9.4549	22.2	5.36	3.53 ± 1.28	2PBC J1228.1-0925	0.2230	SEYFERT ^c
N741	J122906.6+020310	187.2776	2.0529	5.4	31.61	58.49 ± 4.79	3C 273	0.1583	BLAZAR
N742	J123112.7–423529	187.8030	–42.5914	13.4	8.85	5.92 ± 1.34	2RXS J123112.2-423526		CV? ^c
N743	J123136.9–475801	187.9040	–47.9669	14.7	7.29	4.01 ± 1.06	2RXS J123137.3-475800	0.0279	SEYFERT
N744	J123155.3+323239	187.9803	32.5441	19.6	6.31	4.56 ± 1.53	RX J1231.9+3232	0.0654	SEYFERT
N745	J123212.4–421750	188.0518	–42.2973	17.8	7.40	4.28 ± 1.16	XSS J12303-4232	0.1004	SEYFERT
N746	J123216.0–101521	188.0665	–10.2558	18.6	6.27	4.29 ± 1.41	2RXS J123216.4-101514	0.2531	BLAZAR
N747	J123402.7–614310	188.5113	–61.7194	21.0	5.69	2.24 ± 0.75	IGR J12341-6143		HMXB? ^c
N748	J123454.1–643403	188.7252	–64.5675	11.3	10.75	5.77 ± 1.11	RT Cru		CV
N749	J123536.8–395439	188.9034	–39.9108	8.1	16.22	14.40 ± 2.03	NGC 4507	0.0118	SEYFERT
N750	J123630.6–664551	189.1274	–66.7641	13.7	10.17	5.46 ± 1.07	2SXPS J123632.4-664557		CV? ^c

Table A.1. continued.

Id	Name SRGA	RA (J2000)	Dec (J2000)	R98 (")	S/N	Flux (10^{-12} erg s $^{-1}$ cm $^{-2}$)	Conventional name	Redshift	Class
N751	J123744.1+114900	189.4337	11.8165	13.8	8.02	6.74 ± 1.68	NGC 4579	0.0051	SEYFERT
N752	J123816.0-384244	189.5667	-38.7123	10.6	11.25	8.69 ± 1.62	V1025 Cen		CV
N753	J123821.5-253208 ^{b)}	189.5896	-25.5357	10.4	12.64	10.90 ± 2.00			UNIDENT ^{c)}
N754	J123855.3-271832	189.7304	-27.3088	13.1	9.72	8.75 ± 1.82	ESO 506-027	0.0250	SEYFERT
N755	J123907.4-453338	189.7806	-45.5605	15.2	6.80	4.21 ± 1.15	V1129 Cen		CV
N756	J123939.8-052033	189.9157	-5.3424	14.3	9.63	8.15 ± 1.84	NGC 4593	0.0083	SEYFERT
N757	J124125.6-575001	190.3566	-57.8335	6.7	21.44	18.98 ± 2.03	IGR J12415-5750	0.0244	SEYFERT
N758	J124248.7-630324	190.7030	-63.0566	13.6	9.04	5.25 ± 1.10	1H 1249-637		STAR ^{c)}
N759	J124403.4-632220 ^{b)}	191.0141	-63.3723	11.0	10.61	5.54 ± 1.11			HMXB ^{c)}
N760	J124939.5-590518	192.4148	-59.0882	5.4	25.47	23.78 ± 2.24	4U 1246-58		LMXB
N761	J125144.4-512804	192.9351	-51.4678	20.8	5.85	2.60 ± 0.86	2PBC J1251.8-5127	0.1780	SEYFERT
N762	J125212.8-132457	193.0535	-13.4159	17.9	6.88	5.06 ± 1.52	NGC 4748	0.0146	SEYFERT
N763	J125224.4-291456	193.1015	-29.2489	2.9	60.74	130.31 ± 6.26	EX Hya		CV
N764	J125256.4+525915	193.2352	52.9874	20.6	5.51	2.95 ± 1.09	SDSS J125257.94+525925.6	0.1785	SEYFERT
N765	J125341.6-393153	193.4235	-39.5315	15.3	7.05	4.64 ± 1.24	4FGL J1253.5-3934	0.1790	BLAZAR
N766	J125511.0-610309 ^{b)}	193.7958	-61.0526	20.6	5.67	2.60 ± 0.86			UNIDENT
N767	J125608.0-612723	194.0332	-61.4563	15.9	6.62	3.48 ± 0.97	2RXS J125608.2-612714		STAR
N768	J125611.3-054721	194.0472	-5.7892	12.1	11.43	10.38 ± 2.02	3C 279	0.5362	BLAZAR
N769	J125737.1-691719	194.4047	-69.2886	1.2	162.18	437.12 ± 8.79	4U 1254-69		LMXB
N770	J130058.1-491227	195.2421	-49.2075	15.4	6.09	3.04 ± 0.93	V1147 Cen		CV
N771	J130117.0-613615	195.3208	-61.6043	14.1	9.25	5.05 ± 1.12	GX 304-1		HMXB
N772	J130200.1-635815	195.5005	-63.9708	18.3	5.84	2.24 ± 0.72	2RXP J130159.6-635806		HMXB
N773	J130246.1-635003	195.6919	-63.8342	15.6	8.27	4.38 ± 1.00	PSR B1259-63		HMXB
N774	J130259.3+162426	195.7472	16.4072	20.2	6.13	4.42 ± 1.40	Mrk 783	0.0674	SEYFERT
N775	J130321.9-134150	195.8414	-13.6972	23.4	5.76	4.30 ± 1.39	CTS 20	0.0467	SEYFERT
N776	J130415.5-102022	196.0644	-10.3395	16.2	7.70	5.89 ± 1.61	NGC 4939	0.0104	SEYFERT
N777	J130522.0-492823	196.3418	-49.4731	27.1	6.39	3.94 ± 1.17	NGC 4945 XMM4		ULX ^{c)}
N778	J130527.6-492811	196.3649	-49.4697	23.0	5.50	3.07 ± 1.01	NGC 4945	0.0018	SEYFERT
N779	J130534.6-103332	196.3941	-10.5590	26.3	5.36	3.69 ± 1.30	PG 1302-102	0.2784	BLAZAR
N780	J130625.6-402447	196.6069	-40.4131	20.2	6.06	3.34 ± 1.07	ESO 323-77	0.0150	SEYFERT
N781	J130753.9+535130	196.9746	53.8582	21.6	5.97	4.51 ± 1.52	EV UMa		CV
N782	J130905.7+113758	197.2739	11.6328	20.3	5.89	4.42 ± 1.41	IGR J13091+1137	0.0251	SEYFERT
N783	J131036.8-562654	197.6535	-56.4482	15.1	7.53	3.71 ± 0.99	IGR J13107-5626	0.1142	SEYFERT ^{c)}
N784	J131044.6-555214	197.6857	-55.8705	14.8	8.65	4.94 ± 1.16	IGR J13109-5552	0.1040	SEYFERT
N785	J131130.2-012006	197.8758	-1.3349	15.3	8.40	7.95 ± 1.89	Abell 1689	0.1842	CLUSTER
N786	J131239.9-624258	198.1662	-62.7161	13.1	9.01	4.59 ± 0.97	WR 48a		STAR ^{c)}
N787	J131327.4+363545	198.3641	36.5958	18.9	5.68	3.58 ± 1.20	NGC 5033	0.0029	SEYFERT
N788	J131503.8-423648	198.7656	-42.6134	16.3	6.84	4.51 ± 1.21	1E 1312-4221	0.1050	BLAZAR
N789	J131518.0+442426	198.8249	44.4072	17.7	7.50	5.85 ± 1.54	Mrk 248	0.0355	SEYFERT
N790	J131653.6-715529	199.2233	-71.9248	11.1	10.14	5.46 ± 1.07	IGR J13168-7157	0.0705	SEYFERT
N791	J131825.3-625820	199.6055	-62.9723	17.4	7.00	3.35 ± 0.91	IGR J13186-6257		HMXB
N792	J132031.7-701443	200.1320	-70.2454	9.6	12.08	7.24 ± 1.23	2RXS J132032.1-701451		X-RAY BINARY? ^{c)}

Table A.1. continued.

Id	Name SRGA	RA (J2000)	Dec (J2000)	R98 (")	S/N	Flux (10^{-12} erg s $^{-1}$ cm $^{-2}$)	Conventional name	Redshift	Class
N793	J132327.2-165810	200.8634	-16.9695	14.3	7.63	4.44 ± 1.23	XMMSL2 J132326.8-165804	0.0231	AGN? ^c
N794	J132426.3-620128	201.1097	-62.0245	16.5	7.99	4.10 ± 1.00	SAX J1324.4-6200		HMXB
N795	J132450.8+213547	201.2115	21.5964	17.3	7.17	5.73 ± 1.53	RX J1324.8+2135	0.1296	SEYFERT
N796	J132527.7-430110	201.3655	-43.0193	2.2	81.03	185.97 ± 6.89	Cen A	0.0018	SEYFERT
N797	J132532.0-621312	201.3835	-62.2200	19.4	6.32	2.83 ± 0.83	2E 1322.2-6157		UNIDENT ^c
N798	J132636.8-620809	201.6532	-62.1357	3.0	55.11	73.92 ± 3.66	4U 1323-62		LMXB
N799	J133113.8-252413	202.8074	-25.4035	11.6	11.88	10.02 ± 1.87	ESO 509-G038	0.0260	SEYFERT
N800	J133119.5-545830	202.8314	-54.9750	9.0	16.25	13.86 ± 1.87	BV Cen		CV
N801	J133333.6-102810	203.3900	-10.4694	20.2	5.65	3.53 ± 1.19	2RXS J133333.6-102759	0.1026	SEYFERT
N802	J133447.4+371045	203.6975	37.1792	18.1	6.27	4.05 ± 1.23	BH CVn		STAR
N803	J133531.0-295035	203.8793	-29.8430	20.1	6.73	4.71 ± 1.34	4FGL J1335.3-2949		BLAZAR
N804	J133548.2+025953	203.9506	2.9982	17.5	6.59	4.63 ± 1.38	NGC 5231	0.0218	SEYFERT
N805	J133554.1-341748	203.9754	-34.2966	6.7	23.24	29.78 ± 3.08	ESO 383-35	0.0077	SEYFERT
N806	J133816.1+043232	204.5670	4.5422	7.1	19.69	23.91 ± 2.92	NGC 5252	0.0231	SEYFERT
N807	J133836.9-352851	204.6536	-35.4809	17.6	6.23	3.96 ± 1.19	2SXPS J133837.1-352852		AGN? ^c
N808	J133950.6-643002 ^b	204.9609	-64.5006	10.9	9.43	4.71 ± 1.01			UNIDENT ^c
N809	J134105.6+395938	205.2732	39.9939	21.4	6.03	3.67 ± 1.15	RX J1341.0+3959	0.1630	BLAZAR
N810	J134105.6+674015	205.2733	67.6709	17.2	6.45	3.42 ± 1.07	NGC 5283	0.0101	SEYFERT
N811	J134113.1-143845	205.3045	-14.6458	15.5	8.91	6.89 ± 1.62	CTS 23	0.0418	SEYFERT
N812	J134208.7+353900	205.5361	35.6501	19.2	6.04	3.82 ± 1.18	NGC 5273	0.0036	SEYFERT
N813	J134519.6+414236	206.3317	41.7099	18.1	6.47	3.21 ± 1.00	NGC 5290	0.0087	SEYFERT
N814	J134648.7-602435	206.7029	-60.4096	11.7	11.69	8.25 ± 1.51	Cen B	0.0129	SEYFERT
N815	J134735.9-603701	206.8996	-60.6171	4.6	33.26	41.04 ± 3.13	4U 1344-60	0.0129	SEYFERT
N816	J134736.0-325010	206.8999	-32.8362	20.6	6.34	5.89 ± 1.69	Abell 3571	0.0397	CLUSTER
N817	J134742.7-621356	206.9280	-62.2322	20.6	6.11	3.38 ± 1.01	SWIFT J134745.7-621411		SNR ^c
N818	J134919.2-301833	207.3299	-30.3091	3.4	48.88	93.30 ± 5.35	IC 4329A	0.0160	SEYFERT
N819	J134953.2+020445	207.4717	2.0791	11.5	11.61	9.25 ± 1.67	UM 614	0.0329	SEYFERT
N820	J135129.4-181345	207.8727	-18.2291	18.2	6.59	4.95 ± 1.43	CTS 10	0.0122	SEYFERT
N821	J135304.0+691827	208.2665	69.3075	9.6	13.60	11.86 ± 1.85	Mrk 279	0.0305	SEYFERT
N822	J135418.5-374648	208.5772	-37.7801	23.9	5.89	3.97 ± 1.28	Tol 1351-375	0.0517	SEYFERT? ^c
N823	J135534.4+352045	208.8933	35.3460	18.7	6.39	3.58 ± 1.07	PBC J1355.5+3523	0.1021	SEYFERT ^c
N824	J135637.0-193152	209.1543	-19.5310	17.6	6.79	4.38 ± 1.32	CTS 104	0.0350	SEYFERT
N825	J140045.5-632541	210.1897	-63.4280	8.8	15.70	12.70 ± 1.75	IGR J14003-6326		SNR / PULSAR
N826	J140102.4+025220	210.2600	2.8723	14.5	8.81	6.97 ± 1.57	Abell 1835	0.2506	CLUSTER
N827	J140130.2-493239	210.3757	-49.5441	20.4	5.59	2.75 ± 0.95	2SXPS J140131.8-493237		SEYFERT? ^c
N828	J140146.3-501333 ^b	210.4430	-50.2257	14.4	8.27	4.52 ± 1.10			CV? ^c
N829	J140429.6-614716	211.1234	-61.7878	13.4	9.19	6.19 ± 1.31	IGR J14043-6148		UNIDENT
N830	J140503.9-534130 ^b	211.2661	-53.6917	16.8	7.95	4.42 ± 1.07			AGN? ^c
N831	J140716.7-264424 ^b	211.8195	-26.7401	19.9	5.60	2.97 ± 1.05			UNIDENT
N832	J140744.3-430522	211.9346	-43.0893	19.7	5.92	3.52 ± 1.09	XMMSL2 J140743.6-430516		UNIDENT
N833	J140851.3+215118	212.2137	21.8550	21.5	5.80	3.15 ± 1.05	2RXS J140851.5+215150	0.7650	SEYFERT
N834	J140908.1-451720	212.2836	-45.2889	11.9	10.21	7.00 ± 1.45	V834 Cen		CV

Table A.1. continued.

Id	Name SRGA	RA (J2000)	Dec (J2000)	R98 (")	S/N	Flux (10^{-12} erg s $^{-1}$ cm $^{-2}$)	Conventional name	Redshift	Class
N835	J141249.4-402138	213.2058	-40.3605	13.2	8.93	6.29 ± 1.43	V504 Cen		CV ^{c)}
N836	J141309.7-652019	213.2905	-65.3386	6.2	21.79	19.01 ± 2.05	Circinus Galaxy	0.0014	SEYFERT
N837	J141315.1-031229	213.3131	-3.2080	3.7	43.10	74.99 ± 4.77	NGC 5506	0.0061	SEYFERT
N838	J141441.8+165824	213.6743	16.9735	16.5	6.94	3.96 ± 1.09	RX J1414.6+1658	0.2376	SEYFERT
N839	J141648.2+223515 ^{b)}	214.2008	22.5875	17.0	6.45	2.92 ± 0.87		0.1374	SEYFERT
N840	J141650.0-115854	214.2085	-11.9816	14.2	9.04	7.04 ± 1.58	2RXS J141650.3-115847	0.0986	SEYFERT
N841	J141757.0+254328	214.4877	25.7245	15.6	8.83	5.28 ± 1.18	1E 1415.6+2557	0.2400	BLAZAR
N842	J141758.1+091620	214.4922	9.2723	20.6	5.93	3.48 ± 1.12	RX J1417.9+0916	0.1389	SEYFERT
N843	J141759.4+250811	214.4977	25.1364	5.8	25.78	25.76 ± 2.40	NGC 5548	0.0172	SEYFERT
N844	J141903.7-131048	214.7653	-13.1799	26.0	5.58	3.08 ± 1.08	PG 1416-129	0.1289	SEYFERT
N845	J141908.8+075454	214.7867	7.9149	21.8	5.71	3.76 ± 1.19	SDSS J141908.30+075449.6	0.0560	SEYFERT
N846	J141949.9+194412	214.9578	19.7366	17.9	6.53	3.44 ± 1.02	RX J1419.8+1944	0.0771	SEYFERT
N847	J141949.9-192825	214.9581	-19.4735	18.1	6.64	4.05 ± 1.22	PKS J1419-1928	0.1200	SEYFERT
N848	J142006.2-165410 ^{b)}	215.0256	-16.9027	20.5	5.38	3.41 ± 1.18			BLAZAR? ^{c)}
N849	J142112.1-624158	215.3004	-62.6994	2.3	78.12	161.60 ± 6.01	4U 1416-62		HMXB
N850	J142130.3+474719	215.3764	47.7887	10.8	11.82	7.47 ± 1.34	3A 1422+481	0.0723	SEYFERT
N851	J142148.6-630137	215.4526	-63.0270	16.2	7.63	4.17 ± 1.07	2E 1418.0-6247		UNIDENT
N852	J142149.3-380858	215.4555	-38.1494	23.5	5.67	3.72 ± 1.20	2RXS J142149.9-380857		UNIDENT
N853	J142238.3+580154	215.6596	58.0318	14.5	7.04	3.83 ± 1.02	1ES 1421+582		BLAZAR
N854	J142508.7-611903	216.2863	-61.3174	17.7	7.24	4.42 ± 1.16	IGR J14257-6117		CV
N855	J142543.6-310716	216.4318	-31.1212	18.6	6.97	5.18 ± 1.40	2RXS J142544.3-310723		AGN? ^{c)}
N856	J142557.7+374956	216.4904	37.8323	20.0	6.69	4.59 ± 1.26	Abell 1914	0.1660	CLUSTER
N857	J142725.3+194959	216.8556	19.8329	16.1	6.46	3.24 ± 1.01	Mrk 813	0.1099	SEYFERT
N858	J142833.1+424014	217.1379	42.6707	8.1	17.67	15.44 ± 1.95	4U 1444+43	0.1292	BLAZAR
N859	J142906.8+011708	217.2781	1.2855	12.5	10.35	7.32 ± 1.54	Mrk 1383	0.0866	SEYFERT
N860	J142958.7-671435	217.4947	-67.2431	12.7	10.02	5.36 ± 1.14	IGR J14298-6715		LMXB
N861	J143231.2-580932 ^{b)}	218.1299	-58.1590	19.1	5.91	3.43 ± 1.06			UNIDENT
N862	J143307.4-611535	218.2810	-61.2598	17.1	7.12	3.62 ± 1.01	IGR J14331-6112		HMXB
N863	J143342.2-730420	218.4258	-73.0721	20.3	5.75	2.54 ± 0.78	2RXS J143342.2-730430		BLAZAR?
N864	J143352.3+052725	218.4677	5.4570	18.4	7.13	4.88 ± 1.32	NGC 5674	0.0249	SEYFERT
N865	J143446.5+231756	218.6939	23.2989	16.0	7.13	4.16 ± 1.12	RX J1434.7+2317	0.1003	SEYFERT
N866	J143622.8+584742	219.0952	58.7950	21.5	5.84	3.31 ± 0.99	Mrk 817	0.0313	SEYFERT
N867	J143649.6-161342	219.2066	-16.2283	13.4	8.79	6.17 ± 1.46	HE 1434-1600	0.1445	SEYFERT
N868	J143701.5+073508 ^{b)}	219.2564	7.5856	21.0	5.54	3.02 ± 1.05		0.1830	SEYFERT? ^{c)}
N869	J143739.3-361323	219.4139	-36.2231	12.1	12.70	9.28 ± 1.57	XMMSL2 J143739.7-361331		STAR? ^{c)}
N870	J144037.2-384649	220.1548	-38.7804	9.9	12.05	8.95 ± 1.56	2RXS J144037.6-384659		BLAZAR
N871	J144223.9-171514	220.5997	-17.2538	20.3	5.76	3.67 ± 1.15	NGC 5728	0.0093	SEYFERT
N872	J144248.8+120040	220.7032	12.0112	10.4	12.32	10.27 ± 1.75	1ES 1440+122	0.1631	BLAZAR
N873	J144302.9+520124	220.7619	52.0232	22.0	5.41	2.04 ± 0.70	3C 303	0.1412	SEYFERT
N874	J144356.4-390830	220.9849	-39.1418	16.9	7.51	5.33 ± 1.37	PKS 1440-389	0.1385	BLAZAR
N875	J144713.8-631723	221.8077	-63.2897	16.1	7.71	4.83 ± 1.17	IGR J14471-6319	0.0380	SEYFERT
N876	J144720.0-581607	221.8333	-58.2687	17.4	7.68	4.81 ± 1.18	SWIFT J1447.0-5814		CV? ^{c)}
N877	J144739.0-083338	221.9125	-8.5606	22.2	6.28	4.13 ± 1.27	RBS 1431	0.1980	SEYFERT

Table A.1. continued.

Id	Name SRGA	RA (J2000)	Dec (J2000)	R98 (")	S/N	Flux (10^{-12} erg s $^{-1}$ cm $^{-2}$)	Conventional name	Redshift	Class
N878	J144844.1-594209	222.1837	-59.7026	14.5	9.69	5.95 ± 1.28	IGR J14488-5942		HMXB
N879	J144851.5-400844	222.2147	-40.1454	15.4	7.47	4.64 ± 1.25	IGR J14488-4008	0.1230	SEYFERT
N880	J144914.1-553620	222.3088	-55.6056	13.6	9.17	5.87 ± 1.30	IGR J14493-5534	0.0187	SEYFERT ^{c)}
N881	J145134.2-554045	222.8925	-55.6791	14.8	8.74	5.70 ± 1.28	IGR J14515-5542	0.0180	SEYFERT
N882	J145307.6+255441	223.2818	25.9114	15.9	7.36	4.74 ± 1.19	SWIFT J1453.3+2558	0.0485	SEYFERT
N883	J145339.7-552145	223.4156	-55.3624	19.8	5.45	2.95 ± 0.97	IGR J14536-5522		CV
N884	J145517.3-513414	223.8219	-51.5705	11.6	9.93	7.35 ± 1.53	IGR J14552-5133	0.0160	SEYFERT
N885	J145524.8-645953	223.8535	-64.9980	24.8	5.41	2.47 ± 0.85	IGR J14549-6459		AGN? ^{c)}
N886	J145532.6-544636	223.8857	-54.7767	24.4	5.37	2.88 ± 0.99	IGR J14557-5448		AGN? ^{c)}
N887	J145738.5-362411	224.4105	-36.4029	22.6	6.52	4.75 ± 1.37	2RXS J145737.0-362408		AGN? ^{c)}
N888	J145742.2-430803	224.4257	-43.1341	17.6	6.98	4.55 ± 1.27	IGR J14579-4308	0.0157	SEYFERT
N889	J150340.5-154115	225.9188	-15.6874	7.8	17.18	15.43 ± 2.06	EGR J1504-1539		BLAZAR
N890	J150401.5+102619	226.0061	10.4385	9.5	14.66	13.82 ± 2.04	Mrk 841	0.0364	SEYFERT
N891	J150407.2-024810	226.0302	-2.8028	13.3	10.62	9.84 ± 1.89	RXC J1504.1-0248	0.2172	CLUSTER ^{c)}
N892	J150439.9+010745	226.1663	1.1292	19.2	6.24	4.11 ± 1.21	2CXO J150440.4+010734	0.1283	SEYFERT
N893	J150655.7-215923	226.7319	-21.9897	18.1	6.96	4.09 ± 1.16	2RXS J150654.7-215932		BLAZAR?
N894	J150843.5+270900	227.1812	27.1500	21.7	5.86	3.06 ± 0.95	RX J1508.7+2709	0.2696	BLAZAR
N895	J150854.0-001149	227.2251	-0.1969	20.5	5.91	4.10 ± 1.28	Mrk 1393	0.0543	SEYFERT
N896	J150926.8-664923	227.3616	-66.8230	6.8	19.81	16.16 ± 1.87	IGR J15094-6649		CV
N897	J151013.9+332951	227.5579	33.4975	32.0	5.40	2.92 ± 0.97	Abell 2034	0.1132	CLUSTER
N898	J151055.8+054436	227.7325	5.7434	11.9	15.08	19.03 ± 2.56	Abell 2029	0.0773	CLUSTER
N899	J151159.0-211851	227.9957	-21.3143	17.8	6.52	4.97 ± 1.41	IRAS 15091-2107	0.0446	SEYFERT
N900	J151250.8-090600	228.2117	-9.0998	14.2	10.18	7.09 ± 1.47	PKS 1510-08	0.3600	BLAZAR
N901	J151338.1-344046	228.4089	-34.6795	18.5	6.64	4.15 ± 1.23	2RXS J151338.6-344049	0.0382	SEYFERT ^{c)}
N902	J151355.0-590806	228.4793	-59.1350	5.2	30.41	39.78 ± 3.15	PSR B1509-58		SNR / PULSAR
N903	J151425.6-545900 ^{b)}	228.6065	-54.9834	25.5	5.61	3.57 ± 1.16			CV? ^{c)}
N904	J151443.4-812337	228.6810	-81.3935	11.9	11.22	7.02 ± 1.30	SWIFT J1513.8-8125	0.0684	SEYFERT
N905	J151503.3+420251	228.7638	42.0475	18.8	6.73	3.38 ± 0.88	NGC 5899	0.0086	SEYFERT
N906	J151742.1-242221	229.4253	-24.3726	15.6	7.60	4.58 ± 1.23	PKS 1514-24	0.0490	BLAZAR
N907	J151747.1+652518	229.4461	65.4216	11.2	9.78	5.96 ± 1.16	H 1517+656	0.7020	BLAZAR
N908	J151922.2+590822	229.8425	59.1393	16.4	6.51	2.64 ± 0.69	SBSG 1518+593	0.0781	SEYFERT
N909	J151931.6-472604 ^{b)}	229.8817	-47.4345	15.1	6.59	3.65 ± 1.06		0.0342	AGN ^{c)}
N910	J151932.6+653550	229.8858	65.5973	17.3	6.40	2.43 ± 0.75	MCG+11-19-006	0.0440	SEYFERT
N911	J152041.0-571001	230.1710	-57.1668	0.4	604.13	5114.62 ± 33.85	Cir X-1		HMXB
N912	J152102.1+320410	230.2589	32.0693	13.6	9.00	5.10 ± 1.13	2SXPS J152101.8+320415	0.1143	SEYFERT ^{c)}
N913	J152346.6+633929	230.9443	63.6579	13.4	8.72	3.90 ± 0.85	4C +63.22	0.2049	SEYFERT
N914	J152450.8-100558	231.2118	-10.0994	22.5	5.41	3.54 ± 1.21	HE 1522-0955	0.1460	SEYFERT
N915	J152506.9-032658	231.2787	-3.4493	15.2	7.75	4.87 ± 1.22	2RXS J152507.0-032645		CV
N916	J152903.1-671104	232.2629	-67.1845	21.7	5.44	2.93 ± 0.92	2RXS J152906.9-671047		UNIDENT
N917	J152907.6+561607	232.2818	56.2686	19.6	6.20	2.16 ± 0.62	RX J1529.1+5616	0.0997	SEYFERT
N918	J152937.2-442325 ^{b)}	232.4051	-44.3903	20.6	5.43	2.72 ± 0.99			UNIDENT
N919	J153117.8+072731	232.8243	7.4587	22.9	5.44	2.94 ± 0.99	NGC 5940	0.0337	SEYFERT

Table A.1. continued.

Id	Name SRGA	RA (J2000)	Dec (J2000)	R98 (")	S/N	Flux (10^{-12} erg s $^{-1}$ cm $^{-2}$)	Conventional name	Redshift	Class
N920	J153158.5-293020	232.9936	-29.5056	16.1	7.32	5.43 ± 1.42	PKS 1528-29		BLAZAR? ^{c)}
N921	J153309.3-522318	233.2887	-52.3884	15.9	8.07	5.20 ± 1.27	2SXPS J153309.9-522318		CV? ^{c)}
N922	J153311.0+185430	233.2960	18.9083	18.3	6.29	3.70 ± 1.10	RX J1533.1+1854	0.3071	BLAZAR
N923	J153320.9-084212	233.3371	-8.7034	19.1	7.16	5.54 ± 1.50	MCG-01-40-001	0.0227	SEYFERT
N924	J153344.9+690038	233.4369	69.0106	17.0	7.04	3.33 ± 0.85	RX J1533.7+6900	0.1340	SEYFERT
N925	J153412.6+625855	233.5523	62.9819	17.1	6.64	2.24 ± 0.63	RX J1534.2+6259	0.2372	SEYFERT ^{c)}
N926	J153552.4+575400	233.9682	57.8997	8.3	15.46	7.65 ± 1.02	Mrk 290	0.0302	SEYFERT
N927	J153603.0-574849	234.0125	-57.8135	18.9	5.53	2.66 ± 0.89	IGR J15360-5750		AGN? ^{c)}
N928	J153814.2-554215	234.5592	-55.7042	9.6	11.96	8.47 ± 1.49	AX J1538.3-5541		LMXB? ^{c)}
N929	J153844.1-032248	234.6835	-3.3800	20.2	5.98	3.99 ± 1.27	IRAS 15361-0313	0.0239	SEYFERT
N930	J153938.3-833507	234.9094	-83.5852	24.6	5.83	2.96 ± 0.92	RXC J1539.5-8335	0.0728	CLUSTER
N931	J154017.7+815513	235.0738	81.9204	17.5	5.65	2.41 ± 0.77	1ES 1544+820		BLAZAR
N932	J154203.6-291458	235.5148	-29.2495	20.3	5.37	3.12 ± 1.09	4FGL J1541.9-2915		BLAZAR
N933	J154210.6+130758	235.5440	13.1327	19.8	5.88	2.82 ± 0.89	RX J1542.1+1307	0.0928	SEYFERT
N934	J154223.4-522310	235.5974	-52.3862	1.7	104.27	282.94 ± 8.46	4U 1538-52		HMXB
N935	J154426.3-201636	236.1094	-20.2766	22.8	5.66	3.89 ± 1.23	2RXS J154426.1-201636		AGN? ^{c)}
N936	J154500.2-664154	236.2509	-66.6983	14.4	8.22	4.58 ± 1.11	4FGL J1545.0-6642		BLAZAR
N937	J154507.0+170949	236.2792	17.1637	19.6	6.50	3.74 ± 1.09	RX J1545.1+1709	0.0483	SEYFERT
N938	J154623.3+692903	236.5972	69.4842	16.9	5.86	2.65 ± 0.74	SWIFT J1546.3+6928	0.0376	SEYFERT
N939	J154707.6-474008	236.7816	-47.6690	0.7	333.49	2177.64 ± 23.77	4U 1543-47		LMXB
N940	J154743.0-442203	236.9294	-44.3674	19.8	5.68	3.06 ± 1.02	2SXPS J154743.1-442157		AGN? ^{c)}
N941	J154744.0+205214	236.9334	20.8706	20.5	5.69	2.34 ± 0.74	PG 1545+210	0.2643	SEYFERT
N942	J154754.9-623408	236.9786	-62.5688	2.4	72.99	145.46 ± 5.81	4U 1543-624		LMXB
N943	J154815.0-452842	237.0624	-45.4785	6.2	24.93	29.75 ± 2.89	NY Lup		CV
N944	J154824.7-134523	237.1029	-13.7565	9.8	13.25	12.46 ± 2.08	NGC 5995	0.0252	SEYFERT
N945	J154850.2-225055	237.2093	-22.8487	9.2	14.72	13.83 ± 2.15	PMN J1548-2251	0.1920	BLAZAR
N946	J155053.9-541828	237.7248	-54.3078	19.4	6.22	3.88 ± 1.13	1E 1547.0-5408		MAGNETAR
N947	J155247.3+185636	238.1969	18.9434	18.1	6.79	3.46 ± 0.98	PG 1550+191		CV
N948	J155343.0+234833	238.4291	23.8091	13.0	10.17	6.54 ± 1.30	4C +23.42	0.1176	SEYFERT
N949	J155418.2+323832	238.5757	32.6423	21.0	6.01	2.61 ± 0.83	RX J1554.2+3238	0.0483	SEYFERT
N950	J155432.1-334006	238.6338	-33.6683	21.4	6.44	3.84 ± 1.16	2RXS J155431.4-334026		AGN? ^{c)}
N951	J155507.8-540340	238.7824	-54.0611	9.4	13.55	9.65 ± 1.60	SWIFT J1555.2-5402		MAGNETAR
N952	J155543.0+111128	238.9290	11.1910	6.8	20.75	18.75 ± 2.16	PG 1553+113	0.3600	BLAZAR
N953	J155603.4-521610	239.0140	-52.2695	15.2	7.93	5.00 ± 1.24	2RXS J155601.4-521556		CV ^{c)}
N954	J155612.5+662100	239.0520	66.3499	19.9	5.74	2.01 ± 0.63	Abell 2146	0.2337	CLUSTER
N955	J155701.0-791402	239.2541	-79.2338	14.7	8.37	4.83 ± 1.17	PKS 1549-79	0.1522	BLAZAR
N956	J155747.6-542450	239.4485	-54.4138	3.8	43.91	66.10 ± 4.04	2S 1553-542		HMXB
N957	J155827.5+271237	239.6144	27.2103	16.7	7.55	5.12 ± 1.26	Abell 2142	0.0903	CLUSTER
N958	J155901.6-733759	239.7565	-73.6330	19.7	6.06	3.15 ± 1.03	2SXPS J155901.9-733748		AGN? ^{c)}
N959	J155929.6+255508	239.8734	25.9189	11.6	9.74	5.12 ± 1.06	T CrB		CV
N960	J160050.8-514300	240.2118	-51.7166	15.5	8.42	5.56 ± 1.32	2XMM J160050.7-514245		STAR ^{c)}
N961	J160102.3-604418	240.2594	-60.7385	2.1	89.71	213.12 ± 7.19	4U 1556-60		LMXB

S. Sazonov et al.: SRG/ART-XC all-sky X-ray survey: Catalog of sources detected during the first five surveys

Table A.1. continued.

Id	Name SRGA	RA (J2000)	Dec (J2000)	R98 (")	S/N	Flux (10^{-12} erg s $^{-1}$ cm $^{-2}$)	Conventional name	Redshift	Class
N962	J160208.5-423056	240.5356	-42.5155	16.8	6.63	4.69 ± 1.28	2RXS J160209.5-423043		UNIDENT
N963	J160251.8-240201	240.7157	-24.0336	18.7	6.29	3.84 ± 1.15	RX J1602.8-2401B		STAR
N964	J160445.8-103322	241.1908	-10.5562	15.6	7.11	4.42 ± 1.23	2RXS J160446.1-103338	0.0602	SEYFERT
N965	J160455.4-722323	241.2307	-72.3898	17.1	6.61	3.92 ± 1.16	2RXS J160451.8-722257		STAR ^{c)}
N966	J160519.5+542103	241.3313	54.3509	16.4	6.19	1.93 ± 0.53	RX J1605.3+5421	0.2117	BLAZAR
N967	J160534.2+164904 ^{b)}	241.3925	16.8178	20.1	5.76	2.96 ± 0.97		0.1414	SEYFERT ^{c)}
N968	J160546.0+255157	241.4415	25.8659	15.0	7.70	3.97 ± 1.03	2E 1603.6+2600		LMXB
N969	J160552.0-611140	241.4665	-61.1945	17.6	6.33	3.47 ± 1.02	IGR J16056-6110	0.0520	SEYFERT
N970	J160621.5+563014	241.5896	56.5038	12.7	7.81	2.23 ± 0.50	RX J1606.3+5630	0.4500	BLAZAR
N971	J160901.9-390518	242.2579	-39.0883	19.8	5.88	2.74 ± 0.97	THA 15-35		STAR
N972	J160947.4-545110 ^{b)}	242.4474	-54.8529	21.1	5.96	3.54 ± 1.14			AGN? ^{c)}
N973	J161007.2+035236	242.5298	3.8767	15.4	7.59	4.58 ± 1.24	V519 Ser		CV
N974	J161018.6-634242	242.5775	-63.7116	16.5	7.79	5.85 ± 1.49	2RXS J161017.3-634238	0.2094	SEYFERT ^{c)}
N975	J161123.5+585053	242.8480	58.8480	19.7	5.40	1.27 ± 0.41	SBS 1610+589	0.0321	SEYFERT
N976	J161150.2-603755	242.9592	-60.6320	12.5	10.42	7.95 ± 1.56	WKK 6092	0.0156	SEYFERT
N977	J161158.3-494115 ^{b)}	242.9929	-49.6874	20.0	6.30	4.30 ± 1.25			UNIDENT
N978	J161243.3-522523	243.1803	-52.4231	1.9	103.49	310.50 ± 9.32	4U 1608-52		LMXB
N979	J161251.4-052105	243.2140	-5.3515	17.9	6.63	3.61 ± 1.10	2RXS J161250.6-052118	0.0306	SEYFERT ^{c)}
N980	J161354.3-304714 ^{b)}	243.4763	-30.7873	20.5	5.44	3.12 ± 1.08			UNIDENT
N981	J161356.0+654312	243.4833	65.7201	10.1	11.03	4.09 ± 0.71	Mrk 876	0.1211	SEYFERT
N982	J161413.4+260416	243.5560	26.0710	15.5	8.17	4.82 ± 1.13	Ton 256	0.1310	SEYFERT
N983	J161440.3+335126	243.6680	33.8571	12.1	9.56	4.97 ± 1.05	sig CrB		STAR
N984	J161515.2-283722	243.8135	-28.6229	10.3	14.02	12.19 ± 2.01	V893 Sco		CV
N985	J161518.9-093608	243.8288	-9.6022	16.6	7.17	4.34 ± 1.20	XSS J16151-0943	0.0650	SEYFERT
N986	J161537.9+594546	243.9077	59.7629	13.5	8.04	2.39 ± 0.53	RX J1615.6+5945		AGN? ^{c)}
N987	J161545.4-060851	243.9392	-6.1475	18.4	7.56	6.80 ± 1.65	Abell 2163	0.2010	CLUSTER
N988	J161637.8-495847	244.1577	-49.9797	7.9	16.83	16.53 ± 2.25	IGR J16167-4957		CV
N989	J161728.9-502245	244.3706	-50.3793	17.6	6.98	3.74 ± 1.08	IGR J16173-5023		CV? ^{c)}
N990	J161730.0-505514	244.3749	-50.9205	9.9	13.27	4.18 ± 0.64	PSR J1617-5055		SNR / PULSAR
N991	J161735.5+501447 ^{b)}	244.3980	50.2464	17.6	5.70	1.38 ± 0.44		0.0417	SEYFERT ^{c)}
N992	J161742.0+322236	244.4249	32.3768	13.8	9.29	5.22 ± 1.11	3C 332	0.1510	SEYFERT
N993	J161836.1-592729	244.6503	-59.4581	16.9	6.52	4.65 ± 1.38	IGR J16185-5928	0.0346	SEYFERT
N994	J161932.4-494428	244.8850	-49.7412	6.3	22.23	26.36 ± 2.81	IGR J16195-4945		HMXB
N995	J161933.2-280733	244.8883	-28.1259	11.1	13.33	13.29 ± 2.09	IGR J16195-2807		LMXB
N996	J161944.1-132618 ^{b)}	244.9338	-13.4385	19.5	5.81	3.48 ± 1.15		0.0789	SEYFERT ^{c)}
N997	J161947.6+435849 ^{b)}	244.9483	43.9804	19.9	5.51	1.92 ± 0.61		0.8524	SEYFERT? ^{c)}
N998	J161953.5+405840	244.9731	40.9779	20.3	5.68	1.74 ± 0.56	1ES 1618+411	0.0378	SEYFERT
N999	J161955.1-153824	244.9795	-15.6400	0.1	3600.88	206247.34 ± 262.61	Sco X-1		LMXB
N1000	J162046.5-513006	245.1939	-51.5017	8.1	17.89	18.33 ± 2.38	IGR J16207-5129		HMXB
N1001	J162145.5+542720	245.4396	54.4555	8.2	13.18	4.93 ± 0.73	SBS 1620+545	0.0505	SEYFERT
N1002	J162304.9+662410	245.7703	66.4029	18.0	5.84	1.57 ± 0.46	RX J1623.0+6624	0.2010	BLAZAR
N1003	J162312.1-260324	245.8004	-26.0567	24.2	5.51	2.85 ± 1.05	1AXG J162310-2603		AGN? ^{c)}

Table A.1. continued.

Id	Name SRGA	RA (J2000)	Dec (J2000)	R98 (")	S/N	Flux (10^{-12} erg s $^{-1}$ cm $^{-2}$)	Conventional name	Redshift	Class
N1004	J162420.7-331101	246.0862	-33.1837	16.9	6.62	4.19 ± 1.22	SWIFT J1624.5-3317		SEYFERT ^{c)}
N1005	J162458.2-321321	246.2424	-32.2224	25.2	5.38	2.68 ± 1.01	ICRF J162459.6-321324		BLAZAR?
N1006	J162459.3+503538 ^{b)}	246.2473	50.5938	18.8	5.51	1.42 ± 0.45			UNIDENT
N1007	J162526.8+852953	246.3618	85.4979	12.7	9.84	5.73 ± 1.17	IRAS 16360+8536	0.0631	SEYFERT
N1008	J162552.7+434723	246.4694	43.7898	18.0	6.11	1.70 ± 0.50	RX J1625.8+4346	1.0456	BLAZAR
N1009	J162606.4-295123	246.5269	-29.8564	20.0	5.58	2.84 ± 1.01	PKS 1622-29	0.8138	BLAZAR
N1010	J162618.5-392702 ^{b)}	246.5771	-39.4504	20.8	5.83	3.09 ± 1.07			CV? ^{c)}
N1011	J162636.5-515629	246.6522	-51.9415	3.7	42.53	72.35 ± 4.80	SWIFT J1626.6-5156		HMXB
N1012	J162719.3-244146	246.8303	-24.6961	17.7	7.46	4.75 ± 1.31	SR 12		STAR
N1013	J162756.5+552233	246.9854	55.3759	13.2	8.84	2.72 ± 0.57	PG 1626+554	0.1330	SEYFERT
N1014	J162802.6-491153	247.0109	-49.1981	1.0	204.58	1005.15 ± 17.02	4U 1624-49		LMXB
N1015	J162804.2+514631	247.0175	51.7753	6.8	19.04	8.72 ± 0.97	Mrk 1498	0.0547	SEYFERT
N1016	J162808.3+634922	247.0347	63.8228	18.2	6.33	1.51 ± 0.39	RX J1628.1+6349	0.1040	SEYFERT
N1017	J162827.2-502233	247.1133	-50.3759	20.1	6.02	4.11 ± 1.32	IGR J16287-5021		LMXB
N1018	J162827.5-432634 ^{b)}	247.1147	-43.4426	22.0	5.50	2.95 ± 1.05			UNIDENT
N1019	J162838.9+393228	247.1620	39.5411	25.4	8.04	6.05 ± 1.27	Abell 2199	0.0309	CLUSTER
N1020	J162949.1+672240	247.4546	67.3777	19.3	5.79	1.59 ± 0.48	Mrk 885	0.0253	SEYFERT
N1021	J163114.2-474821	247.8090	-47.8059	5.0	30.72	48.94 ± 4.07	MAXI J1631-479		LMXB
N1022	J163148.1-484857	247.9506	-48.8158	10.4	12.45	12.85 ± 2.28	IGR J16318-4848		HMXB
N1023	J163202.0-475230	248.0082	-47.8750	3.4	49.42	110.95 ± 6.29	IGR J16320-4751		HMXB
N1024	J163217.4-672741	248.0727	-67.4613	2.0	92.15	254.95 ± 8.62	4U 1626-67		LMXB
N1025	J163231.8+823218	248.1326	82.5384	19.6	5.60	2.38 ± 0.76	NGC 6251	0.0247	SEYFERT
N1026	J163247.4+053424	248.1976	5.5735	13.6	10.44	8.71 ± 1.71	Abell 2204	0.1511	CLUSTER
N1027	J163402.0-472335	248.5081	-47.3931	2.1	88.04	298.51 ± 10.51	4U 1630-47		LMXB
N1028	J163515.5+380811	248.8144	38.1363	16.9	6.16	2.48 ± 0.73	4C 38.41	1.8140	BLAZAR
N1029	J163529.1-480606	248.8712	-48.1016	16.8	8.64	7.96 ± 1.89	2E 1631.7-4759		X-RAY BINARY? ^{c)}
N1030	J163605.3+661238	249.0221	66.2105	18.6	6.13	1.65 ± 0.44	Abell 2218	0.1709	CLUSTER
N1031	J163816.8-642216	249.5701	-64.3712	23.6	5.89	6.80 ± 1.93	Triangulum Australis Cluster	0.0510	CLUSTER
N1032	J163827.9-441447 ^{b)}	249.6165	-44.2464	21.3	5.86	3.97 ± 1.35			UNIDENT ^{c)}
N1033	J163830.4-205526	249.6266	-20.9240	14.1	8.84	6.83 ± 1.61	IGR J16385-2057	0.0264	SEYFERT
N1034	J163905.7-464211	249.7738	-46.7031	6.5	21.39	31.85 ± 3.60	AX J1639.0-4642		HMXB
N1035	J164017.7+464234	250.0739	46.7094	16.7	7.62	3.74 ± 0.85	Abell 2219	0.2257	CLUSTER
N1036	J164046.2-032813 ^{b)}	250.1925	-3.4703	21.1	5.37	3.11 ± 1.06			CV? ^{c)}
N1037	J164050.9+654718 ^{b)}	250.2123	65.7882	15.7	7.17	1.93 ± 0.46		0.0244	SEYFERT ^{c)}
N1038	J164052.6-061833 ^{b)}	250.2191	-6.3092	19.8	5.68	2.71 ± 0.97		0.0277	SEYFERT
N1039	J164056.1-534506	250.2337	-53.7515	1.5	154.66	726.92 ± 15.90	4U 1636-536		LMXB
N1040	J164150.7-453228	250.4614	-45.5410	5.2	27.93	50.37 ± 4.50	IGR J16418-4532		HMXB
N1041	J164257.9+394850	250.7414	39.8138	19.2	6.29	2.66 ± 0.74	3C 345	0.5934	BLAZAR
N1042	J164356.8-321347 ^{b)}	250.9868	-32.2298	16.3	7.79	5.76 ± 1.58			AGN? ^{c)}
N1043	J164433.4-513411	251.1392	-51.5696	19.5	5.82	4.41 ± 1.44	2RXS J164434.8-513358		AGN? ^{c)}
N1044	J164516.2-733501	251.3175	-73.5836	22.7	5.65	4.04 ± 1.23	PKS 1639-734	0.0692	SEYFERT
N1045	J164547.9-453641	251.4496	-45.6115	0.4	576.04	7958.25 ± 54.98	GX 340+0		LMXB

Table A.1. continued.

Id	Name SRGA	RA (J2000)	Dec (J2000)	R98 (")	S/N	Flux (10^{-12} erg s $^{-1}$ cm $^{-2}$)	Conventional name	Redshift	Class
N1046	J164607.6–392836 ^{b)}	251.5318	–39.4765	22.5	5.48	2.92 ± 1.13			UNIDENT
N1047	J164610.7–112404	251.5444	–11.4012	21.4	5.79	3.61 ± 1.20	H 1643-113	0.0740	SEYFERT
N1048	J164635.8–450707	251.6493	–45.1185	9.8	12.89	17.77 ± 2.82	IGR J16465-4507		HMXB
N1049	J164641.0–602355	251.6708	–60.3987	21.1	6.13	4.60 ± 1.42	CIZA J1646.6-6023	0.1480	CLUSTER
N1050	J164734.4+495000	251.8934	49.8332	13.7	8.14	2.89 ± 0.65	RX J1647.5+4950	0.0475	BLAZAR
N1051	J164807.4–451216	252.0310	–45.2044	8.0	16.82	25.06 ± 3.31	IGR J16479-4514		HMXB
N1052	J164927.6–434907	252.3650	–43.8187	4.7	32.69	57.99 ± 4.82	IGR J16493-4348		HMXB
N1053	J164955.8–330703	252.4826	–33.1175	12.8	10.53	12.64 ± 2.48	IGR J16500-3307		CV
N1054	J165042.8+043615	252.6784	4.6041	13.8	8.72	6.59 ± 1.54	2MASX J16504275+043618	0.0326	SEYFERT
N1055	J165119.4–591403	252.8310	–59.2342	23.3	5.48	3.14 ± 1.15	ESO 138-1	0.0092	SEYFERT
N1056	J165143.2+532539	252.9299	53.4276	15.8	5.95	1.42 ± 0.39	SBS 1650+535	0.0286	SEYFERT ^{c)}
N1057	J165219.7+555422	253.0822	55.9061	9.9	10.56	3.09 ± 0.54	SBS 1651+559	0.0291	SEYFERT
N1058	J165246.9–591303	253.1953	–59.2174	10.5	10.84	9.56 ± 1.91	NGC 6221	0.0050	SEYFERT
N1059	J165251.2+172700	253.2132	17.4500	19.6	5.81	2.56 ± 0.85	4XMM J165251.4+172651	0.0344	AGN? ^{c)}
N1060	J165314.5+234947	253.3105	23.8298	17.6	6.57	2.88 ± 0.86	IRAS 16511+2354	0.1034	SEYFERT
N1061	J165352.1+394536	253.4672	39.7600	4.2	38.11	35.12 ± 2.31	Mrk 501	0.0330	BLAZAR
N1062	J165435.5+330241	253.6480	33.0448	22.0	5.38	2.05 ± 0.70	SDSS J165435.84+330251.4	0.1222	SEYFERT
N1063	J165444.0–191634	253.6832	–19.2761	10.7	13.43	16.65 ± 2.76	IGR J16547-1916		CV
N1064	J165517.8–224021	253.8242	–22.6726	23.9	5.39	4.49 ± 1.60	1BIGB J165517.8-224045		BLAZAR
N1065	J165552.1–495737	253.9669	–49.9604	23.5	5.70	4.01 ± 1.37	IGR J16560-4958	0.0586	SEYFERT ^{c)}
N1066	J165601.6+211241	254.0066	21.2113	14.9	9.44	5.96 ± 1.27	2RXS J165602.3+211238	0.0492	SEYFERT
N1067	J165605.6–520342	254.0232	–52.0618	9.2	14.71	17.06 ± 2.60	IGR J16558-5203	0.0540	SEYFERT
N1068	J165617.1–330203	254.0711	–33.0341	19.3	5.75	3.59 ± 1.29	SWIFT J1656.3-3302	2.4000	BLAZAR
N1069	J165749.8+352032	254.4573	35.3423	1.0	178.98	492.69 ± 8.84	Her X-1		LMXB
N1070	J165833.7+051516	254.6403	5.2543	12.9	9.95	7.65 ± 1.61	PKS 1656+053	0.8790	BLAZAR
N1071	J170004.8–415802	255.0202	–41.9673	18.9	7.27	6.06 ± 1.75	AX J1740.1-2847		HMXB
N1072	J170008.9+683003	255.0369	68.5009	19.5	5.87	1.48 ± 0.41	ICRF J170009.2+683006	0.3010	BLAZAR
N1073	J170025.6–724043	255.1066	–72.6785	15.5	7.75	4.43 ± 1.20	2RXS J170023.5-724040	0.1047	SEYFERT ^{c)}
N1074	J170048.9–413921	255.2039	–41.6558	2.4	79.02	269.82 ± 10.35	OA0 1657-41		HMXB
N1075	J170054.5+400352	255.2269	40.0644	18.8	6.23	2.06 ± 0.61	V1237 Her		CV
N1076	J170109.4+292437	255.2891	29.4103	20.7	6.35	3.42 ± 0.96	Mrk 504	0.0361	SEYFERT
N1077	J170128.1–430621	255.3670	–43.1057	14.6	9.19	8.87 ± 2.01	IGR J17014-4306		CV
N1078	J170144.5–405129	255.4354	–40.8581	2.3	85.18	294.07 ± 10.82	XTE J1701-407		LMXB
N1079	J170228.0+341055	255.6168	34.1821	21.9	5.40	2.18 ± 0.71	2MASX J17022620+3411173	0.1053	SEYFERT
N1080	J170244.7+725317	255.6861	72.8881	22.4	5.47	1.76 ± 0.52	RBS 1620	0.0545	SEYFERT
N1081	J170249.8–484723	255.7074	–48.7898	1.4	142.91	694.97 ± 16.23	GX 339-4		LMXB
N1082	J170330.8+454051	255.8782	45.6808	15.8	7.05	2.25 ± 0.59	IRAS 17020+4544	0.0604	SEYFERT
N1083	J170336.8+620130	255.9035	62.0249	17.0	5.65	0.92 ± 0.25	ASASSN-20hx	0.0167	AGN? ^{c)}
N1084	J170357.0–375039	255.9873	–37.8441	0.8	330.28	2692.29 ± 32.95	4U 1700-37		HMXB
N1085	J170405.8–430534	256.0240	–43.0927	15.0	8.49	8.20 ± 1.96	IGR J17040-4305		CV
N1086	J170412.5–443136	256.0521	–44.5268	9.2	14.42	16.18 ± 2.58	2RXS J170411.4-443113		UNIDENT ^{c)}
N1087	J170442.5+604431	256.1772	60.7419	10.5	8.91	1.80 ± 0.34	3C 351	0.3715	SEYFERT
N1088	J170544.7–362523	256.4362	–36.4231	0.4	654.70	9820.11 ± 61.16	GX 349+2		LMXB

Table A.1. continued.

Id	Name	RA	Dec	R98	S/N	Flux	Conventional name	Redshift	Class
	SRGA	(J2000)	(J2000)	(")		(10^{-12} erg s $^{-1}$ cm $^{-2}$)			
N1089	J170615.3-430210	256.5639	-43.0360	1.6	132.44	625.39 ± 15.71	4U 1702-429		LMXB
N1090	J170616.6-614243	256.5692	-61.7119	6.2	24.04	32.17 ± 3.32	IGR J17062-6143		LMXB
N1091	J170634.6+235821	256.6441	23.9725	5.1	28.17	30.98 ± 2.68	4U 1700+24		LMXB
N1092	J170723.3-194422	256.8470	-19.7394	22.1	5.50	4.35 ± 1.55	2RXS J170721.9-194426		AGN? ^{c)}
N1093	J170746.4+133051	256.9433	13.5140	20.6	5.85	4.63 ± 1.42	RX J1707.7+1330	0.9360	BLAZAR
N1094	J170846.9-400901	257.1954	-40.1504	11.2	11.17	11.44 ± 2.25	1RXS J170849.0-400910		MAGNETAR
N1095	J170854.5-440608	257.2273	-44.1023	0.7	316.63	2663.50 ± 31.47	4U 1705-44		LMXB
N1096	J170854.9-321856	257.2286	-32.3155	9.7	14.67	18.48 ± 2.84	4U 1705-32		LMXB
N1097	J170930.5-263925	257.3772	-26.6570	21.1	6.59	6.23 ± 1.81	XTE J1709-267		LMXB
N1098	J171012.8-280749	257.5532	-28.1301	11.0	10.79	11.32 ± 2.25	XTE J1710-281		LMXB
N1099	J171115.2+530953 ^{b)}	257.8132	53.1648	19.1	5.37	1.09 ± 0.35			AGN? ^{c)}
N1100	J171224.1-405033	258.1003	-40.8425	2.2	82.46	268.65 ± 10.10	4U 1708-40		LMXB
N1101	J171227.4-232203	258.1141	-23.3676	2.8	92.84	37.19 ± 1.01	Oph Cluster	0.0280	CLUSTER
N1102	J171228.8+355313	258.1200	35.8869	17.6	5.69	2.36 ± 0.73	MCG+06-38-005	0.0264	SEYFERT
N1103	J171236.6-241448	258.1525	-24.2467	5.9	26.74	42.64 ± 4.16	V2400 Oph		CV
N1104	J171236.8-373842	258.1535	-37.6451	3.6	45.56	113.88 ± 6.90	SAX J1712.6-3739		LMXB
N1105	J171252.4+640213	258.2184	64.0370	20.1	5.46	0.81 ± 0.21	Abell 2255	0.0801	CLUSTER
N1106	J171255.5+333127	258.2311	33.5242	17.3	7.30	3.28 ± 0.86	V795 Her		CV
N1107	J171334.7-252015	258.3945	-25.3376	18.2	6.37	4.83 ± 1.57	XMMSL2 J171334.6-252015		AGN? ^{c)}
N1108	J171344.7-391200	258.4364	-39.1998	18.5	6.41	5.75 ± 1.76	AX J1714.1-3912		HMXB
N1109	J171456.9+585123	258.7370	58.8563	17.1	6.22	1.03 ± 0.27	V508 Dra		STAR
N1110	J171544.9-232608 ^{b)}	258.9373	-23.4355	19.9	6.26	5.10 ± 1.61			UNIDENT ^{c)}
N1111	J171627.6-283945 ^{b)}	259.1148	-28.6624	20.5	5.69	4.04 ± 1.41			UNIDENT
N1112	J171659.1-624920	259.2463	-62.8223	9.6	13.45	13.41 ± 2.19	NGC 6300	0.0037	SEYFERT
N1113	J171802.2-372633	259.5093	-37.4425	22.5	6.11	4.83 ± 1.62	G349.7+0.2		SNR
N1114	J171823.9-402939	259.5994	-40.4942	17.7	7.44	7.27 ± 1.91	RX J1718.4-4029		LMXB
N1115	J171915.8+485852	259.8157	48.9810	14.0	8.15	2.43 ± 0.54	MCG+08-31-041	0.0242	BLAZAR
N1116	J171935.9-410055	259.8997	-41.0153	7.1	18.25	24.25 ± 3.23	IGR J17195-4100		CV
N1117	J171938.0+043118	259.9084	4.5218	20.2	6.23	4.49 ± 1.45	ASASSN -15kw		CV
N1118	J172002.1+485917	260.0089	48.9880	25.0	5.58	1.63 ± 0.50	1AXG J171959+4859	0.1980	SEYFERT
N1119	J172005.9-311703	260.0247	-31.2840	8.7	17.41	24.05 ± 3.30	IGR J17200-3116		HMXB
N1120	J172009.9+263747	260.0413	26.6296	20.8	5.58	3.34 ± 1.10	RBS 1639	0.1604	CLUSTER
N1121	J172202.0+431525	260.5083	43.2568	12.0	10.78	4.95 ± 0.92	RX J1722.0+4315	0.1393	SEYFERT
N1122	J172240.8+305257	260.6700	30.8824	24.6	5.67	3.35 ± 1.06	Mrk 506	0.0431	SEYFERT
N1123	J172307.4-124806	260.7808	-12.8017	7.7	18.88	25.72 ± 3.34	RY Ser		CV
N1124	J172320.8+341801	260.8367	34.3002	12.0	9.85	6.86 ± 1.37	4C +34.47	0.2060	SEYFERT
N1125	J172324.4+363007	260.8515	36.5020	15.0	8.80	5.71 ± 1.23	IRAS 17216+3633	0.0400	SEYFERT
N1126	J172525.7-325713	261.3570	-32.9537	7.9	18.35	27.15 ± 3.51	IGR J17254-3257		LMXB
N1127	J172711.7+632233	261.7987	63.3758	17.3	5.55	0.64 ± 0.17	SDSS J172711.80+632241.8	0.2173	SEYFERT
N1128	J172733.4-304804	261.8893	-30.8011	3.2	56.39	158.85 ± 8.22	4U 1722-30		LMXB
N1129	J172818.5+501310	262.0770	50.2194	10.1	12.78	5.03 ± 0.77	6C 172704+501607	0.0554	BLAZAR
N1130	J173007.7+624757	262.5321	62.7991	13.9	8.83	1.25 ± 0.23	SDSS J173008.38+624754.7		CV
N1131	J173022.1-055931	262.5921	-5.9920	9.5	14.82	17.67 ± 2.78	V2731 Oph		CV

Table A.1. continued.

Id	Name SRGA	RA (J2000)	Dec (J2000)	R98 (")	S/N	Flux (10^{-12} erg s $^{-1}$ cm $^{-2}$)	Conventional name	Redshift	Class
N1132	J173040.6–212816	262.6692	–21.4710	17.6	7.85	8.39 ± 2.11	Kepler SNR		SNR
N1133	J173144.3–165743	262.9345	–16.9621	0.5	335.23	3181.48 ± 36.17	GX 9+9		LMXB
N1134	J173157.9–335001	262.9912	–33.8336	1.2	181.24	1109.32 ± 21.41	GX 354-0		LMXB
N1135	J173201.6–191401	263.0067	–19.2336	23.1	5.35	4.19 ± 1.47	V2487 Oph		CV
N1136	J173202.0–244444	263.0082	–24.7456	2.1	91.49	359.81 ± 12.32	GX 1+4		LMXB
N1137	J173240.7+741341	263.1696	74.2280	14.3	7.85	2.30 ± 0.51	29 Dra		STAR
N1138	J173250.5–273004	263.2106	–27.5012	5.5	27.95	48.50 ± 4.62	IGR J17329-2731		LMXB
N1139	J173253.5–440735	263.2227	–44.1264	20.8	6.25	5.50 ± 1.72	2SXPS J173253.9-440728		CV? ^c
N1140	J173254.6+653323	263.2276	65.5565	13.6	7.10	0.71 ± 0.15	4C 65.21	0.8560	SEYFERT
N1141	J173324.2–332319	263.3509	–33.3887	3.0	62.34	197.93 ± 9.26	Rapid Burster		LMXB
N1142	J173338.1+363133	263.4086	36.5259	14.3	7.58	4.34 ± 1.09	SWIFT J1733.3+3635	0.0437	SEYFERT ^c
N1143	J173357.6–220200	263.4900	–22.0334	12.2	11.54	13.28 ± 2.54	4U 1730-22		LMXB
N1144	J173523.7–354026	263.8487	–35.6739	16.1	7.36	6.26 ± 1.75	IGR J17353-3539		LMXB
N1145	J173527.4–325549	263.8641	–32.9302	8.2	17.72	25.07 ± 3.37	IGR J17354-3255		HMXB
N1146	J173547.2–302854	263.9467	–30.4817	3.7	45.65	113.12 ± 7.00	XB 1732-304		LMXB
N1147	J173706.9+660102	264.2789	66.0172	13.8	6.83	0.64 ± 0.14	RX J1737.0+6601	0.3580	SEYFERT
N1148	J173728.9–290758	264.3702	–29.1326	5.4	29.79	59.56 ± 5.15	GRS 1734-292	0.0214	SEYFERT
N1149	J173739.6–595625	264.4149	–59.9403	19.9	6.20	4.64 ± 1.42	ESO 139-12	0.0170	SEYFERT
N1150	J173759.2–374622	264.4968	–37.7726	12.5	12.54	14.39 ± 2.58	IGR J17379-3747		LMXB
N1151	J173817.4–265939	264.5726	–26.9943	2.4	75.26	258.59 ± 10.58	SLX 1735-269		LMXB
N1152	J173858.4–442701	264.7435	–44.4503	0.6	372.03	3547.39 ± 37.37	4U 1735-444		LMXB
N1153	J173918.4–545409 ^b	264.8268	–54.9025	23.0	5.36	3.83 ± 1.36			AGN ^c
N1154	J173954.1–282945	264.9755	–28.4959	2.9	65.10	203.91 ± 9.47	XTE J1739-285		LMXB
N1155	J174008.8–284721	265.0368	–28.7891	14.6	9.07	8.46 ± 2.02	AX J1740.1-2847		CV? ^c
N1156	J174026.1+514950	265.1087	51.8305	14.6	6.99	2.24 ± 0.57	2E 1739.2+5151	0.0610	SEYFERT
N1157	J174027.1–365542	265.1130	–36.9285	16.5	8.80	8.56 ± 2.04	IGR J17404-3655		CV ^c
N1158	J174037.7+521138	265.1570	52.1939	18.2	5.60	1.68 ± 0.51	4C 51.37	1.3790	BLAZAR
N1159	J174038.1–273658	265.1586	–27.6161	20.9	6.18	6.29 ± 1.87	SWIFT J174038.1-273712		UNIDENT ^c
N1160	J174043.4–281812	265.1809	–28.3033	15.5	7.71	9.17 ± 2.21	SLX 1737-282		LMXB
N1161	J174046.3+060353	265.1929	6.0647	8.7	15.66	18.04 ± 2.73	PBC J1740.7+0603		CV ^c
N1162	J174104.6–224727 ^b	265.2692	–22.7909	18.2	6.99	6.09 ± 1.79			UNIDENT
N1163	J174128.8+034848	265.3700	3.8134	20.3	6.35	4.83 ± 1.52	RX J1741.4+0348	0.0230	SEYFERT
N1164	J174155.0–121201	265.4793	–12.2003	11.7	11.71	13.33 ± 2.49	2E 1739.1-1210	0.0376	SEYFERT
N1165	J174201.3–605516	265.5056	–60.9210	19.8	6.93	5.07 ± 1.47	PKS 1737-60	0.1520	SEYFERT ^c
N1166	J174207.3+182721	265.5304	18.4558	19.4	5.70	3.09 ± 1.06	4C 18.51	0.1859	SEYFERT
N1167	J174218.1+635119	265.5754	63.8552	12.9	6.82	0.65 ± 0.14	RX J1742.2+6351	0.4019	SEYFERT
N1168	J174242.0+184112	265.6750	18.6868	16.1	7.36	5.17 ± 1.41	2RXS J174241.6+184125		STAR? ^c
N1169	J174317.5+625029	265.8228	62.8415	18.4	5.95	0.61 ± 0.16	2MASX J17431735+6250207	0.0330	SEYFERT
N1170	J174355.0–294444	265.9790	–29.7456	2.7	63.72	216.79 ± 9.63	1E1740.7-2942		LMXB
N1171	J174358.1+193507	265.9921	19.5854	14.9	8.66	6.37 ± 1.55	1ES 1741+196	0.0840	BLAZAR
N1172	J174400.0–035015	265.9999	–3.8374	21.0	5.84	4.12 ± 1.48	PKS 1741-03	1.0540	BLAZAR
N1173	J174414.9+325947	266.0619	32.9964	23.8	5.77	3.71 ± 1.13	RXC J1744.2+3259	0.0757	CLUSTER

Table A.1. continued.

Id	Name SRGA	RA (J2000)	Dec (J2000)	R98 (")	S/N	Flux (10^{-12} erg s $^{-1}$ cm $^{-2}$)	Conventional name	Redshift	Class
N1174	J174445.6-295046	266.1899	-29.8462	14.3	8.89	11.01 ± 2.41	XMMU J174445.5-29504		LMXB ^{c)}
N1175	J174459.8-172643	266.2490	-17.4453	18.2	6.42	4.68 ± 1.50	2RXS J174459.5-172641		BLAZAR
N1176	J174502.1-285443	266.2589	-28.9119	8.9	14.97	22.55 ± 3.34	GRS 1741.9-2853		LMXB
N1177	J174510.2-285237 ^{b)}	266.2926	-28.8771	22.9	5.39	4.85 ± 1.71			UNIDENT
N1178	J174536.0-290133	266.3999	-29.0259	5.1	35.34	92.10 ± 6.48	1A 1742-289		LMXB
N1179	J174538.6+290833	266.4107	29.1426	15.1	7.63	4.56 ± 1.21	SWIFT J1745.4+2906	0.1100	SEYFERT
N1180	J174605.3-293054	266.5220	-29.5149	1.3	165.31	1010.20 ± 20.76	1A 1742-294		LMXB
N1181	J174609.0+673725	266.5374	67.6236	15.0	6.91	0.82 ± 0.18	2E 1746.2+6738	0.0410	SEYFERT
N1182	J174619.4-434619 ^{b)}	266.5809	-43.7720	24.1	5.49	3.43 ± 1.31			UNIDENT
N1183	J174621.1-284342	266.5880	-28.7282	3.4	53.38	152.70 ± 8.16	1E 1743.1-2843		LMXB
N1184	J174701.3+683632	266.7555	68.6088	10.1	11.80	1.79 ± 0.26	2E 1747.3+6837	0.0630	SEYFERT
N1185	J174726.0-300000	266.8584	-30.0001	2.8	58.90	211.81 ± 9.82	SLX 1744-299		LMXB
N1186	J174726.2-300242	266.8591	-30.0451	2.7	63.03	236.65 ± 10.26	SLX 1744-300		LMXB
N1187	J174729.7-225245	266.8738	-22.8793	18.7	6.91	5.37 ± 1.68	IGR J17476-2253	0.0470	SEYFERT
N1188	J174756.2-263349	266.9844	-26.5635	0.6	359.46	3638.55 ± 38.90	GX 3+1		LMXB
N1189	J174836.8+684222	267.1532	68.7062	17.2	5.56	0.67 ± 0.18	Mrk 507	0.0551	SEYFERT
N1190	J174838.8-233523	267.1617	-23.5896	20.0	6.13	4.65 ± 1.54	IGR J17488-2338	0.2400	SEYFERT
N1191	J174850.6+665403 ^{b)}	267.2108	66.9010	12.2	6.64	0.53 ± 0.11		0.0261	SEYFERT ^{c)}
N1192	J174855.2-325450	267.2298	-32.9138	10.6	11.92	13.17 ± 2.46	IGR J17488-3253	0.0200	SEYFERT
N1193	J174913.6-263836	267.3065	-26.6433	3.5	45.83	151.89 ± 8.18	GRO J1750-27		HMXB
N1194	J175004.0-322549	267.5168	-32.4303	7.3	19.18	29.02 ± 3.64	2E 1746.7-3225		LMXB
N1195	J175012.7-370307	267.5529	-37.0519	2.0	87.41	318.49 ± 11.62	4U 1746-371		LMXB
N1196	J175018.0-263605	267.5752	-26.6015	23.8	5.50	6.23 ± 1.98	IGR J17503-2636		HMXB?
N1197	J175113.6-201221	267.8068	-20.2058	19.6	6.85	5.89 ± 1.75	IGR J17513-2011	0.0470	SEYFERT
N1198	J175145.9-434622 ^{b)}	267.9413	-43.7728	20.8	5.78	4.22 ± 1.49			UNIDENT
N1199	J175328.6-244632	268.3693	-24.7756	21.3	6.28	5.40 ± 1.77	V771 Sgr		STAR ^{c)}
N1200	J175340.5+654239	268.4187	65.7109	12.7	7.10	0.35 ± 0.07	7C 1753+6543	0.1487	SEYFERT ^{c)}
N1201	J175403.4+661343	268.5141	66.2286	13.9	5.90	0.22 ± 0.05	RX J1754.0+6613	0.4067	SEYFERT
N1202	J175505.3+651949	268.7720	65.3304	11.8	6.90	0.42 ± 0.08	RX J1755.0+6519	0.0785	SEYFERT
N1203	J175615.4+552214	269.0641	55.3705	17.5	6.50	1.65 ± 0.46	RX J1756.2+5522		BLAZAR
N1204	J175713.0+703337	269.3041	70.5603	13.7	7.24	1.24 ± 0.27	2E 1757.7+7034	0.4070	BLAZAR
N1205	J175721.0-304409	269.3374	-30.7358	12.2	10.82	15.18 ± 2.95	2RXS J175721.1-304403		LMXB? ^{c)}
N1206	J175758.4+042732	269.4932	4.4589	12.2	12.32	14.99 ± 2.72	2E 1755.4+0427		CV ^{c)}
N1207	J175806.5+660038 ^{b)}	269.5271	66.0106	13.8	5.69	0.22 ± 0.05		0.0871	SEYFERT ^{c)}
N1208	J175824.1+653109	269.6005	65.5192	17.3	5.21	0.31 ± 0.08	RX J1758.4+6531	0.3250	SEYFERT
N1209	J175834.7-212321	269.6448	-21.3893	12.6	11.43	14.65 ± 2.84	IGR J17586-2129		HMXB
N1210	J175840.2-334829	269.6676	-33.8081	2.4	79.57	299.97 ± 11.83	4U 1755-33		LMXB
N1211	J180003.1-193915	270.0128	-19.6541	20.6	5.38	4.48 ± 1.63	XMMSL2 J180001.8-193927		UNIDENT
N1212	J180007.3+663654	270.0306	66.6149	3.4	26.83	0.88 ± 0.05	NGC 6552	0.0265	SEYFERT
N1213	J180035.9+081021	270.1495	8.1726	13.4	10.27	9.85 ± 2.11	V2301 Oph		CV
N1214	J180048.9+782806	270.2039	78.4684	16.8	6.12	2.08 ± 0.57	S5 1803+78	0.6800	BLAZAR
N1215	J180108.5-250442	270.2856	-25.0784	0.3	884.01	17413.84 ± 89.61	GX 5-1		LMXB

Table A.1. continued.

Id	Name SRGA	RA (J2000)	Dec (J2000)	R98 (")	S/N	Flux (10^{-12} erg s $^{-1}$ cm $^{-2}$)	Conventional name	Redshift	Class
N1216	J180112.7–254436	270.3028	–25.7434	1.8	100.13	543.12 ± 16.44	GRS 1758-258		LMXB
N1217	J180132.5–203148	270.3856	–20.5299	0.4	711.16	10644.27 ± 70.69	GX 9+1		LMXB
N1218	J180147.1+663835	270.4464	66.6431	6.6	13.57	0.32 ± 0.03	RX J1801.7+6638		AGN?
N1219	J180241.6–201714	270.6734	–20.2872	6.6	20.99	54.33 ± 5.60	IGR J18027-2016		HMXB
N1220	J180246.8–145453	270.6948	–14.9149	12.8	9.93	12.12 ± 2.58	IGR J18027-1455	0.0350	SEYFERT
N1221	J180249.9+660541	270.7078	66.0946	14.5	5.91	0.29 ± 0.06	RX J1802.8+6605	0.2070	SEYFERT
N1222	J180303.5–294947	270.7645	–29.8298	15.8	7.89	8.37 ± 2.21	MAXI J1803-298		LMXB
N1223	J180312.5+045110	270.8021	4.8529	21.4	6.10	5.32 ± 1.76	2RXS J180312.3+045128		AGN? ^{c)}
N1224	J180328.6+673811	270.8693	67.6363	5.6	16.87	1.32 ± 0.13	QSO B1803+6737	0.1360	SEYFERT
N1225	J180342.0+615651	270.9250	61.9474	14.4	7.61	1.33 ± 0.30	2RXS J180340.6+615654	0.4178	SEYFERT ^{c)}
N1226	J180639.3+663247 ^{b)}	271.6639	66.5464	16.3	5.28	0.24 ± 0.06		0.0867	SEYFERT ^{c)}
N1227	J180651.8+694928	271.7159	69.8243	5.9	18.31	3.14 ± 0.32	3C 371	0.0495	BLAZAR
N1228	J180657.9–260545 ^{b)}	271.7410	–26.0958	18.5	6.57	5.92 ± 1.87			UNIDENT
N1229	J180731.6+662950 ^{b)}	271.8815	66.4972	15.1	5.92	0.31 ± 0.07		0.2615	SEYFERT ^{c)}
N1230	J180733.9+501523 ^{b)}	271.8913	50.2563	21.4	5.52	2.44 ± 0.76			UNIDENT
N1231	J180751.9+055145	271.9661	5.8626	8.6	17.57	23.22 ± 3.24	V426 Oph		CV
N1232	J180835.5+101027	272.1481	10.1742	15.6	7.63	6.08 ± 1.71	2RXS J180834.6+101041		CV
N1233	J180839.1–202443	272.1631	–20.4118	22.6	5.98	4.97 ± 1.72	SGR 1806-20		MAGNETAR
N1234	J180849.4+663426	272.2057	66.5740	9.4	9.47	0.57 ± 0.08	RX J1808.7+6634	0.6970	BLAZAR ^{c)}
N1235	J180900.4+670421	272.2518	67.0725	13.4	5.45	0.24 ± 0.06	RX J1809.0+6704	0.6950	SEYFERT
N1236	J181021.0–190411	272.5876	–19.0697	5.8	26.01	51.23 ± 5.17	XTE J1810-189		LMXB
N1237	J181044.5–260902	272.6854	–26.1505	5.6	29.10	57.76 ± 5.29	V4722 Sgr		LMXB
N1238	J181227.8–181237	273.1160	–18.2104	2.6	72.16	264.74 ± 11.31	XTE J1812-182		LMXB ^{c)}
N1239	J181239.8–221924	273.1658	–22.3233	4.5	37.69	89.23 ± 6.68	MAXI J1810-222		LMXB? ^{c)}
N1240	J181414.6–225618 ^{b)}	273.5610	–22.9383	12.4	11.40	14.82 ± 2.87			LMXB
N1241	J181431.2–170926	273.6301	–17.1572	0.7	358.70	4498.58 ± 47.66	GX 13+1		LMXB
N1242	J181506.3–120548	273.7763	–12.0966	3.3	54.40	175.59 ± 9.48	4U 1812-12		LMXB
N1243	J181601.6–140210	274.0065	–14.0362	0.4	593.47	10606.55 ± 74.59	GX 17+2		LMXB
N1244	J181611.8+423938	274.0492	42.6604	8.9	15.52	12.99 ± 1.81	MCG +07-37-031	0.0412	SEYFERT
N1245	J181613.1+495204	274.0547	49.8679	2.6	64.92	90.74 ± 3.86	AM Her		CV
N1246	J181636.0–391251	274.1502	–39.2143	15.9	7.33	6.73 ± 1.92	IGR J18165-3912		CV? ^{c)}
N1247	J181642.9–161322	274.1787	–16.2229	7.4	22.37	47.14 ± 5.26	SWIFT J1816.7-1613		HMXB
N1248	J181721.6–250839	274.3400	–25.1441	18.0	6.49	6.98 ± 2.16	IGR J18170-2511		CV
N1249	J181749.5+234311 ^{b)}	274.4561	23.7196	17.1	7.45	5.76 ± 1.61		0.0813	SEYFERT ^{c)}
N1250	J181815.4–545033 ^{b)}	274.5641	–54.8425	21.0	5.79	4.32 ± 1.46			AGN? ^{c)}
N1251	J181829.0+674124	274.6207	67.6900	6.7	13.13	1.18 ± 0.14	2E 1818.6+6740	0.3140	SEYFERT
N1252	J181837.5–170251	274.6562	–17.0474	11.7	11.41	15.74 ± 3.12	SAX J1818.6-1703		HMXB
N1253	J181921.5–252426	274.8398	–25.4073	5.3	30.04	65.72 ± 6.05	V4641 Sgr		HMXB
N1254	J181934.6–634548	274.8942	–63.7635	20.3	5.58	3.30 ± 1.20	PKS 1814-63	0.0647	SEYFERT
N1255	J182036.0–203022 ^{b)}	275.1500	–20.5062	18.1	6.82	6.06 ± 1.98			UNIDENT
N1256	J182111.0+765816 ^{b)}	275.2957	76.9711	14.1	6.64	1.72 ± 0.44		0.0631	SEYFERT ^{c)}
N1257	J182121.3–060149 ^{b)}	275.3387	–6.0303	20.0	5.87	5.14 ± 1.82			UNIDENT

Table A.1. continued.

Id	Name SRGA	RA (J2000)	Dec (J2000)	R98 (")	S/N	Flux (10^{-12} erg s $^{-1}$ cm $^{-2}$)	Conventional name	Redshift	Class
N1258	J182127.7+595525	275.3654	59.9237	10.1	10.38	3.15 ± 0.54	PBC J1821.2+5957	0.0990	SEYFERT
N1259	J182155.1-134728	275.4794	-13.7912	14.5	9.42	11.76 ± 2.77	IGR J18219-1347		HMXB
N1260	J182156.3+642033	275.4845	64.3426	4.2	32.19	10.19 ± 0.66	H 1821+643	0.2970	SEYFERT ^{c)}
N1261	J182340.7-302140	275.9196	-30.3610	0.7	332.19	3953.18 ± 46.88	4U 1820-30		LMXB
N1262	J182411.3+184610	276.0469	18.7695	18.1	6.50	5.96 ± 1.74	PBC J1824.2+1846	0.0663	SEYFERT
N1263	J182420.4-562211	276.0850	-56.3696	22.5	5.77	4.18 ± 1.46	IGR J18244-5622	0.0169	SEYFERT
N1264	J182456.3-324309	276.2344	-32.7192	19.5	6.11	5.82 ± 1.96	IGR J18249-3243	0.3550	SEYFERT
N1265	J182510.7+645021	276.2947	64.8392	6.9	18.12	4.31 ± 0.45	2E 1824.9+6448		STAR ^{c)}
N1266	J182522.2-000045	276.3425	-0.0124	3.2	55.99	188.03 ± 10.04	4U 1822-00		LMXB
N1267	J182528.9+720905	276.3705	72.1514	15.8	6.27	1.04 ± 0.25	SWIFT J1825.7+7215	0.1108	SEYFERT ^{c)}
N1268	J182546.3+690557	276.4428	69.0992	16.3	6.24	0.61 ± 0.15	RX J1825.7+6905	0.0888	SEYFERT
N1269	J182546.9-370617	276.4456	-37.1048	2.0	100.66	502.24 ± 16.39	4U 1822-37		LMXB
N1270	J182633.0+325126	276.6376	32.8573	18.7	6.83	4.28 ± 1.26	PBC J1826.6+3251	0.0220	SEYFERT
N1271	J182637.3+670646	276.6555	67.1128	13.7	5.84	0.48 ± 0.12	ICRF J182637.5+670644	0.2870	BLAZAR
N1272	J182714.5+195617	276.8105	19.9380	22.6	5.85	3.87 ± 1.41	MCG+03-47-002	0.0402	SEYFERT
N1273	J182733.3+643143	276.8890	64.5285	17.6	5.83	0.95 ± 0.26	RX J1827.5+6431	0.0977	SEYFERT
N1274	J182830.5-022914	277.1271	-2.4872	28.1	5.42	5.16 ± 1.93	XMMSL2 J182831.4-022903		UNIDENT
N1275	J182832.6-592055	277.1358	-59.3485	18.7	6.75	5.10 ± 1.64	2RXS J182831.7-592109		BLAZAR? ^{c)}
N1276	J182848.6+502218	277.2025	50.3715	9.8	14.20	8.96 ± 1.30	Ark 539	0.0169	SEYFERT
N1277	J182928.4-234748	277.3682	-23.7967	0.8	268.07	2840.43 ± 39.91	GS 1826-24		LMXB
N1278	J182931.5+484441	277.3814	48.7448	18.8	7.36	3.92 ± 0.99	3C 380	0.6917	BLAZAR
N1279	J182944.2-095123	277.4342	-9.8565	5.6	29.93	65.19 ± 5.97	XTE J1829-098		HMXB
N1280	J182956.7-023017 ^{b)}	277.4864	-2.5048	23.2	5.67	4.93 ± 1.78			UNIDENT
N1281	J183008.5+373657	277.5354	37.6159	20.7	6.28	3.97 ± 1.24	ASASSN-13bs		CV
N1282	J183023.2+731316	277.5968	73.2210	6.7	18.03	4.53 ± 0.49	IRAS F18315+7310	0.1230	SEYFERT
N1283	J183050.5-123226	277.7103	-12.5405	14.6	8.29	9.48 ± 2.48	IGR J18308-1232		CV
N1284	J183144.1+651130	277.9338	65.1915	14.7	6.40	0.95 ± 0.24	RX J1831.7+6511		CV
N1285	J183219.5-084024	278.0813	-8.6734	16.6	7.50	9.34 ± 2.41	AX J1832.3-0840		CV
N1286	J183234.3+684813	278.1428	68.8037	14.5	5.72	0.56 ± 0.15	7C 1832+6845	0.2050	BLAZAR
N1287	J183333.9-103404	278.3912	-10.5678	7.3	22.07	44.01 ± 5.11	SNR 021.5-00.9		SNR / PULSAR
N1288	J183340.1-210336	278.4170	-21.0599	15.9	10.20	13.77 ± 3.05	PKS 1830-21	2.5070	BLAZAR
N1289	J183503.6+324148	278.7651	32.6968	8.3	17.88	20.68 ± 2.70	3C 382	0.0556	SEYFERT
N1290	J183544.3-325925	278.9347	-32.9902	14.6	9.25	12.04 ± 2.75	XB 1832-330		LMXB
N1291	J183658.5-592406	279.2436	-59.4017	8.4	15.08	20.24 ± 3.16	Fairall 49	0.0200	SEYFERT
N1292	J183754.5+155436	279.4772	15.9099	22.9	5.62	3.78 ± 1.45	2RXS J183753.9+155433		STAR? ^{c)}
N1293	J183803.0-065531	279.5126	-6.9254	17.3	7.69	6.98 ± 2.07	AX J1838.0-0655		SNR / PULSAR
N1294	J183811.5+655457	279.5479	65.9158	13.2	7.55	1.12 ± 0.24	HS 1838+6552	0.2301	SEYFERT ^{c)}
N1295	J183820.4-652541	279.5849	-65.4280	7.6	18.91	26.26 ± 3.40	ESO 103-35	0.0133	SEYFERT
N1296	J183906.5-571501	279.7770	-57.2503	15.4	8.86	7.82 ± 1.98	PBC J1838.9-5714		BLAZAR ^{c)}
N1297	J184006.8+592011 ^{b)}	280.0283	59.3364	19.5	5.64	1.49 ± 0.46		0.0257	AGN? ^{c)}
N1298	J184101.2-053544	280.2551	-5.5956	20.2	6.34	7.90 ± 2.31	AX J1841.0-0536		HMXB
N1299	J184119.5-045617	280.3313	-4.9380	13.0	10.13	14.05 ± 2.90	1E 1841-045/Kes 73		MAGNETAR ^{c)}

Table A.1. continued.

Id	Name SRGA	RA (J2000)	Dec (J2000)	R98 (")	S/N	Flux (10^{-12} erg s $^{-1}$ cm $^{-2}$)	Conventional name	Redshift	Class
N1300	J184210.2+794615	280.5424	79.7707	4.2	32.54	21.08 \pm 1.51	3C 390.3	0.0561	SEYFERT
N1301	J184239.9-042409 ^{b)}	280.6662	-4.4026	8.9	15.60	23.08 \pm 3.65			UNIDENT
N1302	J184425.8+123605 ^{b)}	281.1074	12.6013	22.9	5.38	3.97 \pm 1.51			UNIDENT
N1303	J184455.3-622203	281.2303	-62.3676	17.0	7.01	5.50 \pm 1.66	ESO 140-43	0.0142	SEYFERT
N1304	J184501.2-043404	281.2550	-4.5679	9.8	14.04	19.80 \pm 3.37	AX J1845.0-0433		HMXB
N1305	J184527.3+721101	281.3637	72.1837	7.4	14.83	2.92 \pm 0.37	IRAS 18462+7207	0.0463	SEYFERT
N1306	J184625.3-025831	281.6054	-2.9754	12.7	10.65	17.93 \pm 3.63	PSR J1846-0258		SNR / PULSAR
N1307	J184703.8-783151	281.7659	-78.5307	10.7	11.38	9.85 \pm 1.84	1H 1836-786	0.0741	SEYFERT
N1308	J184817.5-031021	282.0728	-3.1726	10.4	14.13	20.94 \pm 3.53	IGR J18483-0311		HMXB
N1309	J184822.2+653657	282.0924	65.6159	13.0	8.20	1.60 \pm 0.33	2RXS J184822.6+653659	0.3640	BLAZAR
N1310	J184854.8+003502	282.2283	0.5838	15.7	7.32	7.44 \pm 2.21	V603 Aql		CV
N1311	J184901.6-000119	282.2567	-0.0220	17.8	6.70	6.03 \pm 1.96	PSR J1849-0001		SNR / PULSAR
N1312	J185050.8+574503	282.7118	57.7509	18.0	5.39	1.93 \pm 0.59	WISEA J185052.94+574517.5		BLAZAR
N1313	J185304.5+275043	283.2689	27.8454	22.9	5.64	4.19 \pm 1.41	IRAS 18510+2746	0.0619	SEYFERT
N1314	J185304.9-084222	283.2706	-8.7062	5.3	31.21	77.84 \pm 6.87	4U 1850-086		LMXB
N1315	J185357.9+682303	283.4913	68.3840	22.2	6.26	0.89 \pm 0.21	Abell 2312	0.0930	CLUSTER
N1316	J185421.6+083842	283.5899	8.6449	18.6	6.09	4.79 \pm 1.61	IGR J18544+0839		STAR? ^{c)}
N1317	J185438.3-783358	283.6598	-78.8993	14.0	9.62	8.15 \pm 1.72	ESO 25-2	0.0292	SEYFERT
N1318	J185457.5+735130	283.7396	73.8583	12.6	8.21	1.65 \pm 0.33	ICRF J185457.2+735119	0.4610	BLAZAR
N1319	J185502.1-310952	283.7589	-31.1645	5.4	27.82	60.35 \pm 5.99	V1223 Sgr		CV
N1320	J185530.4-023618	283.8767	-2.6049	4.2	42.36	117.71 \pm 7.89	XTE J1855-026		HMXB
N1321	J185600.4+153753	284.0017	15.6315	15.4	7.87	8.96 \pm 2.22	IGR J18559+1535	0.0844	SEYFERT
N1322	J185707.3-782828	284.2806	-78.4746	18.0	6.21	4.03 \pm 1.24	2E 1849.2-7832	0.0420	SEYFERT
N1323	J185721.0+713124	284.3377	71.5234	13.4	6.66	1.08 \pm 0.26	HS 1857+7127		CV
N1324	J190038.1+700108	285.1587	70.0190	19.1	5.58	0.72 \pm 0.21	Abell 2315	0.0936	CLUSTER
N1325	J190140.6+012628	285.4191	1.4411	8.2	18.05	31.06 \pm 4.21	XTE J1901+014		LMXB ^{c)}
N1326	J190245.6+763052	285.6898	76.5144	11.1	9.33	2.36 \pm 0.45	RX J1902.7+7630	0.2710	SEYFERT
N1327	J190308.3+733241	285.7847	73.5448	15.0	5.80	1.00 \pm 0.28	2RXS J190303.7+733241		AGN? ^{c)}
N1328	J190407.5+052712	286.0315	5.4533	18.7	5.95	5.07 \pm 1.74	3C 396		SNR
N1329	J190526.1+422742	286.3589	42.4618	15.3	8.60	6.34 \pm 1.52	Zwicky 229-015	0.0279	SEYFERT
N1330	J190529.2-263916	286.3719	-26.6545	22.9	5.73	5.10 \pm 1.86	1AXG J190529-2639		AGN? ^{c)}
N1331	J190544.8+780436	286.4366	78.0767	16.3	6.03	1.75 \pm 0.48	RX J1905.7+7804	0.1394	SEYFERT
N1332	J190629.4-044655 ^{b)}	286.6224	-4.7819	20.2	6.07	6.39 \pm 2.04			AGN ^{c)}
N1333	J190717.4+440102	286.8224	44.0172	22.8	5.92	3.77 \pm 1.17	MV Lyr		CV
N1334	J190722.1-204641	286.8423	-20.7781	10.5	13.56	21.12 \pm 3.65	V1082 Sgr		CV? ^{c)}
N1335	J190824.8+522540	287.1034	52.4279	13.7	8.80	4.72 \pm 1.04	V1762 Cyg		STAR
N1336	J190938.1+094948	287.4086	9.8300	3.0	58.61	187.84 \pm 9.72	4U 1907+09		HMXB
N1337	J191048.3+073553	287.7013	7.5981	3.2	58.70	201.68 \pm 10.29	4U 1909+07		HMXB
N1338	J191115.9+003504	287.8161	0.5843	2.9	65.33	243.93 \pm 11.74	Aql X-1		LMXB
N1339	J191149.6+045859	287.9566	4.9830	5.2	32.99	77.06 \pm 6.34	SS 433		HMXB
N1340	J191404.1+095255	288.5173	9.8819	5.3	30.04	63.52 \pm 5.73	IGR J19140+0951		HMXB
N1341	J191438.9+502846	288.6620	50.4794	18.7	6.16	2.73 \pm 0.86	2RXS J191438.6+502857		AGN? ^{c)}

Table A.1. continued.

Id	Name SRGA	RA (J2000)	Dec (J2000)	R98 (")	S/N	Flux (10^{-12} erg s $^{-1}$ cm $^{-2}$)	Conventional name	Redshift	Class
N1342	J191456.9+103641	288.7369	10.6113	10.7	13.04	17.35 ± 3.16	IGR J19149+1036		HMXB? ^{c)}
N1343	J191511.4+105644	288.7973	10.9455	3.4	53.65	177.60 ± 10.05	GRS 1915+105		LMXB
N1344	J191628.1+711619	289.1171	71.2720	17.1	6.50	1.06 ± 0.27	2RXS J191627.3+711610		SEYFERT ^{c)}
N1345	J191847.9-051418	289.6994	-5.2384	3.2	55.68	195.84 ± 10.45	4U 1916-053		LMXB
N1346	J191928.0-295810	289.8665	-29.9695	25.0	5.49	5.51 ± 1.98	PKS 1916-300	0.1668	SEYFERT
N1347	J192111.4+435651	290.2976	43.9476	25.0	6.17	6.30 ± 1.81	Abell 2319	0.0559	CLUSTER
N1348	J192114.2-584017	290.3092	-58.6714	9.9	15.48	19.34 ± 3.00	ESO 141-55	0.0371	SEYFERT
N1349	J192149.7-585835	290.4572	-58.9763	23.6	5.40	3.96 ± 1.45	6dF J1921494-585831	0.0371	SEYFERT
N1350	J192214.5+691110	290.5604	69.1861	9.1	12.64	3.16 ± 0.44	4C 69.26	0.0970	SEYFERT
N1351	J192403.4+552921	291.0143	55.4891	18.9	5.56	2.06 ± 0.67	2RXS J192405.0+552948		BLAZAR
N1352	J192413.0+665631	291.0543	66.9419	18.8	5.50	1.01 ± 0.30	2RXS J192413.2+665637		AGN? ^{c)}
N1353	J192433.1+501430	291.1378	50.2418	5.9	23.43	21.88 ± 2.22	CH Cyg		CV
N1354	J192501.9+504316	291.2581	50.7211	11.7	9.52	5.60 ± 1.16	2E 1923.7+5037	0.0680	SEYFERT ^{c)}
N1355	J192718.9+653352	291.8286	65.5645	16.8	6.17	1.46 ± 0.38	1ES 1927+654	0.0170	SEYFERT
N1356	J192747.5+735800	291.9480	73.9664	8.9	12.77	3.51 ± 0.51	4C 73.18	0.3021	BLAZAR
N1357	J192832.4-500143	292.1350	-50.0285	19.8	6.00	4.58 ± 1.59	CTCV J1928-5001		CV
N1358	J192955.6+181831	292.4816	18.3087	22.3	5.84	5.11 ± 1.77	IGR J19294+1816		HMXB
N1359	J193013.6+341042	292.5567	34.1783	19.4	5.85	3.85 ± 1.28	SWIFT J1930.5+3414	0.0629	SEYFERT
N1360	J193346.0+325424	293.4418	32.9066	14.5	9.25	8.92 ± 2.09	SWIFT J1933.9+3258	0.0630	SEYFERT ^{c)}
N1361	J193355.3+654029	293.4806	65.6748	17.8	5.58	1.13 ± 0.33	ICRF J193357.3+654016	1.6870	BLAZAR
N1362	J193707.1+660811	294.2794	66.1363	15.7	6.17	1.24 ± 0.33	2RXS J193708.1+660821	0.0714	SEYFERT ^{c)}
N1363	J193732.8-061306	294.3868	-6.2183	12.3	11.06	14.16 ± 3.03	1H 1934-063	0.0103	SEYFERT
N1364	J193804.4-510950	294.5184	-51.1638	20.0	7.10	7.94 ± 2.24	1H 1927-516	0.0400	SEYFERT
N1365	J193929.4+700749	294.8726	70.1301	10.7	10.04	2.06 ± 0.38	2RXS J193929.8+700752	0.1200	SEYFERT
N1366	J193938.9-660352	294.9120	-6.0643	23.9	5.97	6.70 ± 2.29	HD 185510		STAR
N1367	J194011.3-102525	295.0472	-10.4235	11.2	15.46	28.45 ± 4.39	V1432 Aql		CV
N1368	J194016.1-301549	295.0670	-30.2635	22.3	5.67	4.87 ± 1.81	IGR J19405-3016	0.0530	SEYFERT
N1369	J194212.6-204549	295.5525	-20.7637	24.4	5.47	5.40 ± 1.85	RX J1942.2-2045		STAR
N1370	J194241.2-101928	295.6715	-10.3243	10.0	13.85	21.34 ± 3.76	NGC 6814	0.0052	SEYFERT
N1371	J194251.9+223336	295.7163	22.5601	25.0	5.53	4.00 ± 1.57	2SXPS J194252.1+223334		UNIDENT
N1372	J194355.9+211826	295.9829	21.3071	16.1	7.33	7.89 ± 2.17	IGR J19443+2117		BLAZAR
N1373	J194412.5-243619	296.0519	-24.6054	20.0	6.45	5.71 ± 1.90	XMMSL2 J194412.4-243621	0.1402	SEYFERT ^{c)}
N1374	J194438.6-043223 ^{b)}	296.1610	-4.5396	25.0	5.31	4.39 ± 1.76			CV? ^{c)}
N1375	J194638.0+704554	296.6584	70.7650	7.0	19.01	6.24 ± 0.65	2RXS J194639.7+704551		CV ^{c)}
N1376	J194718.9+444939	296.8286	44.8275	11.4	10.74	8.23 ± 1.62	XSS J19459+4508	0.0530	SEYFERT
N1377	J194845.0+054156 ^{b)}	297.1876	5.6988	20.8	5.76	5.19 ± 1.93			UNIDENT
N1378	J194907.3+774426	297.2804	77.7404	11.4	9.96	2.74 ± 0.51	AB Dra		CV
N1379	J195226.6+380011	298.1109	38.0031	19.0	5.81	4.31 ± 1.38	2RXS J195225.6+380017	0.0767	SEYFERT ^{c)}
N1380	J195512.1+004533	298.8006	0.7591	15.2	7.85	11.57 ± 2.88	IGR J19552+0044		CV
N1381	J195542.3+320548	298.9263	32.0968	3.6	49.93	124.79 ± 7.15	4U 1954+31		LMXB
N1382	J195702.7+615028	299.2613	61.8410	17.0	7.15	2.80 ± 0.69	2RXS J195702.4+615038	0.0586	SEYFERT ^{c)}
N1383	J195814.3+323245	299.5596	32.5457	14.6	9.12	8.34 ± 1.96	V2306 Cyg		CV

Table A.1. continued.

Id	Name	RA	Dec	R98	S/N	Flux	Conventional name	Redshift	Class
	SRGA	(J2000)	(J2000)	(")		(10^{-12} erg s $^{-1}$ cm $^{-2}$)			
N1384	J195814.8-301105	299.5615	-30.1846	15.6	9.16	11.03 ± 2.75	2RXS J195815.7-301118	0.1193	BLAZAR
N1385	J195815.6+194141	299.5648	19.6947	20.8	6.05	4.93 ± 1.75	IGR J19583+1941	0.0310	SEYFERT ^{c)}
N1386	J195821.9+351206	299.5913	35.2016	0.5	540.65	6254.25 ± 47.71	Cyg X-1		HMXB
N1387	J195924.1+114230	299.8505	11.7083	2.0	99.60	531.29 ± 17.69	4U 1957+115		LMXB
N1388	J195927.9+404358	299.8664	40.7327	5.8	27.93	45.81 ± 4.06	Cyg A	0.0561	CLUSTER ^{c)}
N1389	J195958.4+650857	299.9933	65.1492	2.1	83.57	77.17 ± 2.49	1ES 1959+650	0.0470	BLAZAR
N1390	J200022.1+321115	300.0920	32.1876	11.8	10.66	10.07 ± 2.09	IGR J20006+3210		HMXB
N1391	J200055.5-181003	300.2314	-18.1676	24.9	5.91	6.70 ± 2.31	IRAS 19580-1818	0.0371	SEYFERT
N1392	J200206.8+413240	300.5283	41.5445	22.8	5.91	4.09 ± 1.35	RX J2002.0+4132		BLAZAR? ^{c)}
N1393	J200227.2-711926	300.6132	-71.3238	20.2	5.84	4.14 ± 1.38	4FGL J2002.4-7119		BLAZAR?
N1394	J200331.8+701331	300.8823	70.2253	14.4	6.68	1.45 ± 0.36	2RXS J200332.1+701331	0.0976	SEYFERT ^{c)}
N1395	J200431.2+610218	301.1301	61.0384	16.7	5.54	2.17 ± 0.66	2RXS J200433.8+610235		SEYFERT ^{c)}
N1396	J200632.4+562054	301.6349	56.3483	18.8	5.55	2.11 ± 0.68	SWIFT J2006.5+5619	0.0430	SEYFERT
N1397	J200658.6-343309	301.7440	-34.5526	19.4	6.16	5.91 ± 2.08	CTS 28	0.0253	SEYFERT
N1398	J200845.3+335637	302.1888	33.9437	20.4	5.96	4.07 ± 1.37	XMMSL2 J200844.1+335627		UNIDENT
N1399	J200846.3-610604	302.1929	-61.1012	14.6	10.60	12.72 ± 2.58	NGC 6860	0.0149	SEYFERT
N1400	J200911.0+323354	302.2958	32.5651	13.7	8.56	8.72 ± 2.11	2RXS J200911.9+323345		STAR
N1401	J201116.5+600418	302.8188	60.0716	16.6	8.00	3.84 ± 0.86	2RXS J201118.0+600421		CV ^{c)}
N1402	J201459.0+252302	303.7457	25.3839	22.5	5.78	4.62 ± 1.59	SWIFT J2015.2+2526	0.0457	SEYFERT
N1403	J201529.0+371105	303.8708	37.1848	20.5	6.54	4.91 ± 1.55	ZOAG G074.87+01.22	0.8590	BLAZAR
N1404	J201633.2+705525 ^{b)}	304.1384	70.9235	18.8	5.44	1.09 ± 0.34		0.2579	SEYFERT ^{c)}
N1405	J201733.7-033945	304.3905	-3.6626	19.7	6.29	6.07 ± 2.09	V794 Aql		CV
N1406	J201921.1+300257 ^{b)}	304.8378	30.0491	21.1	6.07	4.58 ± 1.55			CV? ^{c)}
N1407	J202027.6+435120	305.1148	43.8557	15.8	7.04	4.75 ± 1.34	WR 140		STAR
N1408	J202424.1-572352	306.1005	-57.3977	16.3	7.13	5.67 ± 1.64	PKS 2020-57	0.3520	SEYFERT
N1409	J202630.5+764444	306.6269	76.7455	10.0	11.31	3.63 ± 0.61	4FGL J2026.1+7645		BLAZAR
N1410	J202733.2+354338 ^{b)}	306.8882	35.7271	22.8	5.43	4.12 ± 1.48			UNIDENT
N1411	J202835.2+254401	307.1465	25.7337	18.6	7.36	8.13 ± 2.21	MCG +04-48-002	0.0136	SEYFERT ^{c)}
N1412	J202931.7-614911	307.3822	-61.8198	18.7	7.78	6.44 ± 1.81	XMMSL2 J202930.4-614903	0.1243	SEYFERT ^{c)}
N1413	J203215.5+373812	308.0646	37.6367	2.0	93.55	337.62 ± 11.41	EXO 2030+375		HMXB
N1414	J203225.9+405729	308.1080	40.9581	0.6	419.55	4333.41 ± 39.62	Cyg X-3		HMXB
N1415	J203317.2-225334	308.3216	-22.8926	22.4	6.29	7.69 ± 2.51	PKS 2030-23	0.1315	SEYFERT
N1416	J203431.4-303727	308.6308	-30.6242	12.9	12.54	20.59 ± 3.75	2RXS J203433.3-303720	0.0194	SEYFERT
N1417	J203515.3+220628 ^{b)}	308.8139	22.1078	20.5	6.30	5.28 ± 1.78			CV? ^{c)}
N1418	J204149.7-373346	310.4573	-37.5627	22.9	5.35	5.82 ± 2.18	RBS 1691	0.0985	BLAZAR? ^{c)}
N1419	J204237.4+750803	310.6556	75.1342	4.7	30.03	16.00 ± 1.20	4C 74.26	0.1040	SEYFERT
N1420	J204318.6+443820 ^{b)}	310.8273	44.6390	9.0	14.49	14.41 ± 2.32			HMXB ^{c)}
N1421	J204409.7-104325	311.0403	-10.7235	8.9	16.54	33.11 ± 4.97	Mrk 509	0.0344	SEYFERT
N1422	J204547.9+672640	311.4496	67.4446	10.1	11.24	3.57 ± 0.60	2RXS J204548.4+672629		CV ^{c)}
N1423	J205202.1-570419	313.0088	-57.0720	16.2	8.53	8.03 ± 2.10	IC 5063	0.0114	SEYFERT
N1424	J205353.8+442304	313.4740	44.3846	19.5	6.85	5.28 ± 1.51	V1794 Cyg		STAR
N1425	J205522.2+401808	313.8423	40.3022	21.4	5.66	3.34 ± 1.23	2RXS J205524.3+401757		STAR ^{c)}

Table A.1. continued.

Id	Name SRGA	RA (J2000)	Dec (J2000)	R98 (")	S/N	Flux (10^{-12} erg s $^{-1}$ cm $^{-2}$)	Conventional name	Redshift	Class
N1426	J205642.8+494008	314.1783	49.6690	8.4	16.56	18.59 ± 2.64	4C 49.35		BLAZAR
N1427	J205847.3+414634	314.6972	41.7762	19.0	5.73	4.06 ± 1.36	GRO J2058+42		HMXB
N1428	J210335.9+454505	315.8996	45.7515	2.6	71.34	171.87 ± 7.04	SAX J2103.5+4545		HMXB
N1429	J210501.3-353121 ^{b)}	316.2554	-35.5226	21.9	5.41	4.26 ± 1.71			AGN ^{c)}
N1430	J210809.7-033240	317.0403	-3.5445	25.4	5.39	5.22 ± 1.98	2RXS J210808.5-033318	0.0683	SEYFERT
N1431	J210906.7+480643	317.2780	48.1118	17.2	5.89	3.90 ± 1.28	2E 2107.4+4754		CV ^{c)}
N1432	J210910.2-094010	317.2925	-9.6695	18.6	6.60	6.97 ± 2.19	H 2106-099	0.0270	SEYFERT
N1433	J210932.5+353309	317.3855	35.5524	22.3	7.14	5.90 ± 1.78	RX J2109.4+3532	0.2023	BLAZAR?
N1434	J211148.9+722812 ^{b)}	317.9539	72.4699	15.9	6.04	1.58 ± 0.44		0.1061	SEYFERT ^{c)}
N1435	J211335.2+542226	318.3965	54.3739	13.1	11.42	7.20 ± 1.38	2RXS J211336.1+542224		CV
N1436	J211402.9+820451	318.5122	82.0808	9.0	13.37	5.55 ± 0.83	S5 2116+81	0.0840	SEYFERT
N1437	J211644.6+533408	319.1858	53.5690	18.9	7.58	5.14 ± 1.26	2RXS J211648.1+533347		CV ^{c)}
N1438	J211703.9-485605	319.2661	-48.9347	22.4	5.49	4.95 ± 1.79	2RXS J211704.0-485615	0.2478	AGN ^{c)}
N1439	J211747.2+513848	319.4465	51.6466	9.0	13.75	10.96 ± 1.76	IGR J21178+5139	0.0534	BLAZAR ^{c)}
N1440	J212044.9-543755	320.1872	-54.6320	18.2	6.56	5.74 ± 1.89	2RXS J212043.2-543801		STAR
N1441	J212345.0+421811	320.9376	42.3031	16.5	9.04	8.42 ± 1.96	V2069 Cyg		CV
N1442	J212411.7+050251	321.0489	5.0476	18.8	6.97	7.93 ± 2.42	SWIFT J2124.6+0500		CV
N1443	J212439.0+505822	321.1625	50.9728	3.7	44.90	72.77 ± 4.38	4C +50.55	0.0200	SEYFERT
N1444	J212744.8+565636	321.9366	56.9434	8.3	18.52	13.84 ± 1.61	IGR J21277+5656	0.0140	SEYFERT
N1445	J212901.0+363110	322.2541	36.5195	16.9	7.09	5.32 ± 1.56	2RXS J212902.0+363102		CV ^{c)}
N1446	J212912.5-153841	322.3022	-15.6448	21.2	5.97	6.56 ± 2.23	PKS 2126-158	3.2680	BLAZAR
N1447	J212958.6+121001	322.4942	12.1670	4.7	37.44	104.64 ± 7.79	4U 2129+12		LMXB
N1448	J213136.5-120659	322.9022	-12.1163	18.8	6.30	6.59 ± 2.24	PKS 2128-12	0.5000	BLAZAR
N1449	J213151.0-251555	322.9624	-25.2652	22.2	5.63	5.11 ± 1.97	RBS 1755		BLAZAR
N1450	J213152.0+491400 ^{b)}	322.9667	49.2333	21.5	5.88	3.07 ± 1.03			CV ^{c)}
N1451	J213202.1-334252	323.0089	-33.7144	12.7	12.40	17.56 ± 3.51	CTS 109	0.0300	SEYFERT
N1452	J213343.6+510727	323.4317	51.1241	7.2	20.12	20.48 ± 2.40	RX J2133.7+5107		CV
N1453	J213419.4+473757	323.5807	47.6324	7.4	18.97	21.08 ± 2.61	IGR J21347+4737		HMXB
N1454	J213553.4+472822	323.9725	47.4727	11.3	10.52	9.06 ± 1.76	IGR J21358+4729	0.0253	SEYFERT
N1455	J213622.8-622402	324.0948	-62.4006	12.1	10.98	12.83 ± 2.52	RBS 1763	0.0586	SEYFERT
N1456	J213744.6-143253	324.4360	-14.5482	16.8	7.60	9.62 ± 2.65	PKS 2135-14	0.2005	SEYFERT
N1457	J213806.2+261953	324.5260	26.3313	16.7	7.51	6.25 ± 1.89	V627 Peg		CV
N1458	J213833.5+320514	324.6396	32.0872	18.7	7.92	6.69 ± 1.81	2RXS J213832.7+320505	0.0244	SEYFERT
N1459	J213943.1+595024	324.9295	59.8401	15.1	6.85	3.07 ± 0.80	IGR J21397+5949	0.1142	SEYFERT
N1460	J214242.9+433510	325.6787	43.5861	1.9	105.10	356.61 ± 10.86	SS Cyg		CV
N1461	J214331.7+102854 ^{b)}	325.8819	10.4817	22.0	5.32	4.32 ± 1.68			CV ^{c)}
N1462	J214441.2+381917	326.1715	38.3214	0.5	518.85	7334.70 ± 57.64	Cyg X-2		LMXB
N1463	J214503.7+634527	326.2654	63.7575	17.6	5.95	2.07 ± 0.63	2RXS J214504.0+634540		AGN ^{c)}
N1464	J215155.2-302755	327.9799	-30.4651	17.6	6.52	8.26 ± 2.52	PKS 2149-306	2.3400	BLAZAR
N1465	J215706.5-694132	329.2772	-69.6923	20.3	6.98	5.48 ± 1.61	PKS 2153-699	0.0280	SEYFERT ^{c)}
N1466	J215727.0-061030	329.3624	-6.1749	19.7	6.61	7.25 ± 2.37	RBS 1801	0.1760	SEYFERT
N1467	J215900.1-175251	329.7504	-17.8810	20.8	5.38	5.18 ± 1.95	RBS 1808	0.0934	SEYFERT

Table A.1. continued.

Id	Name SRGA	RA (J2000)	Dec (J2000)	R98 (")	S/N	Flux (10^{-12} erg s $^{-1}$ cm $^{-2}$)	Conventional name	Redshift	Class
N1468	J220041.3+103303	330.1721	10.5507	19.5	6.98	8.40 ± 2.54	Mrk 520	0.0266	SEYFERT
N1469	J220201.4-315204	330.5056	-31.8677	12.5	10.15	12.16 ± 2.83	NGC 7172	0.0087	SEYFERT
N1470	J220243.5+421641	330.6812	42.2782	15.4	7.50	6.19 ± 1.58	BL Lac	0.0668	BLAZAR
N1471	J220355.8+613222	330.9826	61.5394	11.0	10.46	5.20 ± 0.99	2RXS J220358.0+613220		CV? ^{c)}
N1472	J220420.0+033400	331.0831	3.5667	22.6	5.78	5.85 ± 2.13	IRAS 22017+0319	0.0611	SEYFERT
N1473	J220455.6+471410	331.2317	47.2360	14.6	8.19	5.83 ± 1.36	HK Lac		STAR
N1474	J220706.9+360935	331.7789	36.1597	20.4	5.43	4.04 ± 1.43	2RXS J220708.5+360934		AGN? ^{c)}
N1475	J220755.6+543113	331.9816	54.5204	3.5	44.46	25.15 ± 1.44	4U 2206+543		HMXB
N1476	J220840.6+454430	332.1694	45.7418	11.3	11.32	7.95 ± 1.51	AR Lac		STAR
N1477	J220914.4-471016	332.3102	-47.1710	14.4	10.14	11.52 ± 2.66	NGC 7213	0.0058	SEYFERT
N1478	J221025.3-361049 ^{b)}	332.6053	-36.1802	22.7	5.47	5.17 ± 1.89			UNIDENT
N1479	J221058.4+320342	332.7434	32.0617	19.1	6.16	4.77 ± 1.53	2RXS J221058.4+320329		BLAZAR?
N1480	J221105.1-685058 ^{b)}	332.7711	-68.8494	24.3	5.45	4.23 ± 1.47			UNIDENT
N1481	J221144.7-034940	332.9362	-3.8279	26.3	6.07	7.22 ± 2.47	MCXC J2211.7-0349	0.3970	CLUSTER
N1482	J221402.2+124210	333.5091	12.7028	15.3	7.61	7.73 ± 2.11	RU Peg		CV
N1483	J221712.3+141420	334.3013	14.2390	16.3	7.41	7.92 ± 2.11	Mrk 304	0.0658	SEYFERT
N1484	J221755.3-082107	334.4805	-8.3519	8.1	19.36	41.32 ± 5.34	FO Aqr		CV
N1485	J221913.5+362004 ^{b)}	334.8063	36.3346	23.5	5.74	4.17 ± 1.43		0.1467	SEYFERT ^{c)}
N1486	J221948.8+261323	334.9531	26.2230	16.3	8.11	8.13 ± 2.21	IRAS F22175+2558	0.0850	BLAZAR
N1487	J222516.9+012242	336.3204	1.3782	14.6	8.81	11.46 ± 2.87	PI Aqr		STAR ^{c)}
N1488	J222913.4+664648	337.3059	66.7799	10.8	10.44	4.48 ± 0.84	IGR J22292+6647	0.1130	SEYFERT
N1489	J223132.7-750114 ^{b)}	337.8861	-75.0205	21.3	5.66	4.04 ± 1.33			CV? ^{c)}
N1490	J223221.6+624939	338.0899	62.8276	23.0	5.45	1.72 ± 0.55	RX J2232.3+6249		BLAZAR?
N1491	J223453.0-843445	338.7206	-84.5791	19.1	6.32	3.66 ± 1.07	2RXS J223456.0-843450	0.1630	SEYFERT ^{c)}
N1492	J223545.6-260304	338.9400	-26.0512	11.5	12.01	17.54 ± 3.45	NGC 7314	0.0048	SEYFERT
N1493	J223602.5+335828	339.0103	33.9745	21.3	6.34	4.65 ± 1.54	NGC 7319	0.0225	SEYFERT
N1494	J223646.2-123243	339.1927	-12.5453	20.2	6.66	8.12 ± 2.50	Mrk 915	0.0241	SEYFERT
N1495	J223715.8+402944	339.3159	40.4955	21.0	5.82	4.12 ± 1.40	1WGA J2237.2+4029	0.0582	SEYFERT ^{c)}
N1496	J223920.7+611627	339.8361	61.2741	7.3	16.36	9.14 ± 1.18	4U 2238+60		HMXB
N1497	J224238.9+294327	340.6622	29.7242	15.0	7.29	6.23 ± 1.76	Ark 564	0.0247	SEYFERT
N1498	J224548.5+394113	341.4521	39.6870	18.8	6.24	4.01 ± 1.21	3C 452	0.0815	SEYFERT
N1499	J224618.3-120655	341.5764	-12.1153	20.8	6.28	6.18 ± 2.17	PKS 2243-123	0.6320	BLAZAR
N1500	J224841.2-510950	342.1716	-51.1640	21.6	6.78	8.57 ± 2.35	SWIFT J2248.7-5109	0.1017	SEYFERT
N1501	J225051.7-085458	342.7156	-8.9162	21.0	6.56	5.76 ± 1.94	2MASX J22505170-0854572	0.0650	SEYFERT
N1502	J225302.3+165030	343.2597	16.8416	19.4	6.36	6.37 ± 1.99	IM Peg		STAR
N1503	J225354.7+624334	343.4781	62.7261	12.1	10.71	5.05 ± 0.95	IGR J22534+6243		HMXB
N1504	J225357.6+160855	343.4900	16.1486	18.4	7.11	6.23 ± 1.91	3C 454.3	0.8579	BLAZAR
N1505	J225405.3-173456	343.5220	-17.5822	8.4	17.10	31.58 ± 4.58	MR 2251-178	0.0640	SEYFERT
N1506	J225413.1+690700	343.5545	69.1167	17.1	6.81	2.07 ± 0.59	2RXS J225416.1+690705		CV ^{c)}
N1507	J225517.7-031040	343.8238	-3.1778	10.1	15.80	28.90 ± 4.59	AO Psc		CV
N1508	J225636.8+052508	344.1534	5.4188	23.4	5.76	5.49 ± 2.03	RX J2256.6+0525	0.0660	SEYFERT
N1509	J225933.0+245510	344.8874	24.9196	18.9	7.72	7.13 ± 2.00	RX J2259.5+2455	0.0345	SEYFERT

Table A.1. continued.

Id	Name SRGA	RA (J2000)	Dec (J2000)	R98 (")	S/N	Flux (10^{-12} erg s $^{-1}$ cm $^{-2}$)	Conventional name	Redshift	Class
N1510	J230108.3+585248	345.2848	58.8801	15.1	7.57	2.98 ± 0.75	1E 2259+586		MAGNETAR
N1511	J230200.6+155754	345.5025	15.9650	13.6	9.11	9.42 ± 2.27	NGC 7465	0.0066	SEYFERT
N1512	J230315.2+085231	345.8135	8.8752	9.6	15.06	23.37 ± 3.66	NGC 7469	0.0163	SEYFERT
N1513	J230338.2+465214 ^{b)}	345.9093	46.8706	18.4	6.15	3.24 ± 0.99		0.0460	SEYFERT ^{c)}
N1514	J230443.2-084111	346.1799	-8.6865	13.3	12.12	19.95 ± 3.91	Mrk 926	0.0470	SEYFERT
N1515	J230631.0+155633 ^{b)}	346.6291	15.9424	23.2	5.65	4.63 ± 1.64		0.4386	SEYFERT ^{c)}
N1516	J230641.7+550827	346.6738	55.1409	16.0	7.63	4.07 ± 1.03	2RXS J230644.7+550817		CV ^{c)}
N1517	J230702.8+043259	346.7617	4.5497	14.2	9.41	11.67 ± 2.74	PG 2304+042	0.0430	SEYFERT
N1518	J230757.3+401644	346.9888	40.2788	15.1	8.08	5.85 ± 1.44	SWIFT J2308.1+4014	0.0716	SEYFERT
N1519	J230821.7-782225 ^{b)}	347.0902	-78.3735	20.2	6.07	3.27 ± 1.04		0.0593	AGN ^{c)}
N1520	J231856.7+001440	349.7364	0.2444	20.1	7.27	8.01 ± 2.27	NGC 7603	0.0288	SEYFERT
N1521	J231951.5+564446	349.9644	56.7460	14.1	7.52	3.31 ± 0.83	2RXS J231950.8+564411		AGN ^{c)}
N1522	J232036.0+643046	350.1500	64.5129	13.1	7.87	3.86 ± 0.90	IGR J23206+6431	0.0732	SEYFERT
N1523	J232038.1+482320	350.1588	48.3890	22.6	5.63	2.47 ± 0.85	2RXS J232039.7+482317	0.0420	SEYFERT ^{c)}
N1524	J232115.7-265901	350.3154	-26.9836	16.5	9.38	11.47 ± 2.57	HD 220096		STAR
N1525	J232245.6-173903	350.6901	-17.6510	19.4	6.15	5.76 ± 2.01	RBS 1994	0.1676	SEYFERT
N1526	J232313.8+584837	350.8074	58.8103	4.1	50.45	115.80 ± 5.08	Cas A		SNR
N1527	J232554.1+215317	351.4754	21.8879	18.9	5.71	4.96 ± 1.70	RX J2325.9+2153	0.1202	SEYFERT
N1528	J232846.1+033035	352.1923	3.5096	22.3	5.80	4.91 ± 1.71	NGC 7679	0.0171	SEYFERT
N1529	J232900.7-294707	352.2529	-29.7853	20.3	7.56	7.49 ± 2.10	VY Scl		CV
N1530	J233032.3-022806	352.6344	-2.4685	23.7	5.58	4.79 ± 1.84	MCG-01-59-027	0.0340	SEYFERT
N1531	J233758.0+430851	354.4916	43.1476	20.7	6.20	3.80 ± 1.15	2RXS J233800.2+430849		CV
N1532	J234024.0+123723	355.0999	12.6231	23.1	5.46	4.36 ± 1.65	HX Peg		CV
N1533	J234333.6+343950	355.8901	34.6638	19.3	7.28	4.40 ± 1.24	2RXS J234332.7+344000	0.3600	BLAZAR
N1534	J234620.9+812214	356.5869	81.3706	20.0	5.42	1.80 ± 0.57	XMMSL2 J234618.4+812222		CV ^{c)}
N1535	J234704.3+514215	356.7680	51.7043	9.0	14.71	9.75 ± 1.44	1ES 2344+514	0.0440	BLAZAR
N1536	J234753.1+543629	356.9714	54.6079	13.9	7.93	4.33 ± 1.05	4FGL J2347.9+5436		BLAZAR?
N1537	J234940.7+362541	357.4195	36.4280	19.8	5.43	3.01 ± 1.06	OU And		STAR
N1538	J235153.1+261936	357.9714	26.3266	20.9	5.51	3.88 ± 1.31	RBS 2055	0.0377	SEYFERT
N1539	J235156.4-010905	357.9849	-1.1514	17.9	6.56	6.17 ± 1.74	PKS 2349-01	0.1738	SEYFERT
N1540	J235250.7-170448	358.2112	-17.0799	19.5	6.90	5.86 ± 1.91	SWIFT J2352.6-1707	0.0550	SEYFERT ^{c)}
N1541	J235335.2-454210	358.3968	-45.7027	25.9	5.56	5.16 ± 1.82	2RXS J235335.6-454217		AGN ^{c)}
N1542	J235729.6-171810	359.3734	-17.3028	13.1	10.29	12.74 ± 2.74	RBS 2066		BLAZAR
N1543	J235908.2-303753	359.7842	-30.6314	25.8	5.80	5.52 ± 2.05	H 2356-309	0.1654	BLAZAR
N1544	J235911.3-040730	359.7971	-4.1250	21.3	5.93	5.03 ± 1.62	IC 1524	0.0192	SEYFERT
N1545	J235958.2+083410	359.9923	8.5693	27.2	5.71	4.30 ± 1.45	RX J2359.9+0833	0.0830	SEYFERT

Notes. ^(a) For the description of columns see Section 4. ^(b) Sources detected in X-rays for the first time by *SRG/ART-XC*. ^(c) Additional information on identification and classification is provided in Section A.